

5-2013

# A Model-free Approach to Vehicle Stability Control

Chinmay Pandit

Clemson University, cpandit@clemson.edu

Follow this and additional works at: [https://tigerprints.clemson.edu/all\\_theses](https://tigerprints.clemson.edu/all_theses)



Part of the [Mechanical Engineering Commons](#)

---

## Recommended Citation

Pandit, Chinmay, "A Model-free Approach to Vehicle Stability Control" (2013). *All Theses*. 1637.

[https://tigerprints.clemson.edu/all\\_theses/1637](https://tigerprints.clemson.edu/all_theses/1637)

This Thesis is brought to you for free and open access by the Theses at TigerPrints. It has been accepted for inclusion in All Theses by an authorized administrator of TigerPrints. For more information, please contact [kokeefe@clemson.edu](mailto:kokeefe@clemson.edu).

A MODEL-FREE APPROACH TO VEHICLE STABILITY CONTROL

---

A Thesis  
Presented to  
the Graduate School of  
Clemson University

---

In Partial Fulfillment  
of the Requirements for the Degree  
Master of Science  
Mechanical Engineering

---

by  
Chinmay Milind Pandit  
May 2013

---

Accepted by:  
Dr. E. Harry Law, Committee Chair  
Dr. John Wagner  
Dr. Beshah Ayalew

## ABSTRACT

This project explored the feasibility of using measured responses of a passenger car together with a fuzzy logic based control algorithm to sense the onset of under-steer (or loss of steering control) and mitigate or eliminate it. The controller is simple and robust and, unlike existing controllers, instead of comparing the vehicle response to that of an idealized model it makes decisions based solely upon the measured response of the car.

Simulations were conducted (using CarSim) of various vehicles executing the skid pad and the double lane change tests to characterize the vehicle behavior. Consistent and qualitatively similar patterns in vehicle response during the inception of and at limit under-steer were observed. A fuzzy logic routine was developed that analyzes real-time measurements of steering wheel angle (SWA) and lateral acceleration ( $A_y$ ). Based on the relative 'trends' of the signals, the control algorithm decides upon the presence and extent of under-steer in the vehicle. The degree of under-steer then defines the corrective action.

The fundamental concept is to measure a drop in the instantaneous lateral acceleration gain, i.e.,  $A_y/SWA$ , indicating a lack of response. It is quantified as a normalized error and transformed into an under-steer number between 0 and 10 using a pair of fuzzy inference systems. Once incipient under-steer is detected, the brakes and engine throttle are managed to limit the lateral deviation from the travel lane. The controller also senses vehicle velocity, master cylinder brake pressure and normalized throttle input to improve controllability. This approach eliminates the need for either a simple or a complex vehicle model and the associated dependence on the model parameters.

Controller performance was validated using a braking-in-turn maneuver developed by the author and the standard double lane change maneuver. The results have shown clear improvement in the tracking ability of a vehicle. The simulations were conducted at different speeds with each of several vehicles and with different tire-to-ground friction values without any changes to the control algorithm. This has shown that the controller is robust across different conditions. The controller is successful in increasing the maximum safe speed for a negotiating a curve for all vehicles on various road conditions.

The last part of the controller was to combine it with an existing over-steer controller, developed at Clemson University, which also uses fuzzy logic. This was successfully completed to obtain a fully functional ESC system, independent of a vehicle model. Future work will include tuning the controller based on track data from real vehicles.

## DEDICATION

This thesis is dedicated to the memory of my father.

## ACKNOWLEDGMENTS

I would like to thank my advisor, Dr. E. H. Law, for his invaluable guidance and encouragement through the course of my graduate studies. I greatly appreciate his time and dedication on this project. I am grateful for his suggestions and his efforts to review and edit this manuscript. I also want to thank Dr. John Wagner and Dr. Beshah Ayalew for their suggestions and for serving on my committee.

I wish to thank Mr. Jeffery Anderson for allowing me the use of his work and to Mr. Judhajit Roy for exchanging ideas and providing objectivity to my work.

Special thanks go to my mother, Hina Pandit, for encouraging and supporting me to pursue my degree and follow my passion.

Finally, I want to thank my wife, Ritu Pandit, for her steadfast support and patience as I worked toward my degree. She inspires me to strive for excellence in all my endeavors.

# TABLE OF CONTENTS

	Page
TITLE PAGE .....	i
ABSTRACT .....	ii
DEDICATION .....	iv
ACKNOWLEDGMENTS .....	v
LIST OF TABLES .....	viii
LIST OF FIGURES .....	ix
CHAPTER	
I. INTRODUCTION .....	1
Introduction .....	1
Literature Survey .....	2
Research Motivation .....	4
II. BACKGROUND .....	8
‘Limit’ Under-steer .....	8
Fuzzy Logic .....	18
Over-steer Controller: Overview and Modifications .....	26
III. ELECTRONIC STABILITY CONTROLLER.....	28
Under-steer Control Module .....	28
Under-steer Actuator Module .....	37
The Combined ESC .....	41
IV. RESULTS .....	45
Vehicle Models .....	46
Test Maneuvers .....	46
Test Configurations.....	49

Table of Contents (Continued)

	Page
Case Studies .....	50
Summary .....	97
V.    CONCLUSIONS AND RECOMMENDATIONS .....	99
Conclusion .....	99
Future Work .....	100
APPENDICES .....	101
A:    Vehicle Parameters .....	102
B:    Tire Data .....	103
C:    MATLAB and Simulink Documentation.....	112
D:    Fuzzy Inference Systems .....	125
REFERENCES .....	143



## LIST OF TABLES

Table		Page
2.1	Fractional Drop at Under-steer Handling Limit: Two Vehicles .....	17
3.1	CarSim Import and Export Parameters .....	44
4.1	Case Studies .....	45
4.2	Maximum Safe Speed: Case 1 .....	54
4.3	Maximum Safe Speed: Case 3 .....	61
4.4	Maximum Safe Speed: Case 4 .....	67
4.5	Maximum Safe Speed: Case 5 .....	73
4.6	Maximum Safe Speed: Case 6 .....	80
4.7	Maximum Safe Speed: Case 7 .....	86
4.8	Maximum Safe Speed: Case 8 .....	92
4.9	Percent Improvement in Maximum Speed: Braking-in-Turn .....	98
A.1	Vehicle Parameters .....	102

## LIST OF FIGURES

Figure	Page
1.1 Overview of a model based ESC system .....	7
2.1 Free Body Diagram of a 2 DOF vehicle model .....	9
2.2 Friction Ellipse.....	10
2.3 Circle Test: Vehicle Dynamics .....	13
2.4 Circle Test: SWA vs. $A_y$ .....	14
2.5 Circle Test: $A_y$ vs. Time .....	14
2.6 Circle Test: $A_y$ gain.....	14
2.7 Circle Test: $A_y$ Gain vs. Time: Two vehicles.....	16
2.8 Circle Test: $A_y$ vs. Time: Two vehicles .....	16
2.9 Circle Test: Fractional Drop: Two vehicles .....	17
2.10 Non-Fuzzy and Fuzzy sets defining {Temperature about 150°C} .....	19
2.11 Logical Operators: Fuzzy Logic vs. Conventional Logic .....	21
2.12 Overview of a Fuzzy Inference System .....	24
2.13 Defuzzification Methods.....	25
3.1 Under-Steer Control Module .....	29
3.2a Under-steer Computation Block .....	31
3.2b Fractional Drop: Two vehicles.....	31
3.3 Overview: FIS ‘Indicated Under-steer’ .....	33

List of Figures (Continued)

Figure	Page
3.4 Overview: FIS ‘Under-steer’ .....	36
3.5 Brake Distribution Parameters .....	40
3.6 Input to the Decision Module .....	41
3.7 Output of the Decision Module.....	42
3.8 Schematic Diagram for the Braking System.....	43
4.1 Lateral Deviation: BMW Mini at two speeds .....	48
4.2 ISO 3888 Double Lane Change .....	48
4.3 Lateral Deviation: Case 1.....	50
4.4 Vehicle Response: Case 1 .....	52
4.5 Brake Torque: Case 1.....	53
4.6 Vehicle Speed: Case 1 .....	54
4.7 Lateral Force per Axle: Case 1 .....	55
4.8 Trajectory: Case 2.....	57
4.9 Brake Torque: Case 2.....	58
4.10 Vehicle Response: Case 2.....	59
4.11 Lateral Force per Axle: Case 2 .....	60
4.12 Lateral Deviation: Case 3.....	62
4.13 Brake Torque: Case 3.....	63
4.14 Vehicle Response: Case 3.....	64
4.15 Vehicle Speed: Case 3 .....	65

List of Figures (Continued)

Figure	Page
4.16 Lateral Force per Axle: Case 3 .....	66
4.17 Lateral Deviation: Case 4.....	68
4.18 Vehicle Response: Case 4.....	69
4.19 Brake Torque: Case 4.....	70
4.20 Vehicle Speed: Case 4 .....	71
4.21 Lateral Force per Axle: Case 4 .....	72
4.22 Lateral Deviation: Case 5.....	74
4.23 Vehicle Response: Case 5.....	75
4.24 Brake Torque: Case 5.....	76
4.25 Vehicle Speed: Case 5 .....	77
4.26 Lateral Force per Axle: Case 5 .....	78
4.27 Lateral Deviation: Case 6.....	80
4.28 Vehicle Response: Case 6.....	81
4.29 Brake Torque: Case 6.....	82
4.30 Vehicle Speed: Case 6 .....	83
4.31 Lateral Force per Axle: Case 6 .....	84
4.32 Lateral Deviation: Case 7.....	86
4.33 Vehicle Response: Case 7.....	87
4.34 Brake Torque: Case 7.....	88
4.35 Lateral Force per Axle: Case 7 .....	89

List of Figures (Continued)

Figure	Page
4.36 Vehicle Speed Case 7.....	90
4.37 Lateral Deviation: Case 8.....	92
4.38 Vehicle Response: Case 8.....	93
4.39 Brake Torque: Case 8.....	94
4.40 Vehicle Speed: Case 8 .....	95
4.41 Lateral Force per Axle: Case 8 .....	96
4.42 Percent Improvement in Maximum Speed .....	98
B.1 BMW Mini: Nominal: $F_y$ vs. $\alpha$ .....	104
B.2 BMW Mini: Nominal: $F_x$ vs. $\kappa$ .....	105
B.3 BMW Mini: Degraded Tires: $F_y$ vs. $\alpha$ .....	106
B.4 BMW Mini: Degraded Tires: $F_x$ vs. $\kappa$ .....	107
B.5 CarSim Sedan: Nominal: $F_y$ vs. $\alpha$ .....	108
B.6 CarSim Sedan: Nominal: $F_x$ vs. $\kappa$ .....	109
B.7 CarSim SUV: Nominal: $F_y$ vs. $\alpha$ .....	110
B.8 CarSim SUV: Nominal: $F_x$ vs. $\kappa$ .....	111
C.1 Complete ESC: Overview.....	113
C.2 CarSim ABS.....	114
C.3 ESC Control Module.....	116
C.4 US Hold Time.....	117
C.5 Actuator Module .....	122

List of Figures (Continued)

Figure	Page
C.6 US Throttle Control .....	123
C.7 Brake Force Distributor .....	124
D.1 Under-Steer Computation Block.....	126
D.2 FIS Indicated Under-steer: Input and Output Membership Functions .....	127
D.3 Indicated Under-Steer: Rule 1 Evaluation and Defuzzified Output.....	128
D.4 Under-Steer Control Module .....	130
D.5 FIS Under-steer: Input and Output Membership Functions .....	131
D.6 Under-steer: Rule 1 Evaluation and Defuzzified Output.....	132
D.7 Over-Steer Indicating Block .....	135
D.8 FIS Possible Unstable Event: Input and Output Membership Functions .....	136
D.9 Possible Unstable Event: Input Membership Function for Input [0.4 0.8] .....	137
D.10 Possible Unstable Event: Evaluation of Rules for Input [0.4 0.8] .....	137
D.11 Under-Steer Brake Force Distributor Block .....	140
D.12 Brake Balance: Input and Output Membership Functions .....	141
D.13 Brake Balance: Input Membership Function for Input [1.5 0.8] .....	142

List of Figures (Continued)

Figure	Page
D.14 Brake Balance: Evaluation of Rules and Defuzzified Outputs .....	142

# CHAPTER 1

## INTRODUCTION

### Introduction

The final NHTSA report <sup>[1]</sup> on effectiveness of electronic stability control (ESC) showed that ESC reduced all fatal single-vehicle run-off-road crash involvements by 36 percent in passenger cars and 70 percent in light trucks. Moreover, in this study, it was found that rollover involvements in fatal crashes decreased by 70 percent in passenger cars and 88 percent in light trucks. It is clear that the ESC is a critical part of the active safety system in any vehicle. One of the functions of the ESC is to reduce skidding due to under-steer of the vehicle.

Milliken and Milliken have described the behavior of an under-steering vehicle by stating that“.... As lateral acceleration (i.e. side force) is applied it ‘under-steers’ the geometric path established by the Ackermann Steering Angle.”<sup>[2]</sup> In other words, the vehicle traverses along the outside of the geometrically defined trajectory. A useful physical analogy they provide is that of a weather cock: “Under-steer is the tendency of the vehicle to align its (longitudinal) axis with its velocity vector.” However, these definitions, by their admission, “apply to sublimit operations.”

At the under-steer limit “... the stabilizing moment from the rear takes over, the path tends to straighten and the vehicle aligns itself with the path. With front steer, control



moments can no longer be generated.”<sup>[2]</sup> One function of the electronic stability control (ESC) is to prevent just such an event from occurring.

This project is focused on developing an ESC that reduces the under-steer tendency of a vehicle without the use of either a complex or simple vehicle and tire model. The prediction and correction of vehicle motion is done entirely based on real time measurements of the actual vehicle response and a physical understanding of vehicle dynamics. Fuzzy logic<sup>[3]</sup> is used to design the controller. The majority of the project focuses on controlling under-steer. The last part of the project, however, combines an existing over-steer controller<sup>[4,5]</sup> to give a complete ESC system.

### Literature Survey

The electronic stability control (ESC) was first introduced in 1995 with the Bosch ESP equipped Mercedes-Benz S-Class<sup>[6]</sup>. The main function of the ESC, according to that paper, is to prevent loss of control of the vehicle during emergency maneuvers. It may be integrated with either Anti-lock Braking System (ABS) or Traction Control System (TCS) or both to modify the slip angles at individual wheels in order to maintain yaw rate and side-slip angle values within allowable limits<sup>[7]</sup>.

The first controller developed by Bosch used an idealized 2 degree of freedom bicycle model of the vehicle to determine the allowable or “safe” values for yaw rate and side slip angle<sup>[6]</sup>. The system used observers and estimators to generate the side slip angle value. Since then, there has been extensive research in trying to improve the performance

of the vehicle stability controller as well as to incorporate other functions along with lateral handling. Guo et al <sup>[8]</sup>, Yuan et al <sup>[9]</sup> and Jangyeol et al <sup>[10]</sup> are only three recent examples from a vast body of work.

In the original paper by van Zanten <sup>[6]</sup>, he has listed the goals of an active system as defined by McLellan <sup>[11]</sup> to be:

1. Keep the driver in charge.
2. Intervene on a 'smart' basis and only when needed.
3. Emulate the expert, or race, driver to assist the novice, or average, driver in realizing the performance potential of the vehicle.

The last point in particular is important because it indicates that the principles of human driver modeling can be applied to a stability program.

In 1990, Sutton <sup>[12]</sup> wrote a book on modeling human operators. He discusses the various issues involved in modeling human operators and the approaches that various authors have taken to tackle these issues. The latter part of his book focuses on modeling the non-linear aspects of human behavior. When dealing with uncertainty he has quoted a few authors advocating the use of fuzzy logic <sup>[13,14]</sup>. Tong <sup>[13]</sup> in particular makes a strong case of using fuzzy logic to model human operators when the system has high non-linearity as well as unpredictable changes in systems parameters. He recommends fuzzy logic because of its robustness in such situations. A number of other papers <sup>[15-17]</sup> exist that demonstrate the superiority of fuzzy logic over conventional logic. However, to quote Sutton, "little work has been carried out using fuzzy set theory to describe and analyze the human operators who control man-machine systems."

In 1999, Vaduri <sup>[18]</sup> developed an expert system that used fuzzy logic to diagnose under-steer and over-steer in vehicles. The system was based on vehicle dynamics patterns described by Fey in his book on data acquisition <sup>[19]</sup> and eliminated the use of a vehicle model. In effect, the system acted like an expert engineer that pinpoints the sections on a road course where instability is observed, independent of the type of car, tire wear and road surface condition. This would save a lot of time for a race engineer who can then utilize his time to address the underlying issues. Anderson <sup>[4,5]</sup> extended this concept to correct over-steer in real time on passenger vehicles. Once again the use of a vehicle model was eliminated. The system was found to be very robust. The current work extends Anderson's work to control understeer. The final objective is to obtain a fully functional ESC that can control both under- and over-steer in a vehicle.

### Research Motivation

A schematic overview of a model based ESC system commonly used is shown in Figure 1.1. The control decisions are based on two sets of signals:

- 'Ideal' vehicle response
- Actual vehicle response

Most ESC systems use a simple 2 degree of freedom 'bicycle' model to generate the 'ideal' or reference values of vehicle response. Steady state equations for yaw rate ( $r$ ), side slip angle ( $\beta$ ) and steering wheel angle ( $\delta$ ) are developed mathematically. These expressions define the reference values for the controller.

Desired Yaw rate:

$$r_{desired} = \frac{V}{L} * \left( \frac{1}{1 + \frac{K_{us} * V^2}{L * g}} \right) * \delta \dots\dots\dots(1.1)$$

Desired Side slip angle:

$$\beta_{desired} = \frac{b}{L} * \left( \frac{1}{1 + \frac{K_{us} * V^2}{L * g}} \right) * \left( 1 - \frac{a m V^2}{b L C_2} \right) * \delta \dots\dots\dots(1.2)$$

Where,

$$K_{us} = \frac{b C_2 - a C_1}{L C_1 C_2} * m g = \text{Understeer Gradient, rad/G}$$

V = Vehicle speed, m/s

L = Wheelbase, m

$$g = 9.81 \text{ m/s}^2$$

a, b = Front and rear axle distance from C.G. respectively, m

m = Vehicle mass, kg

C<sub>1</sub>, C<sub>2</sub> = Cornering stiffness per axle, front and rear respectively, N/ rad

The accuracy of the reference signals depends on an exact description of the vehicle being controlled by the variables described above. However, variables such as vehicle mass, front and rear axle distance and cornering stiffness vary with the loading condition, load distribution, tire wear, etc. The Equations 1.1 and 1.2 are valid only in the linear regime of tire operation because the concept of cornering stiffness is defined only for small values of tire slip angle. When there is incipient ‘limit’ under-steer, the front tires are at the point of saturation and are no longer in their linear range of operation.

The second set of signals, the actual vehicle response, is generated, in most cases, by using some sort of an observer <sup>[6,20,21]</sup>. The observer incorporates tire models that require knowledge of tire properties such as tire stiffness, cornering stiffness, etc. These values also vary with load and tire wear.

To address the issues highlighted above, OEMs conduct extensive tests <sup>[22]</sup> to characterize the vehicle and to generate predictive values of the various parameters for the vehicle model. The stability program is then tuned to account for road banking, road crown, hill descent and ascent, etc. Still, changing the vehicle ride height or installing a new set of tires by the vehicle owner can affect the overall performance of the stability program.

This work focuses on developing a model-free controller that can provide robust control over vehicle motion. The primary issue addressed in this work is limit under-steer. Under-steer progresses relatively slowly and more often than not can be detected by the driver. However, it becomes an issue of concern on low friction surfaces where driver intervention in the form of braking is not sufficient to fix the situation. An ESC then reroutes braking forces to make the best use of the prevailing conditions to maintain driver control over the vehicle.

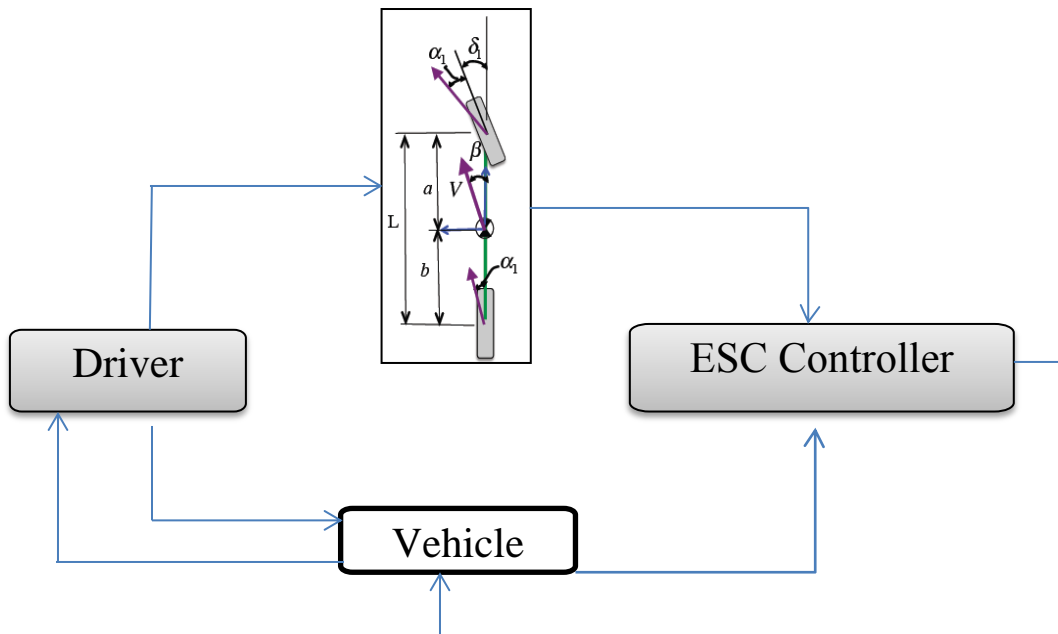


Figure 1.1 Overview of a Model-based ESC system

## CHAPTER 2

### BACKGROUND

#### 'Limit' Under-steer

#### **Principle**

The basic premise of 'limit' under-steer is the inability of the vehicle to increase its lateral acceleration and yaw rate upon increasing the steering input. This occurs "in the transitional and frictional ranges of tire operation when one end (in this case the front) of the vehicle is reaching its limit lateral force capability"<sup>[2]</sup>.

To explore this phenomenon let us look at the free body diagram of a simple 2 degree of freedom model of a vehicle executing a constant radius turn (Figure 2.1). The various terms used in the figure are:

'm' – Vehicle Mass, kg

' $I_z$ ' – Vehicle Moment of Inertia, kg-m<sup>2</sup>

'a' – Distance from Vehicle C.G. to front axle, m

'b' – Distance from Vehicle C.G. to rear axle, m

'L' – Vehicle Wheelbase i.e. 'a' + 'b', m

' $F_{yf}$ ' & ' $F_{yr}$ ' – Front and Rear Lateral force per axle respectively, N

'V' – Instantaneous Longitudinal Speed, m/s

'R' – Radius of curvature of the trajectory, m

' $\psi$ ' – Yaw Angle of the vehicle, rad

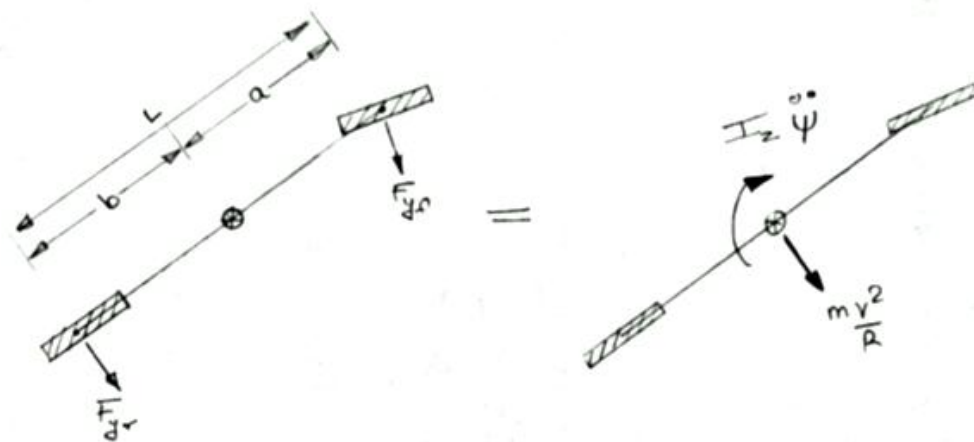


Figure 2.1 Free Body Diagram of a 2 DOF vehicle model

If the radius of curvature is assumed large enough, i.e.  $R \gg L$ , the lateral forces at the front and rear axle are nearly parallel.

Thus, by Newton's Laws of motion:

$$\sum \text{Forces} : F_{yf} + F_{yr} = \frac{m \cdot v^2}{R} \dots\dots\dots(2.1)$$

$$\sum \text{Moments} : F_{yf} \cdot a - F_{yr} \cdot b = I_{zz} \cdot \ddot{\psi} \dots\dots\dots(2.2)$$

For a free rolling tire (i.e. no longitudinal force), the maximum lateral force a tire, and hence an axle, can generate depends on the normal force and the surface friction at that tire-to-ground interface. A tire is said to 'saturate' when the maximum force (limit lateral force) is reached.

The limit lateral force ( $F_y$ ) is also affected by the presence of any longitudinal force ( $F_x$ ). The larger the longitudinal force, the smaller is the lateral force capability. The resultant of the two forces is equal to the total frictional force at the tire-to-ground interface. The relationship between the two forces can be represented by a friction ellipse



(Figure 2.2). The friction ellipse establishes the maximum resultant force that the tire can generate for a given normal load ( $F_z$ ).

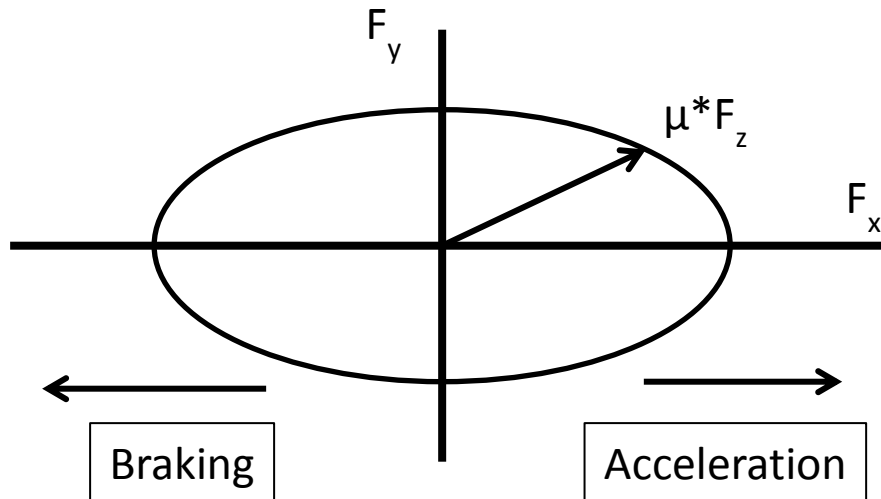


Figure 2.2 Friction Ellipse

In order to ‘de-saturate’ the front tires, the normal load on the front tires must be increased. This can be accomplished by applying the brakes resulting in a longitudinal load transfer. This in turn reduces the normal load on the rear axle. As long as the rear axle stays ‘sublimit’ (resultant tire force remains within its friction ellipse) the increase in normal load at the front axle has the effect of increasing the yaw rate of the vehicle (from Equation (1.2)). Braking also results in reducing the longitudinal velocity of the vehicle and hence the lateral acceleration ( $(V^2)/R$ ) required for a given curve. This makes the vehicle easier to ‘turn-in’.

It is important to remember that the rear axle must remain sublimit during this process. If not, the lateral force at the rear tires is quickly reduced resulting in an excessive increase in yaw rate and ‘snapping’ the vehicle into over-steer (spin-out). Excessive

braking of either axle will also result in instability due to the ‘friction ellipse’ effect. As before, depending on the axle that reaches its limit first, the vehicle will either under-steer or over-steer. Thus, to attenuate under-steer, the braking strategy must maximize the lateral force for the front axle while ensuring the rear axle stays within its ‘friction ellipse’ limit.

### **Pattern Recognition from Vehicle Response**

In order to make the controller robust the first step is to recognize generic patterns that indicate imminent limit under-steer. The fuzzy logic rules that need to be developed depend on an accurate understanding and description of the physics of the phenomenon. To that end the behavior of various vehicles executing the circle test was studied. Although the patterns to be expected during an under-steer event have been defined in [18] and [19], they were limited to a race car at its handling limit. The ESC has to detect under-steer (as well as over-steer) before the limit conditions are realized and prevent them. The controller that is described in this work was developed using Simulink and simulations are carried out in the MATLAB workspace. The vehicle and driver models are based in CarSim in place of an actual vehicle and driver.

Simulations of a circle test were done using CarSim to analyze vehicle behavior during an under-steer event. In this test, the car traverses a constant radius circle and gradually increases speed and, hence, lateral acceleration. The vehicle dynamic signals as well as the steering wheel angle (SWA) versus lateral acceleration ( $A_y$ ) curve for a vehicle are shown in Figures 2.3 and 2.4. The vehicle is an under-steering vehicle

because the slope of the SWA vs.  $A_y$  plot is positive. The peak value of lateral acceleration achieved is 0.694 Gs at 24.3 s. The steer input at this time is 139.7 deg.

Now, the slope of SWA vs.  $A_y$  plot begins increasing much earlier as compared to the point at which the vehicle reaches its limit lateral acceleration. The lateral acceleration at this point for the vehicle in Figure 2.4 is 0.5705 Gs. From Figure 2.5, the time at which the slope starts to increase, i.e.  $A_y = 0.5705$  Gs is 21.63 s. The steering rate also begins to increase at this time. Physically, the driver is required to supply a larger and larger steer input to increase the lateral acceleration of the vehicle as the vehicle approaches its under-steer handling limit. To characterize this behavior this author took a ratio of lateral acceleration ( $A_y$ ) to steering wheel angle (SWA) to compute, in real time, the  $A_y$  gain, shown in Figure 2.6.

The gain reaches a peak value at the same time (21.63 s) that the slope in the SWA vs.  $A_y$  plot begins to increase. It subsequently drops and the size of the fall from the peak value of the gain indicates the proximity of the vehicle to its under-steer handling limit. The larger the fall the closer is the vehicle to its handling limit.

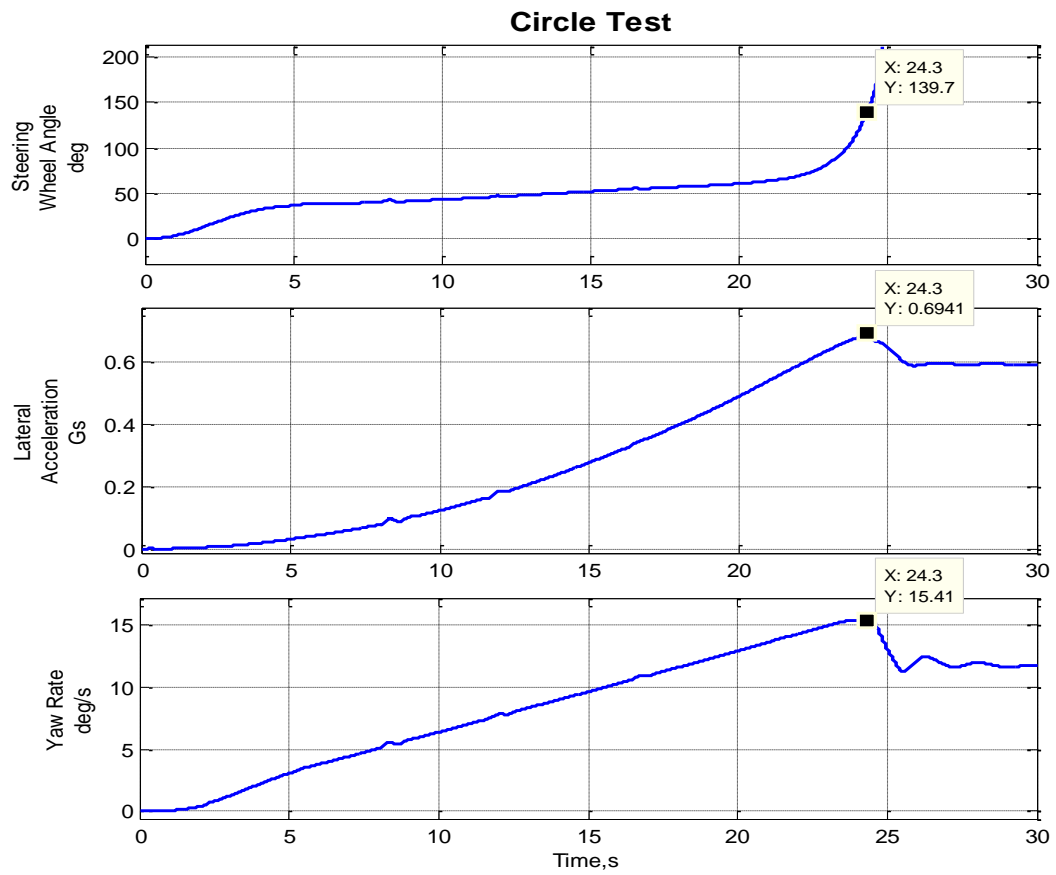


Figure 2.3 Circle Test: Vehicle Dynamics

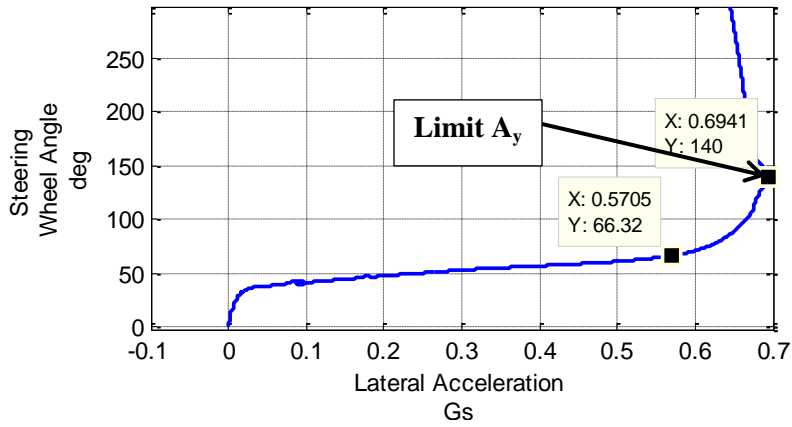


Figure 2.4 Circle Test: SWA vs.  $A_y$

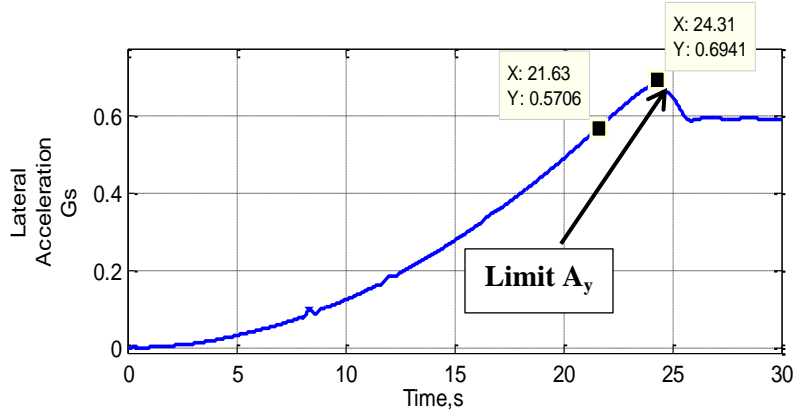


Figure 2.5 Circle Test:  $A_y$  vs. Time

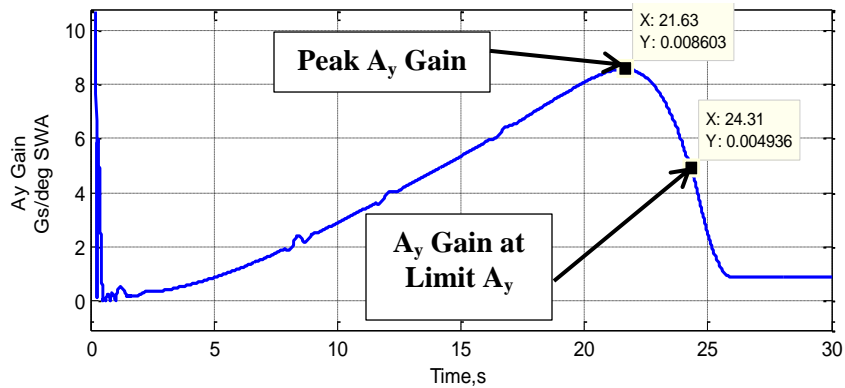


Figure 2.6 Circle Test:  $A_y$  Gain

The start of the drop in the gain plots indicates imminent under-steer. The gain values begin to drop before the limit lateral force for the front axle is reached. So, it gives an advance warning of limit under-steer. However, different vehicles have different characteristics and hence different characteristic curves and peak  $A_y$  gain values. The author observed that the magnitude of the fall in  $A_y$  gain from the peak value before a vehicle reaches its handling limit is in proportion to the magnitude of the peak value of  $A_y$  gain. Shown in Figure 2.7 are the  $A_y$  gain plots for two vehicles, a mid-size sedan and a BMW Mini. The Mini with a higher peak gain value (**0.0178 Gs/deg** against **0.01161 Gs/deg** for the Sedan) has a larger fall in gain (**0.01 Gs/deg** against **0.006 Gs/deg**) before it reaches its limit  $A_y$  value (Figure 2.8). If the magnitude of the fall is divided by the value of the peak gain value then at the limit  $A_y$  value, the ‘fractional’ drop is approximately (-0.5), irrespective of vehicle type (Figure 2.9). This was verified for a number of vehicles, tire conditions and road conditions. This consistent measure is a useful indicator of how close a vehicle is to its under-steer handling limit. The closer the fractional drop at any time to (-0.5), the closer is the vehicle to its under-steer handling limit. The relevant values are tabulated in Table 2.1. The control strategy is based on evaluating and minimizing the fractional drop.

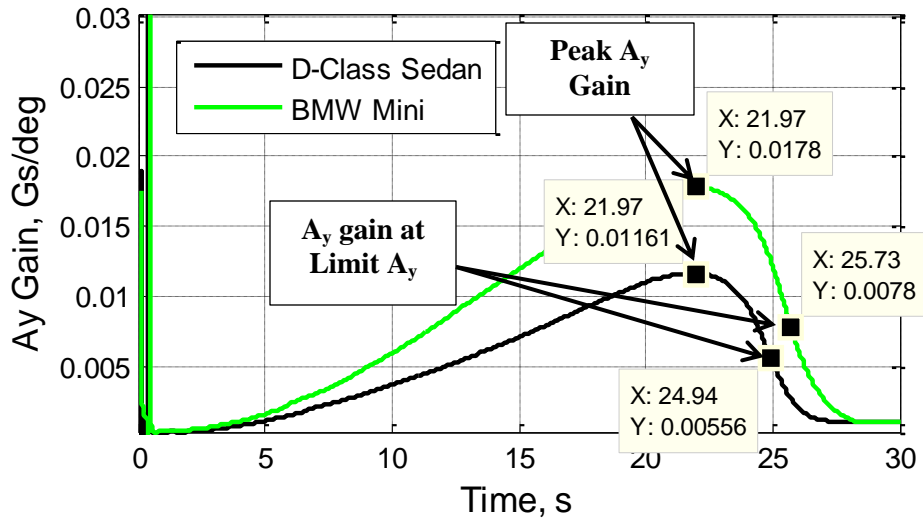


Figure 2.7 Circle Test:  $A_y$  Gain versus time: Two vehicles

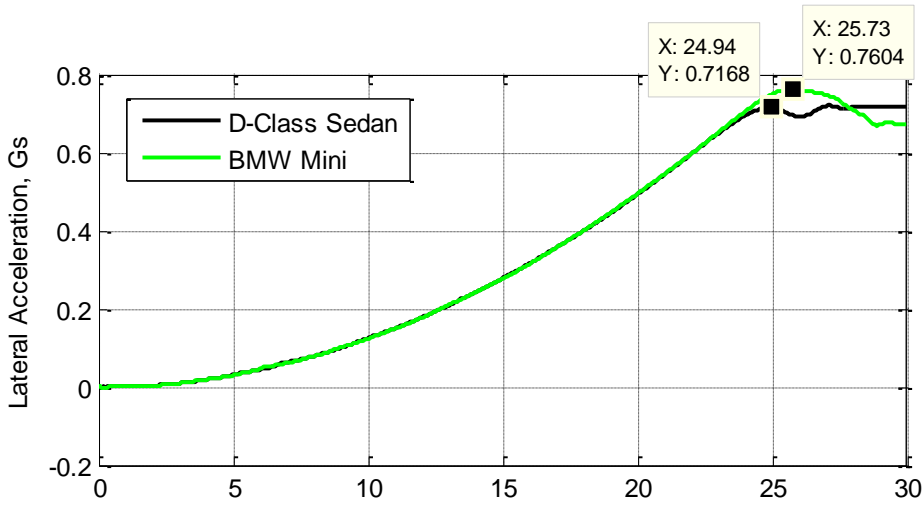


Figure 2.8 Circle Test:  $A_y$  vs. Time: Two vehicles

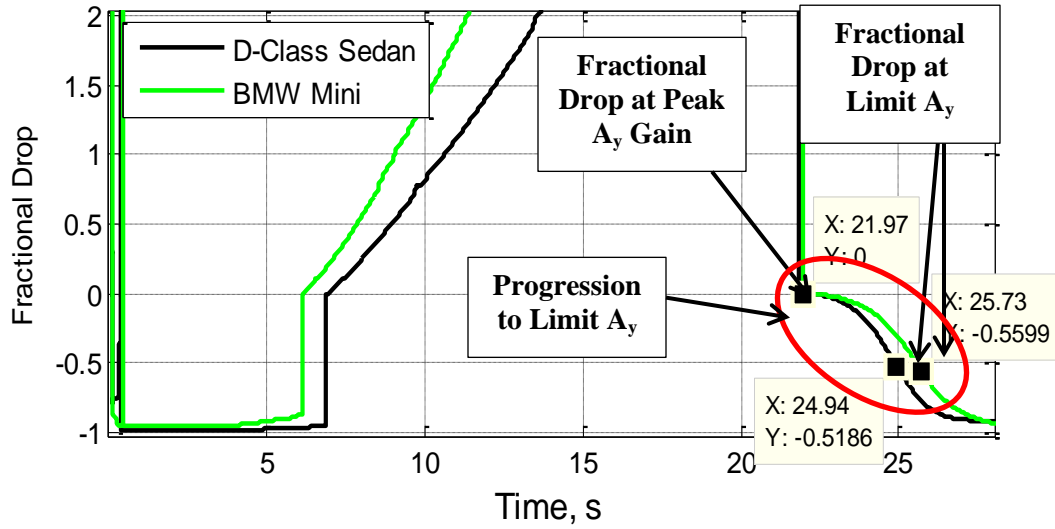


Figure 2.9 Circle Test: Fractional Drop: Two Vehicles

Table 2.1 Fractional Drop at Under-steer Handling Limit: Two Vehicles

At the $A_y$ limit			
Vehicle Model	Time(s)	Drop in Gain from Peak (Gs/ deg)	Fractional Drop
Sedan	24.94	0.006	-0.52
Mini	25.73	0.01	-0.56



## Fuzzy Logic

This work uses fuzzy logic to make control and actuation decisions. A brief overview of fuzzy logic and its application to this work is given below.

Fuzzy logic is based on the theory of fuzzy sets proposed by Zadeh in 1965 <sup>[3]</sup>. It allows the use of linguistic variables for the evaluation of if-then statements, called fuzzy rules. The power of fuzzy logic lies in its ability to incorporate vagueness. Tong <sup>[13]</sup> states that ‘the idea of a fuzzy set allows imprecise and qualitative information to be expressed in an exact way, and, as the name implies, is a generalization of the ordinary notion of a set’. Vaduri <sup>[18]</sup> has dedicated significant material to explain the concepts of fuzzy logic, fuzzy sets and the various terms associated with the evaluation of fuzzy inference systems. A quick overview of the material is given below.

He explains that unlike conventional set theory, where an object either does or does not belong to a given set, in fuzzy set theory the same object may only partially belong to a fuzzy set. It can take a membership value anywhere between 0 (does not belong) and 1 (does belong), called its degree of membership, with respect to that set. A membership function (MF) is a curve that defines to what degree each point in the universe of discourse belongs to the associated fuzzy set. A membership function can be of any shape. Membership functions for a non-fuzzy set and a fuzzy set defining the measure {temperatures about 150°C} are shown in Figure 2.10. For the non-fuzzy set, there is a fixed threshold value at which the description of the temperature goes from ‘not about 150°C’ (membership value ‘0’) to ‘about 150°C’ (membership value ‘1’). However,

human perception is better represented by the fuzzy set. As the temperature rises the description ‘about 150°C’ becomes gradually more appropriate. So, 124°C is definitely not close to 150°C but 145°C can certainly be described as ‘about 150°C’. All values in between have a gradually increasing truth value for the set {temperatures about 150°C}. Meaning that they have increasing membership values to that set. They increasingly belong to a larger extent to the given set. The grade can take any shape and the distribution can be as narrow or as wide as the designer wants based on the system that is being represented.

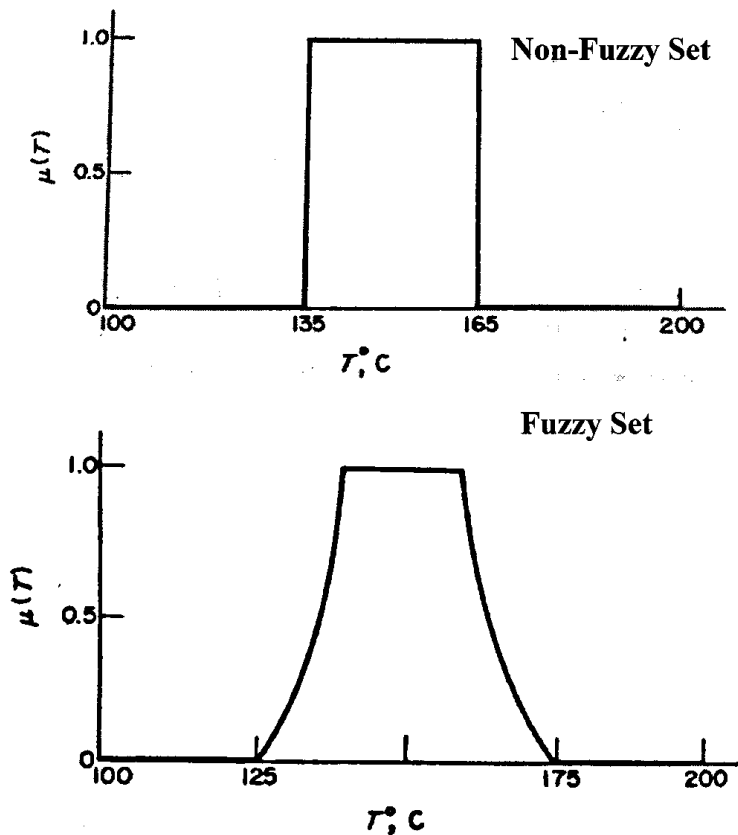


Figure 2.10 Non-Fuzzy and Fuzzy sets defining {Temperature about 150°C}  
(Reproduced, with permission and modifications, from [13])

The Fuzzy Logic Toolbox <sup>[23]</sup> in MATLAB evaluates Fuzzy Inference Systems (FIS) using one or more fuzzy rules (if-then statements). All rules are evaluated in parallel and the order is unimportant. Each rule has an antecedent (the ‘if’ part of the statement) and a consequent (the ‘then’ part of the statement). The antecedent can have multiple parts and different parts are connected through logical operators, called connectives, such as ‘AND’ and ‘OR’. Figure 2.11 highlights the difference between the logical operators as applied to conventional logic and fuzzy logic. Although the operators are similarly defined for both forms of logic, fuzzy logic allows the resolved values to have ‘truth’ values between ‘0’ and ‘1’. The ‘AND’ operator is defined as an intersection of two sets, ‘OR’ is the union of two sets and ‘NOT’ is the complement of the original set.

For example, for a pair of fuzzy sets ‘A’ and ‘B’ (Figure 2.11) if any given input value has a membership value of 0.2 (20% true) in ‘A’ and 0.6 (60% true) in ‘B’ then it is *at least* 20% true in ‘A’ AND ‘B’. Similarly, the input value is *at the most* 60% true in either ‘A’ OR ‘B’. This ‘truth’ value is then used to evaluate the fuzzy rule that uses the operator (‘AND’, ‘OR’, etc.) as a connective for its various inputs. The evaluation of an FIS is explained next.

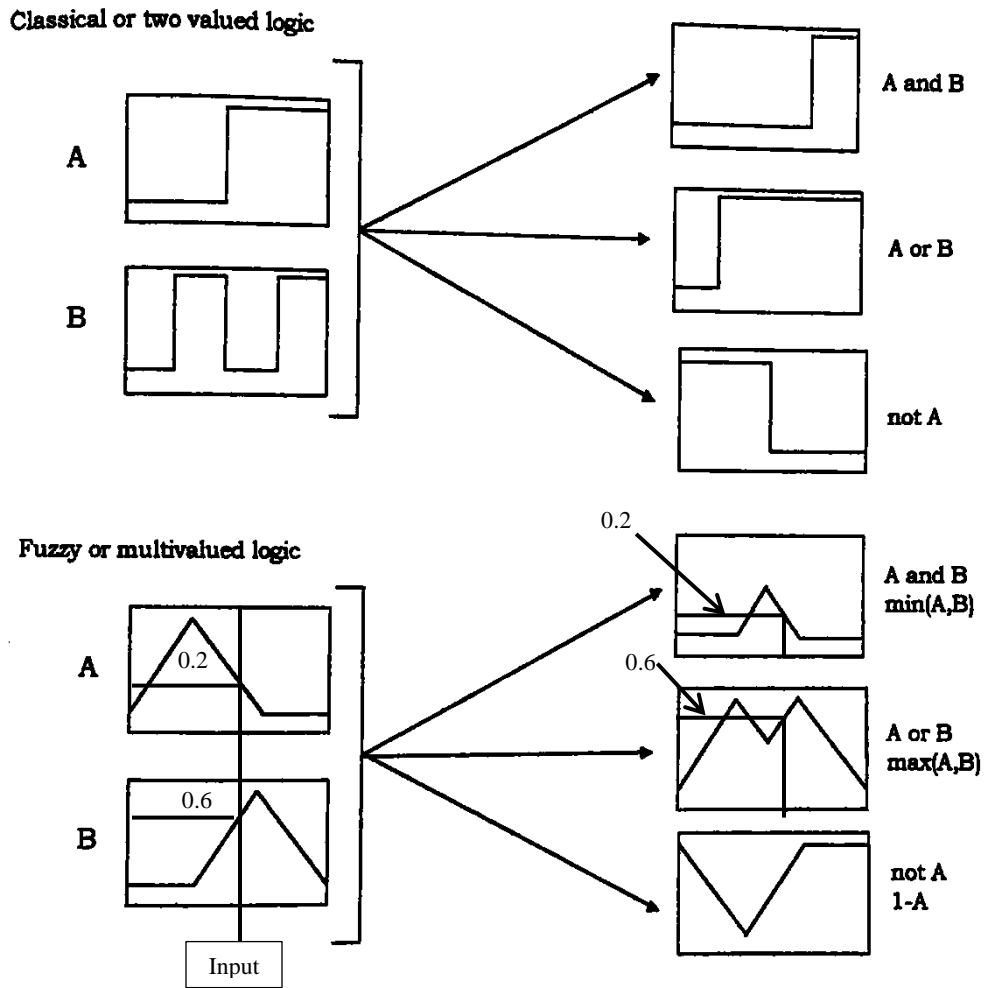


Figure 2.11 Logical Operators: Fuzzy Logic vs. Conventional Logic  
(Reproduced, with permission and modifications, from [18])

The FIS process, as followed in the MATLAB Fuzzy Logic Toolbox, has five parts or steps. An overview of an FIS is shown in Figure 2.12. The FIS shown has two inputs, one output and two rules. Each variable (inputs and output) has two membership functions each, say 'High' and 'Low':

Input 1: Figure 2.12a and 2.12b

Input 2: Figure 2.12c and 2.12d

Output: Figure 2.12e and 2.12f

The rules relating the inputs to the output are:

1. If Input 1 is 'Low' *OR* Input 2 is 'Low' then Output is 'Low'
2. If Input 1 is 'High' *OR* Input 2 is 'High' then Output is 'High'

The steps involved in the evaluation of the fuzzy inference system are explained below.

1. **Fuzzify the inputs:** Each of the inputs is assigned a degree of membership for each fuzzy set associated with that input. A fuzzy set is represented by a membership function. The input values are transformed into membership values between 0 and 1 based on the shape of the membership functions. Hence, Input 1 has a degree '0.2' for 'Low' (Figure 2.12a) and '0' for 'High' (Figure 2.12b). Input 2 has a degree '0' for 'Low' (Figure 2.12c) and '0.6' for 'High' (Figure 2.12d).

2. **Apply the fuzzy operator:** The fuzzy operator resolves the overall antecedent using connectives, if any, into a single number between 0 and 1. The FIS shown in Figure 2.12 uses the 'OR' operator. The maximum value of degree of membership from among the inputs is the value of the antecedent for the associated rule. Hence, Rule 1 resolves to '0.2' and Rule 2 resolves to '0.6' in Figure 2.12.

3. **Apply the implication operator:** The consequent for the fuzzy rule is evaluated. The consequent is the shape of an output variable membership function as defined by the implication operator. The antecedent statement is a mapping from a single input value to

a single truth-value, whereas, the consequent statement is the assignment of an entire fuzzy set to the output variable. The fuzzy set is truncated based on the degree of ‘truthfulness’ of the antecedent. If the antecedent is ‘true’ to a certain degree then consequent is also ‘true’ to the same degree. In Figure 2.12, Rule 1 sections off an area from ‘Low’ membership function of the output (Figure 2.12e) such that the highest degree of membership in that area is ‘0.2’ (Figure 2.12f). Similarly, Rule 2 sections off an area having ‘0.6’ as the highest membership degree for ‘High’ membership function i.e. Figure 2.12g becomes Figure 2.12h.

4. **Aggregate the outputs:** The fuzzy sets for each output variable are combined, i.e. the areas added (overlapped), to obtain a single aggregate fuzzy set for each output variable. This results in an aggregate membership function for each output. In Figure 2.12 the only output variable has the two sections from the two rules added to form the aggregate membership function (Figure 2.12i).

5. **Defuzzify the aggregate fuzzy set:** The defuzzification function reduces the output membership function into a single value for each output variable. There are different defuzzification methods such as centroid, bisector, largest of maximum, etc. Figure 2.12 shown the centroid method of defuzzification. The output value associated with the centroid of the area in Figure 2.12i is the defuzzified output.

In this work, two fuzzy inference systems use the ‘smallest of maximum’ method of defuzzification. This method is part of a group of three similar defuzzification methods:

- LOM: Largest of maximum
- SOM: Smallest of maximum

- MOM: Middle of maximum

All three methods assign the final defuzzified output value based on the maximum membership value of the aggregate membership function of the output. Figure 2.13 shows an example of an aggregate membership function. In the example, the maximum value for the degree of membership has a plateau and the three methods have distinct values. The defuzzified output for the SOM method is that number whose absolute value is the smallest from a range of output values for which the degree of membership is maximum. If the maximum value was a unique number then all three methods would have given the same value for the output.

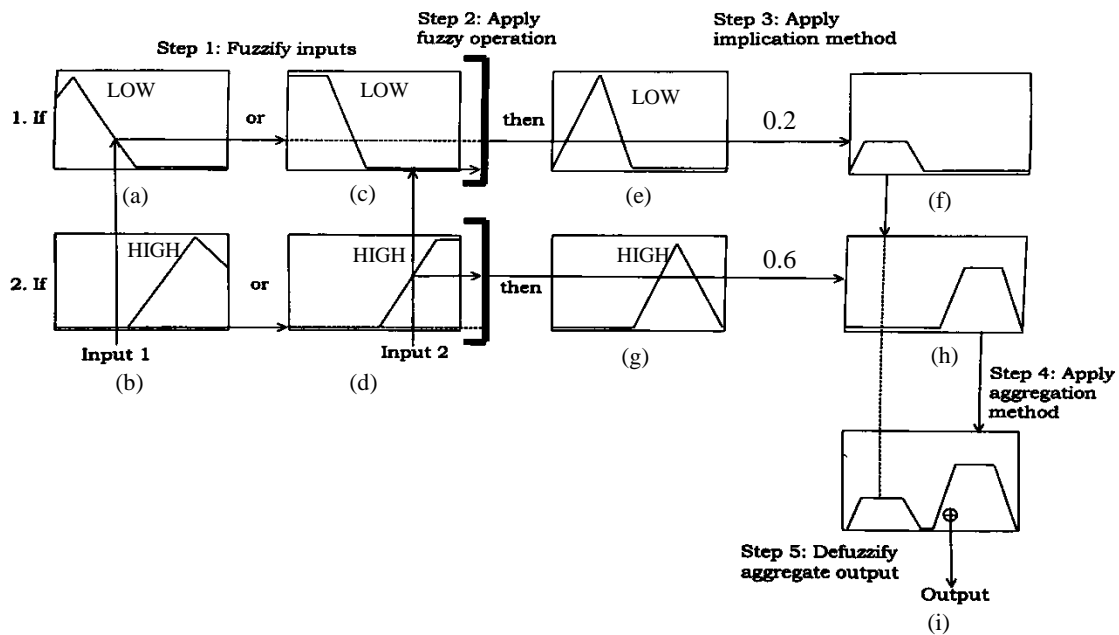


Figure 2.12 Overview of a Fuzzy Inference System  
(Reproduced, with permission and modifications, from [18])

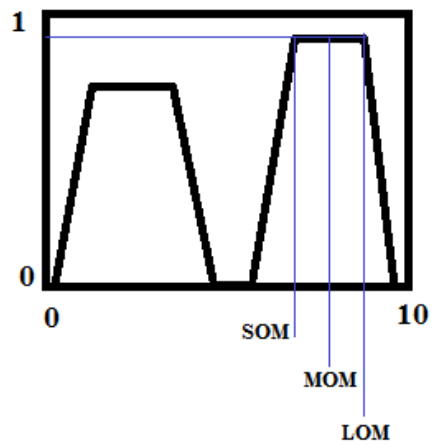


Figure 2.13 Defuzzification Methods



## Over-steer Controller: Overview and Modifications

The over-steer controller previously developed by Anderson <sup>[4,5]</sup> was incorporated with the newer under-steer modules to obtain a complete ESC system. The reader may refer to his work for a detailed working of the over-steer controller. A quick overview is provided here.

The OS controller uses steering wheel angle, lateral acceleration and yaw rate to detect over-steer. The vehicle response signals are passed through two low pass filters, one with a cut-off frequency of 0.5 Hz and another of 3.5 Hz to obtain two sets of vehicle dynamic traces. The 0.5 Hz filtered signals represent the 'ideal' behavior of the vehicle. The difference between the magnitudes of the two traces for steering wheel angle and lateral acceleration along with the absolute value of the yaw rate are sent to a Fuzzy Inference System (FIS) that computes an over-steer number between 0 and 10. Another FIS computes the possibility of over-steer based on the magnitude of the lateral acceleration and the speed of the vehicle. If the possibility of over-steer is greater than the threshold value of 4 then the over-steer number from the first FIS is passed on and actuation carried out.

The actuation of the brakes during an over-steer event is based on reducing the yaw acceleration of the vehicle. The actuator uses the yaw angle of the vehicle to decide which side of the vehicle is on the outside of the turn. It then actuates the brake on the outside front wheel to generate a counter-acting yaw moment that will correct any over-

steer tendency. The Over-steer Stability Control is imported with modifications into the new controller. The modifications made are explained next.

Firstly, the FIS that Anderson used to compute the possibility of instability in a vehicle has been changed. The original controller used lateral acceleration ( $A_y$ ) and longitudinal speed ( $V_x$ ) as inputs to the FIS. The basic idea of the FIS was to give a higher instability number when either  $A_y$  or  $V_x$  or both are high. This method works well if only over-steer is to be detected. However, at high speed and lateral acceleration a typical vehicle may over-steer or under-steer. Hence, this author has changed the inputs to absolute value of lateral acceleration and yaw acceleration. The fuzzy rules are essentially the same with only the range of values changed to make them compatible with the new inputs. The FIS will give a high possibility of instability if either the lateral acceleration or the yaw acceleration or both are high. A threshold block allows the over-steer number generated from the first FIS, 'Over-steer Indicating Fuzzy Logic,' to pass if the instability number is greater than 3. Values lower than 3 are typical for initial turn-in (very low Lateral Acceleration and high Yaw Acceleration), steady turning (very low Yaw Acceleration, moderate to high Lateral Acceleration) or straight-ahead driving (both inputs being low). The 'Over-steer Indicating Fuzzy Logic' remains the same as described in [4,5]. The modified FIS is discussed in detail in the Appendix D.

Apart from the OS Hold block developed by Anderson an additional block, 'Hold Time,' is introduced to keep track of the beginning and the end of over-steer events. An identical block is placed in the under-steer module. This function is explained in greater detail in the following chapter.

## CHAPTER 3

### ELECTRONIC STABILITY CONTROLLER

The Fuzzy Logic based ESC system has two key modules:

- Control Module
- Actuator Module

Each of these modules has subsystems for under-steer and over-steer attenuation. An overview of the controller can be found in the appendix. The control module has an additional subsystem, the decision module, which blends the control signals from the two controllers. The following sections detail the working of the under-steer modules.

#### Under-Steer Control Module

##### **Data Conditioning**

Before the signals can be processed to generate the under-steer number, data conditioning needs to be carried out (Figure 3.1). The lateral acceleration and steering wheel angle signals are passed through 0.5 Hz low pass filters. A cut-off frequency of 0.5 Hz is found to be appropriate for detecting under-steer, which is a low frequency event. Next, the absolute values of the filtered data are used to compute the instantaneous  $A_y$  gain. This is sent to the Under-Steer Computation block (Figure 3.2) where the control strategy is implemented.

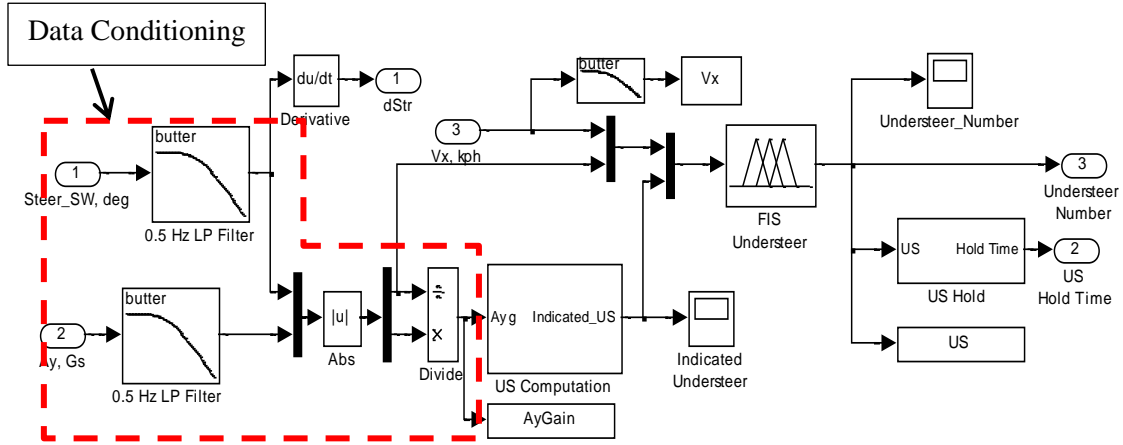


Figure 3.1 Under-steer Control Module

### Control Strategy

The control strategy contained in the Under-Steer Computation block can be split into two main sections:

- Identify the ‘drop’ in  $A_y$  gain
- Quantify the under-steer

The identification of the drop in  $A_y$  gain is fairly easy. When the derivative of the gain ( $d(A_y Gain)/dt$ ) becomes zero or negative, the value of gain at which the zero or negative value for  $d(A_y Gain)/dt$  is observed corresponds to the top of the  $A_y$  gain plot. This value is then assigned to be the peak value of gain from which the fractional drop is computed. In order to quantify the under-steer, the fractional drop as defined in Equation 3.1 and described in chapter 2 is computed.

$$\text{Fractional Drop at time } 't' = \frac{(\text{Gain at time } 't' - \text{Peak Gain})}{\text{Peak Gain}} \dots\dots\dots 3.1$$

When the gain value is decreasing the instantaneous gain will be lower than the peak gain and hence the value of the fractional drop will be negative. At the top of the drop the instantaneous value of gain and peak value of gain will be the same.

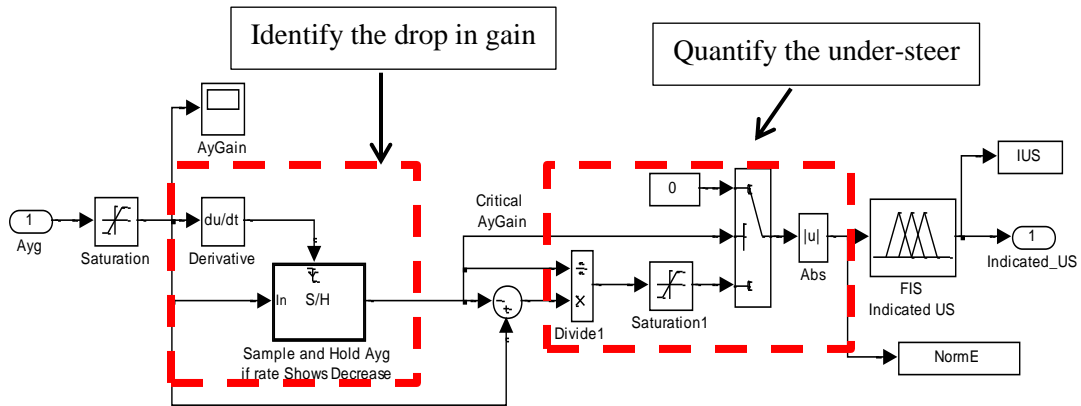


Figure 3.2a Under-Steer Computation Block

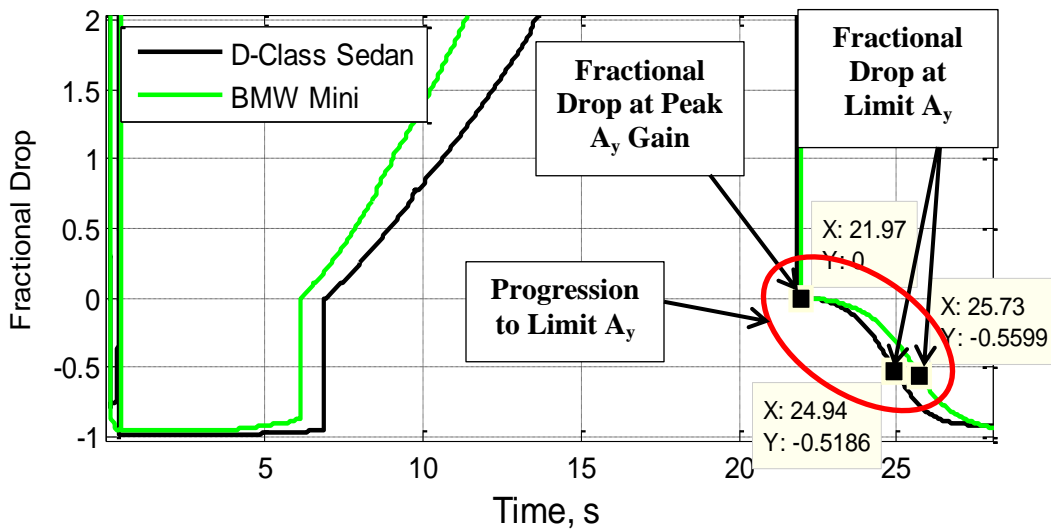


Figure 3.2b Fractional Drop: Two vehicles

Figure 2.9 (repeated here as Figure 3.2b for the convenience of the reader) also shows positive values for the fractional drop. These are computed when the lateral acceleration is increasing in sync with the steering input. Since these values do not indicate under-steer a saturation block with a ceiling value of 0 restricts positive values from being

transmitted. The sharp fall from positive values to zero observed in Figure 3.2b occurs as the ‘critical’ value is reset at the beginning of the drop.

During a direction change or at the beginning of turn-in, the steer input is very close to zero. The gain value as a result is high and then falls back to within the typical range of values for the given vehicle-tire-road combination as the vehicle begins to respond. This ‘fall’ can be misdiagnosed as under-steer. To prevent this from happening, a threshold block restricts signal flow if the peak value of  $A_y$  gain is significantly higher than the typical values. The absolute value of the output of the threshold block is the control signal for the fuzzy inference systems discussed next.

### **Fuzzy Inference Systems**

There are two FISs used in the control module:

- Indicated Under-Steer
- Under-Steer

An overview of the FIS ‘Indicated Under-steer’ is shown in Figure 3.3. It is a single input, single output FIS with one rule:

If NormE (Fractional Drop) is high then IUS is high

This means that the degree of membership (‘truth’ value) of the output will be the same as the degree of membership of the input. The working of the FIS is explained in detail in Appendix D. This FIS effectively works like a proportional controller, transforming values of ‘NormE’ (fractional drop) between 0 and 1 to ‘IUS’ between 0

and 10. This transformation is carried out primarily to maintain congruence between the under-steer and over-steer controllers because the OS number is between 0 and 10.

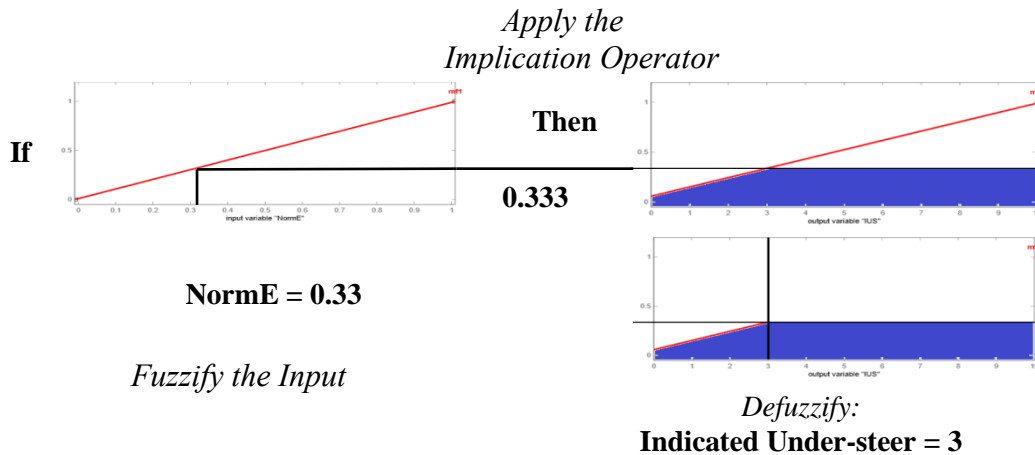


Figure 3.3 Overview: FIS 'Indicated Under-steer'

However, the FIS has another important function. When a vehicle is traveling in a straight line the steering wheel angle and the lateral acceleration are zero. The ratio of two zero values will generate an indeterminate number. In such a situation the output of the FIS will be the average of the output range i.e. '5'. The FIS thus filters out unusable indeterminate numbers and gives a usable real number as an output for all situations. The defuzzification method used here is 'smallest of maximum'.



Misdiagnoses of under-steer as well as unnecessary actuation are filtered by the next FIS 'Under-steer'. An overview of the FIS 'Under-steer' is shown in Figure 3.4. It has three inputs:

- Vehicle Velocity in kph
- Steering Wheel Angle in degrees
- IUS

This FIS also has only one rule:

If  $V_x$  is *high* 'and' SWA is *high* 'and' IUS is *high* then US is *high*

The use of AND operator means that the input with the lowest degree of membership will dominate the output value. Hence, if either the steering wheel angle or vehicle velocity is low, the controller will not send a control signal to the actuator. This eliminates false positives in two driving situations:

- Parking lot driving (Low  $V_x$ ): Unnecessary Control
- Straight line driving (Low SWA): Impossible to Under-steer

The advantage of fuzzy logic is that a clear definition of 'low' for  $V_x$  and SWA is not necessary.

The shape of the output membership function is chosen so as to increase sensitivity during the initial stages of under-steer. It was found that this improves the performance of the controller. This FIS also uses the 'smallest of maximum' method of defuzzification (i.e. the smallest output value associated with the maximum degree of membership in the aggregate membership function). A detailed procedure for the evaluation of the FIS is

provided in Appendix D. The computation of the under-steer number is complete at this stage.

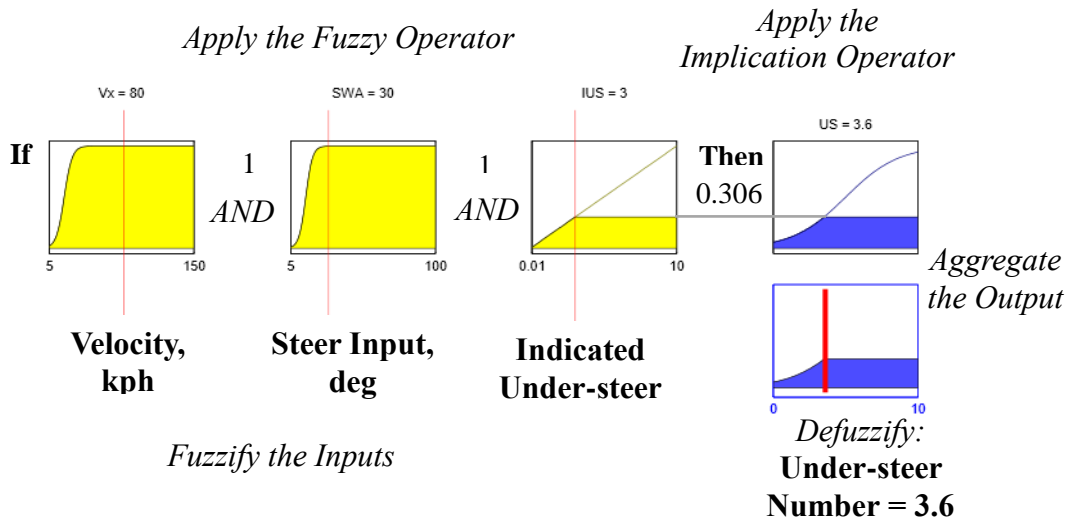


Figure 3.4 Overview: FIS 'Under-Steer'

## Under-Steer Actuator Module

The final under-steer number along with the under-steer hold time is sent to the actuator module. The other inputs to the actuator are:

- Steering Wheel Angle, deg
- Steering Rate, deg/s
- Master Cylinder Pressure, MPa
- Vehicle Velocity, kph
- Yaw Rate, deg/s
- Throttle Input from Driver as a fraction of full throttle
- Yaw Angle, deg

This section details the working of the under-steer actuator. The actuator controls five variables:

- Brake Line Pressure for the four wheels (4)
- Engine Throttle (1)

The throttle control is simple. When under-steer is detected the engine throttle is reduced to zero. Any throttle applied by the driver is over-ridden to avoid increasing the vehicle speed. This results in the front tires having a lower longitudinal slip as well as a load transfer onto the front tires thus increasing the lateral force capability of the front tires and helping the vehicle to ‘turn-in’.

The brake force distribution for the individual wheels is split into three distinct stages during an under-steer event. The stages depend on the extent of under-steer in the vehicle

and the amount of effort needed to contain the under-steer. For all three stages any braking requested by the driver is overridden till the vehicle is stabilized. The computation of the individual brake pressures is done by an embedded MATLAB script.

In the first stage, for an under-steer number up to '3', the braking distribution is commanded by a fuzzy inference system. This FIS is used to generate values for total brake pressure and the proportion of front axle braking pressure with respect to the rear axle. A detailed working is explained in the appendix. The inputs to the FIS are the under-steer number obtained above and the absolute lateral acceleration in Gs. The rules of the FIS are set up such that:

1. Increasing under-steer will reduce front axle braking
2. Higher  $A_y$  will result in greater braking pressure

The first requirement is based on the fact that under-steer occurs because of the lateral force saturation of the front tires. Reducing the front axle braking ensures the tires at the front continue to function within the friction limit and retain steering capability. The proportion of front axle brake pressure drops from '1.77' to '0.126' times the rear axle brake pressure.

The second set of rules regulates the total braking pressure in the system with respect to lateral acceleration. The lateral acceleration at which under-steer is detected indicates the type of surface the vehicle is on. Since tires on a low friction surface will have smaller friction circles the total braking force that can be applied without causing instability will be less than that for a high friction surface.

The purpose of the high initial braking force is to slow the vehicle down as far as possible while the front axle is well below its saturation limit. This will reduce the required lateral acceleration and hence the lateral force to be generated for the given trajectory. Also, during this stage the inside wheels have 20% higher braking pressure than the outside wheels. The differential braking generates a yaw moment necessary to keep the vehicle turning. In most cases, the first stage of braking is sufficient to contain the under-steer.

The second stage occurs if the under-steer number rises above '3'. With the braking at the front axle reduced, the ratio of brake pressure at the inside wheels to the outside wheels is increased from '1.2' to '3.5' as the under-steer number increases from '3' to '5'. The braking strategy gradually changes to "heavy braking at the inside rear wheel" with a small braking force at the front axle.

The last stage is for situations when there is extreme under-steer, i.e.  $US > 5$  (beyond the steady state handling limit). The braking at the front axle is cut-off while the brake pressure at the inside rear wheel is maintained at '3.5' times the pressure at the outside wheel. For an under-steer number greater than '5', strong inside rear wheel braking is the best chance of getting the vehicle to rotate. At this stage the front tires have almost completely saturated and the vehicle wants to move along the tangent to the required trajectory.

The brake control also has to decide the side of the vehicle that needs higher braking. To do this the intent of the driver is examined in the form of the steering wheel angle and rate. A positive steering wheel angle with a positive rate indicates intent to turn left. In

this case, the left side wheels are the inside wheels. Once the driver begins to reduce his input, i.e. the steering angle is positive (left) but the steering rate is negative the outside front wheel (in this case the right front) gets 20% higher braking pressure till the vehicle straightens out or the driver initiates a right turn. This is done to restrict overshoot in the yaw rate and the side slip angle of the vehicle.

A plot of the two parameters, front brake proportion and inside to outside wheel brake ratio, is shown against under-steer number in Figure 3.5. The product of the two parameters results in the brake pressure at the front-inside wheel, shown by the red curve. The green line at '1' shows the nominal pressure.

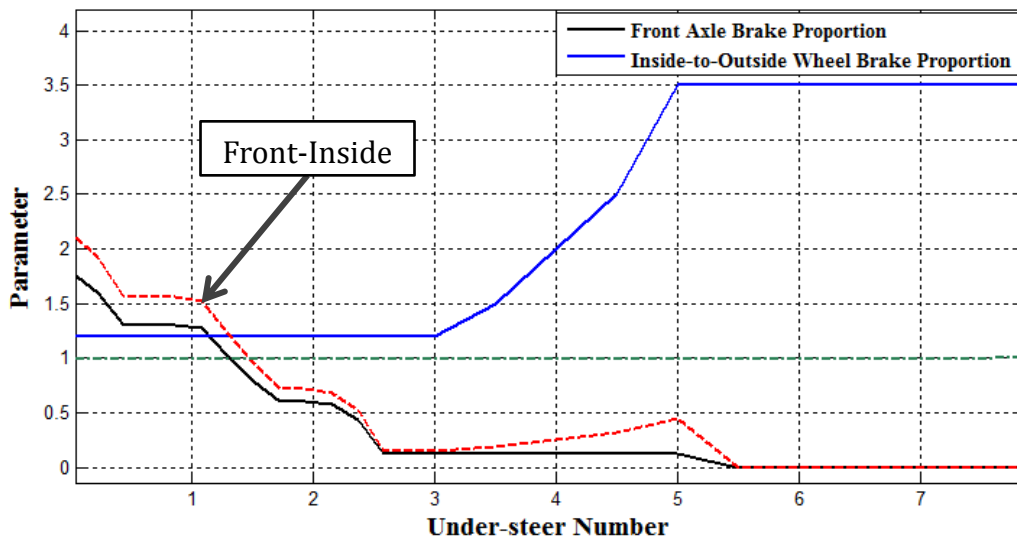


Figure 3.5 Brake Distribution Parameters

## The Combined ESC

Anderson mentioned in his work <sup>[4]</sup> that the application of brakes during an over-steer event will result in the subsequent time step to appear as an under-steer event. The reverse is also found to be true. In order to blend the two controllers effectively the actuator-induced control signals need to be eliminated. A decision module plays an important role at this stage to separate the actual under-steer/over-steer from the actuator-induced under-steer/over-steer.

Along with the over-steer and under-steer numbers a hold time for each block is also sent to the decision module. The hold time, for each block, is reset to zero every time the associated number, US or OS, crosses the zero line. In other words the hold time keeps track of the start and end of each under-steer and over-steer event.

BMW Mini: Braking-in-Turn  
 $\mu = 0.5$  (wet asphalt) at 95 kph

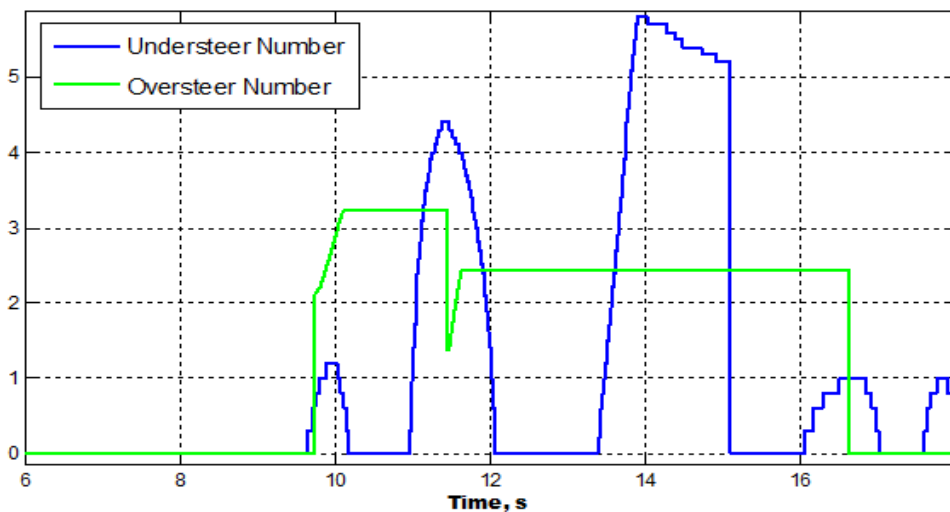
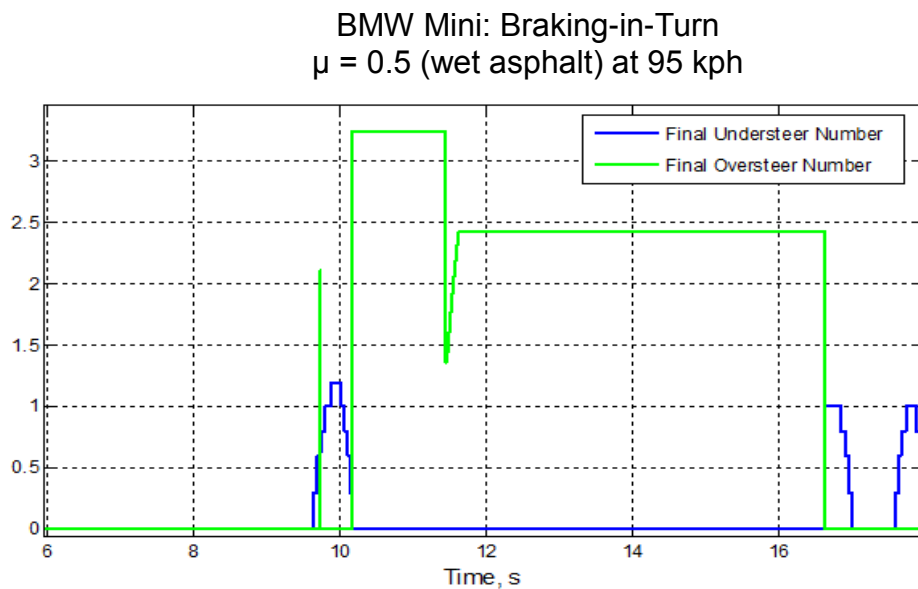


Figure 3.6 Input to the Decision Module



Shown in Figure 3.6 are the input signals to the decision module. At approximately 9.5 s the under-steer module detects under-steer and send a signal to actuate the brakes. The resulting increase in yaw rate makes the over-steer module generate an over-steer signal. However, because the under-steer number was generated before the over-steer number, the value of the under-steer hold time will be larger than the over-steer hold time. So, the decision module will suppress the over-steer signal till the under-steer event is complete. The same occurs when under-steer is detected after the start of the over-steer event. The output of the decision module is shown in Figure 3.7. A large period of over-steer indication is observed. This is due to the presence of a hold block within the over-steer module as designed by Anderson <sup>[4,5]</sup>. This block holds the value of the over-steer number for up to 5 seconds after the end of the over-steer event because over-steer is more critical and must be avoided. The associated MATLAB file is placed in Appendix C.



**Figure 3.7 Output of the Decision Module**

Unlike the over-steer module, the under-steer module overrides only the line pressure in the braking system. This is done to remove the ABS from the control loop during ESC intervention but allows it to function normally during straight line braking. The over-steer module, on the other hand, computes the necessary brake cylinder pressure and is therefore added directly to the final chamber pressure. A schematic diagram of the braking system with the intervention points is shown in Figure 3.8. The final brake chamber pressure along with the throttle control signal is sent to the vehicle model.

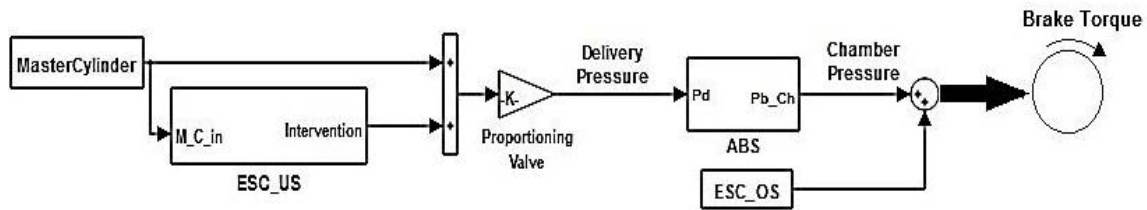


Figure 3.8 Schematic Diagram for the Braking System

The vehicle models used to test the controller are multi-degree of freedom models in CarSim. Simulink and CarSim interact in real-time and the simulation runs are based in the MATLAB workspace. The controller samples data at 100 Hz to ensure smooth transitions between under-steer and over-steer, if necessary. The input and output control signals are listed in Table 3.1.

**Table 3.1 CarSim Import and Export Parameters**

	<b>Variable</b>	<b>Symbol</b>	<b>Unit</b>
<b>Imported from CarSim</b>	Steering Wheel Angle	Steer_SW	deg
	Lateral Acceleration	$A_y$	Gs
	Yaw Rate	$AV_z$	deg/s
	Vehicle Velocity	$V_x$	kph
	Master Cylinder Pressure	Pb_MC	MPa
	Driver Throttle	Th_Itl	-
<b>Exported to CarSim</b>	Front Left Brake Pressure	FL	MPa
	Front Right Brake Pressure	FR	MPa
	Rear Left Brake Pressure	RL	MPa
	Rear Right Brake Pressure	RR	MPa
	Engine Throttle	Eng_Th	-

## CHAPTER 4

### RESULTS

The primary advantage of fuzzy logic is its inherent robustness. The controller described above is designed to be robust to changes in vehicle type, road conditions, tire wear, etc. To demonstrate the robustness a number of cases with different conditions (vehicles, road conditions, etc.) were simulated. Table 4.1 lists the cases that will be presented in this work.

Table 4.1 Case Studies

<b>Vehicle</b>	<b>Configuration</b>	<b>Maneuver</b>	<b>Tire-to-Road Friction Co-efficient</b>
<b>BMW Mini</b>	Nominal	Braking-in-Turn (BIT)	$\mu = 0.5$
<b>BMW Mini</b>	Nominal	Double Lane Change (DLC)	$\mu = 0.85$
<b>BMW Mini</b>	Nominal	BIT	$\mu = 0.2$
<b>BMW Mini</b>	Gross Vehicle Weight	BIT	$\mu = 0.5$
<b>BMW Mini</b>	Degraded Front Tires	BIT	$\mu = 0.85$
<b>D-Class Sedan</b>	Nominal	BIT	$\mu = 0.5$
<b>D-Class Sedan</b>	Nominal	BIT	$\mu = 0.85$
<b>E-Class SUV</b>	Nominal	BIT	$\mu = 0.5$

## Vehicle Models

The primary vehicle model used is the BMW Mini. This is the same vehicle model used by Anderson and was extensively validated by test results in the laboratory and on the track <sup>[24]</sup>. Three configurations for the model are:

- Nominal: Curb + Driver with original equipment tires
- Degraded Front Tires: 25% reduction in lateral force capability
- Gross Vehicle Weight: Maximum number of passengers + Cargo

In addition, some CarSim internal vehicle models were also used. All vehicle and tire data can be found in the Appendices A and B.

## Test Maneuvers

### **Braking-in-Turn**

In order to verify the performance of the under-steer controller the author developed a test maneuver that simulates a likely limit under-steer situation. The maneuver needed to be independently developed because of the lack of any regulated test maneuver to establish performance criterion for limit under-steer <sup>[25,26]</sup>.

The maneuver, braking-in-turn (BIT), simulates a situation most likely to result in limit under-steer. Often drivers enter a turn a little too fast and need to brake sharply to avoid running off the road. This can be particularly hazardous on low-friction surfaces,

such as wet or icy roads. Often, braking initiated by the driver only worsens the situation because most braking systems are programmed to brake the front wheels by a larger proportion. This further reduces the lateral force capability of the front axle.

The maneuver is simulated as described below:

1. Drive along a straight 200 m approach road. The lane width is 4 m, typical of a highway lane, and the driver tries to maintain the vehicle at the center of the lane. The distance is sufficient for the vehicle to attain constant speed.
2. At the end of 200 m, the vehicle enters an 180°, 500 ft. radius turn while maintaining constant speed.
3. If the lateral deviation of the vehicle is more than 1 m to the outside of the turn then the driver removes throttle input and applies a constant braking force of 3 MPa, unless otherwise specified.
4. The driver attempts to return to the center of the lane and continues to apply braking pressure till the lateral deviation is below 1 m.

A vehicle with a lateral deviation larger than 2 m is considered to fail the maneuver.

Figure 4.1 shows a BMW mini executing the same maneuver at two speeds. It can be seen that the vehicle travelling at 95 kph (green curve) fails the maneuver because its lateral deviation is greater than 2 m boundary highlighted by the blue dashed line. The maneuver is simulated for different tire-to-ground friction coefficients and speeds (Table 4.1).

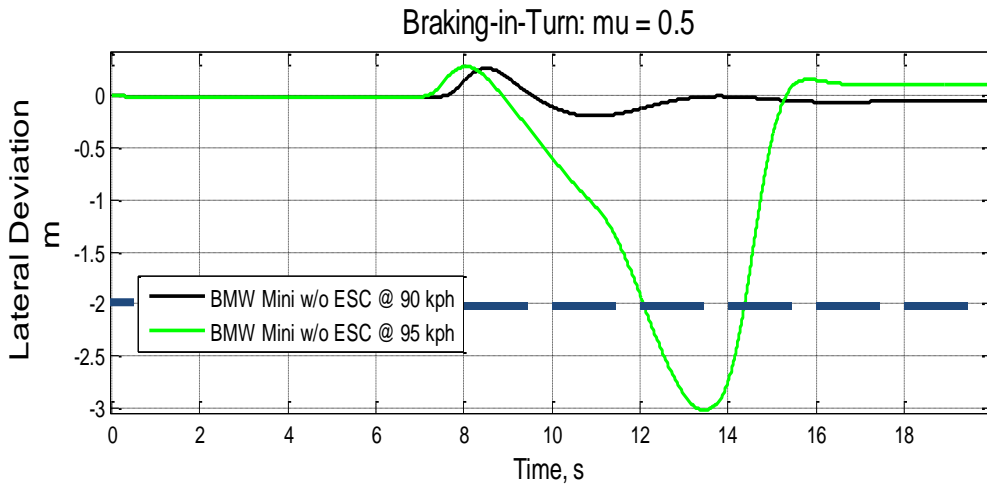


Figure 4.1 Lateral Deviation: BMW Mini at two speeds

### Double Lane Change

A double lane change maneuver as detailed in ISO 3888 is used to test the over-steer module of the controller. This is a standard procedure. It is used to imitate a sudden obstacle avoidance maneuver. Figure 4.2 shows the target path of the vehicle with the position of the cones shown by the yellow dots.

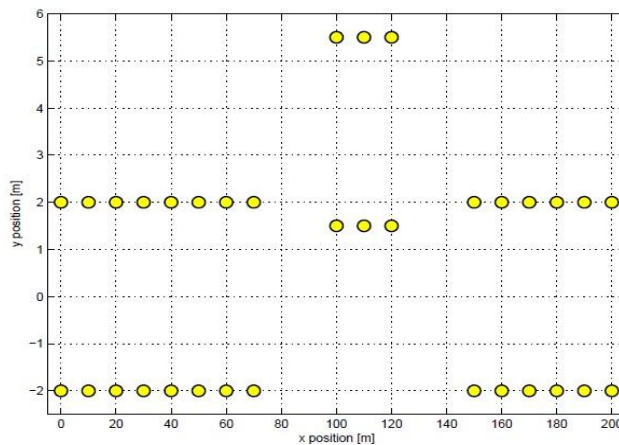


Figure 4.2 ISO 3888 Double Lane Change

## Test Configurations

In this work, up to four test configurations are simulated for each case. The configurations vary with the presence (or absence) of electronic stability control and the type of ESC used. The four configurations used are:

1. **ESC OFF:** As the name suggests, this configuration will not have any electronic aid to improve the road holding capability of the vehicle. This is the base configuration over which any improvements are measured. All the cases studied have this test configuration.

2. **Fuzzy C-ESC:** This is the combined ESC developed in this work. It uses both the over- and under-steer control modules to control the vehicle. This configuration is of primary interest in this work and is simulated for all cases.

3. **Fuzzy OSC:** This is the fuzzy logic based over-steer control developed by Anderson <sup>[4,5]</sup>. The control logic is unchanged from that developed previously and has been used here with permission from the original author. This configuration is simulated for cases 1 and 2.

4. **CarSim ESC:** CarSim has an internal parametric ESC that is used to represent a conventional model-based ESC. The parameters are based in CarSim and have not been modified by the author. The internal CarSim ESC strategy was used because of the difficulty in obtaining authentic data for a commercially available ESC. The details of the ESC are placed in the appendix.



## Case Studies

### Case 1: Nominal BMW Mini, Braking-in-Turn, $\mu = 0.5$ (Wet Asphalt)

The first case is the simulation of a nominal BMW Mini executing the Braking-in-Turn maneuver at **98 kph** on a low friction surface like wet asphalt. All four test configurations are simulated for this case.

Figure 4.3 shows the lateral deviation for the four cases. It is evident that the Fuzzy C-ESC offers significant improvement over the vehicle without any ESC. It is also the only configuration to not fail the maneuver.

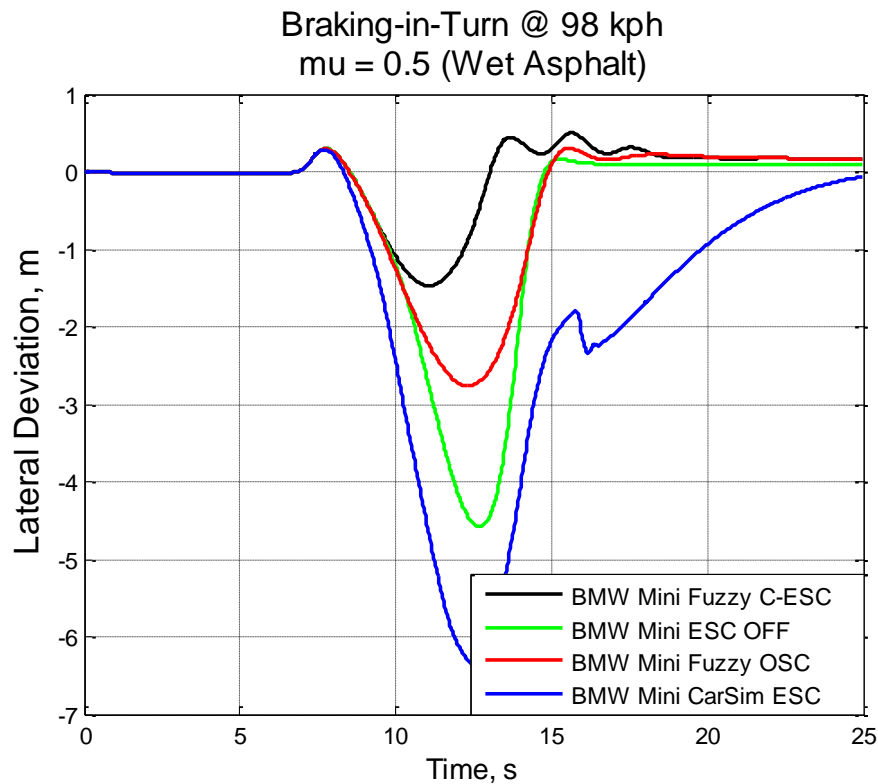


Figure 4.3 Lateral Deviation: Case 1

The vehicle with Fuzzy C-ESC successfully completes the maneuver without any extra effort from the driver. The peak steering input is less than 50 degrees, which is less than a third of that required for the vehicle without ESC (Figure 4.4). The vehicle returns to the center of the lane without a large increase in either the vehicle yaw rate or side slip angle ( $\beta$ ). Excessive increase in side slip angle is a major problem in systems using purely yaw moment control. This can be seen in the plots for the vehicle equipped with the CarSim ESC. There is a large increase in yaw rate accompanied by an increase in vehicle side slip angle. In effect, the CarSim ESC equipped vehicle ‘floats’ off the road with the driver unable to control the vehicle. This occurs due to excessive rear wheel braking (Figure 4.5). Also shown are results for a vehicle equipped with only fuzzy over-steer control (Fuzzy OS). It appears to control under-steer in the vehicle. However, the lateral deviation is too large and the vehicle fails the maneuver. The reason for this becomes apparent when we look at the brake torque plot. The Fuzzy OSC begins actuating the outside front wheel brake from 7.5s. This slows the vehicle down and the vehicle should be able to successfully complete the maneuver. However, only the outside front wheel brake is actuated and results in the vehicle resisting the turn. The vehicle slows down but does not turn-in as efficiently. However, the performance is better than that of the CarSim ESC equipped vehicle. The brake torque applied by the Fuzzy OSC is much lower and does not result in the vehicle floating off the road.

The Fuzzy controllers are also the least intrusive. Figure 4.6 shows a plot of vehicle speed versus time. The final speeds for the vehicles equipped with Fuzzy controllers are much higher than for the other two cases.

Braking-in-Turn @ 98 kph  
 $\mu = 0.5$  (Wet Asphalt)

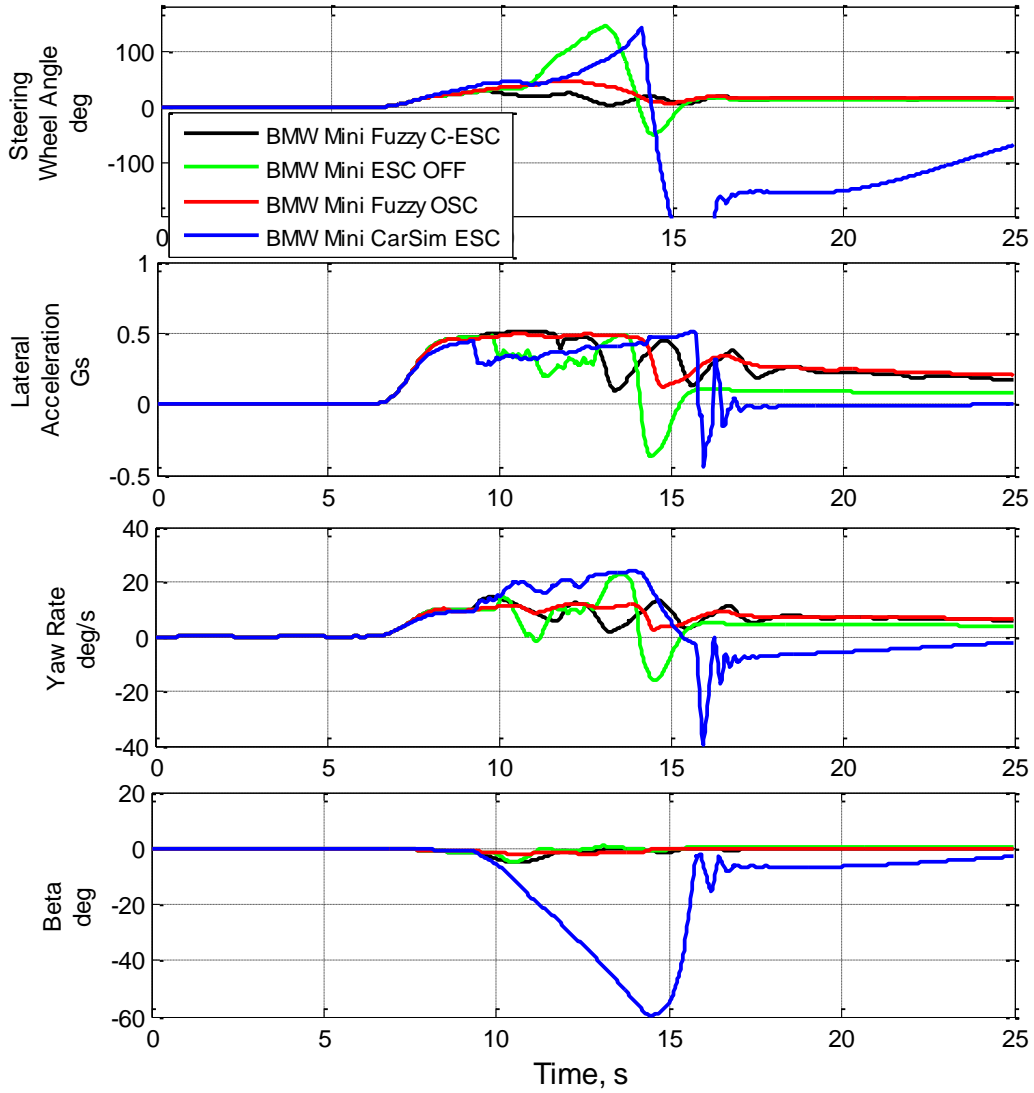
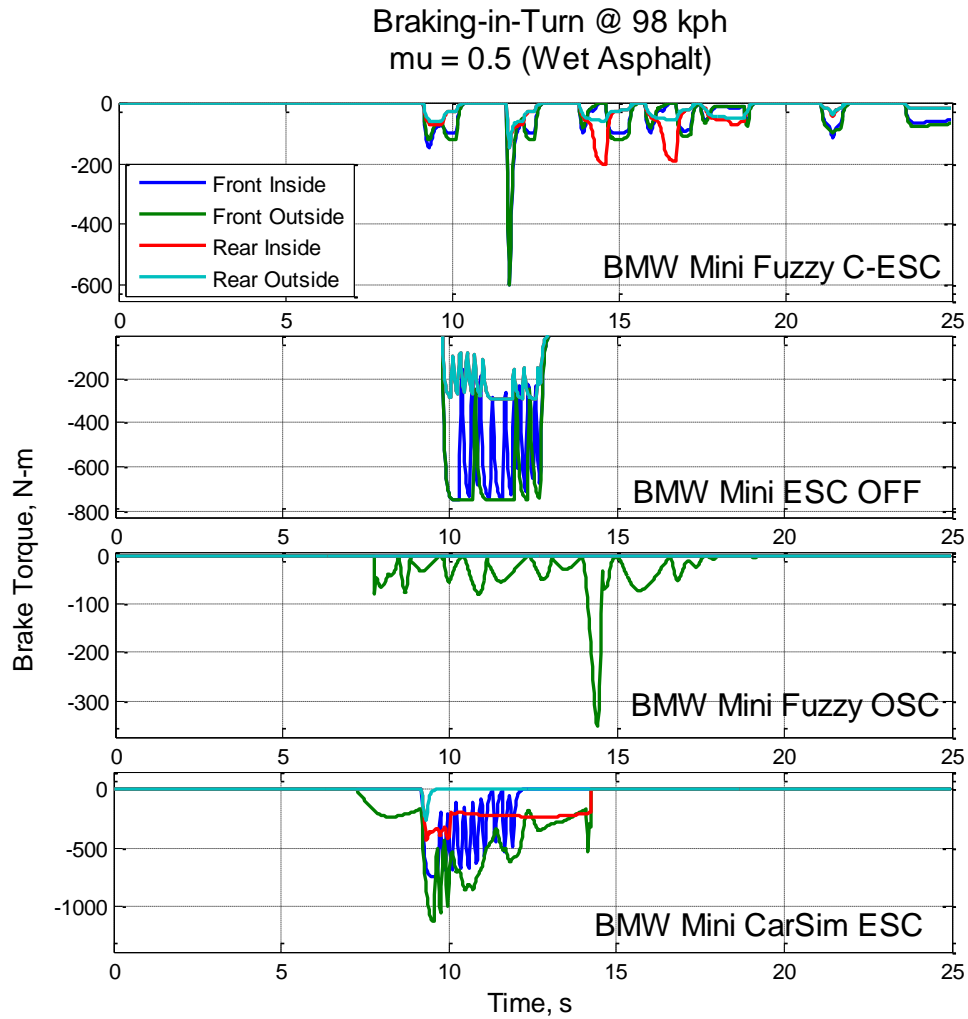


Figure 4.4 Vehicle Response: Case 1



**Figure 4.5 Brake Torque: Case 1**

Unlike the ESC OFF and the CarSim ESC cases, the Fuzzy C-ESC is able to maximize the grip of the vehicle by keeping the lateral forces near their peak value and only gradually allowing them to be reduced as the vehicle slows down (Figure 4.7). The rear axle lateral force is manipulated to ensure that the front axle lateral force is maintained at its peak value. Table 4.2 lists the maximum safe speeds (lateral deviation < 2 m) for the three configurations.

**Table 4.2 Maximum Safe Speed: Case 1**

	<b>Maximum Safe Speed (kph)</b>
<b>ESC OFF</b>	94
<b>Fuzzy C-ESC</b>	99.5
<b>CarSim ESC</b>	87

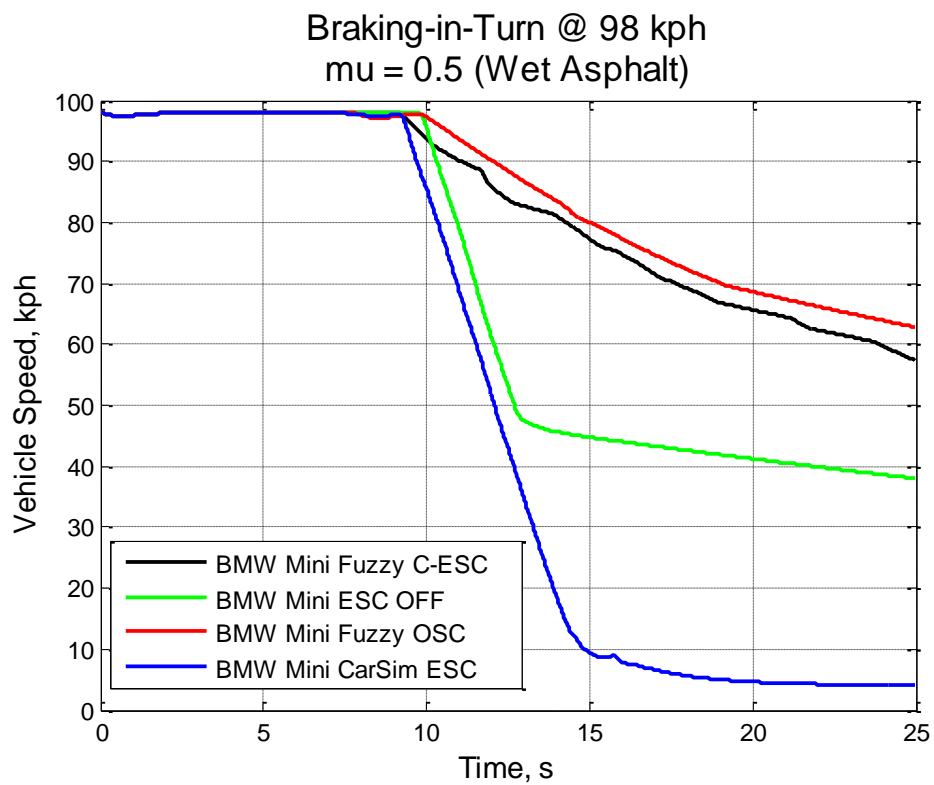


**Figure 4.6 Vehicle Speed: Case 1**

Braking-in-Turn @ 98 kph  
 $\mu = 0.5$  (Wet Asphalt)

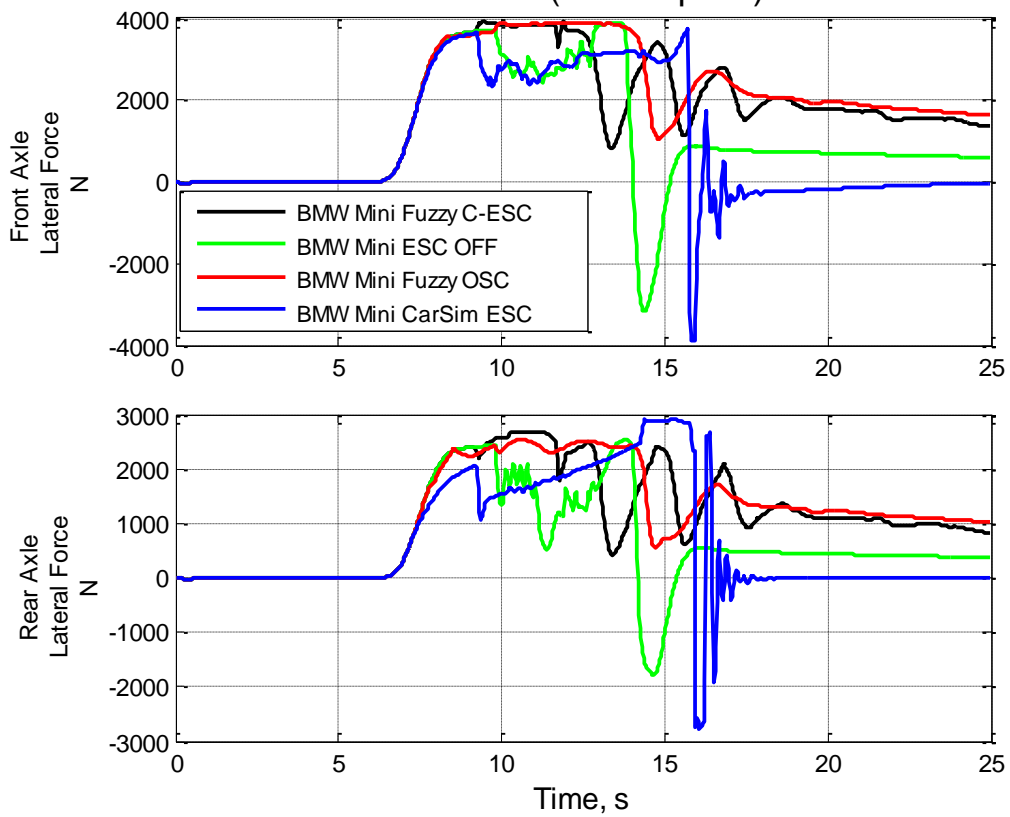


Figure 4.7 Lateral Force per Axle: Case 1

## Case 2: Nominal BMW Mini, Double Lane Change, $\mu = 0.85$ (Dry Asphalt)

This case is identical to the first case presented by Anderson <sup>[4,5]</sup>. It is included here to compare the performance of the complete Fuzzy C-ESC against the existing over-steer controller (Fuzzy OSC) in an over-steer situation. The Nominal Mini executes the Double Lane Change maneuver at **185 kph**. The CarSim driver model was used in all simulations in this project. The performance of this driver is extremely good and has been said by some to emulate that of a “Formula 1 driver on steroids”. It is questionable whether the performance of an actual driver would be this good. The performance of the vehicle with the internal CarSim ESC as well as without any ESC system is also included in the plots.

Figure 4.8 shows the trajectories for the four cases. All vehicles equipped with any kind of ESC system are able to prevent spin-out. However, there are subtle differences in their performance. It can be observed that the vehicle with the CarSim ESC lacks the early stage responsiveness and hits at least one cone during the first lane change. Also, the CarSim ESC equipped vehicle takes much longer to return to the original lane. This is due to the excessive brake actuation by the controller. The CarSim ESC actuates the brakes at all four wheels (Figure 4.9), two at a time, to control the vehicle trajectory. Although this reduces the vehicle side-slip, it makes the vehicle response sluggish and the driver has to work harder to get the vehicle to return to its original lane.

The two Fuzzy Logic based systems have very similar performances. The newer system (Fuzzy C-ESC) has slightly larger overshoots. This is due to the shorter pulses in brake actuation by the Fuzzy C-ESC (Figure 4.9). Unlike the Fuzzy OSC, the new system has to eliminate possible under-steer before applying the brakes. This does not lead to a

large degradation in performance or exceptionally higher braking effort. In fact, the peak braking force for the Fuzzy C-ESC is slightly lower. The brakes are used more efficiently. The vehicle dynamics plots for the two fuzzy controllers are also very similar (Figure 4.10). The Fuzzy C-ESC has marginally larger yaw rate and side-slip angle. However, this is compensated by the extended peaks in lateral acceleration and lateral forces. The excessive braking for the CarSim ESC equipped vehicle results in the driver working a lot harder and can be seen in the larger steering input required (Figure 4.10). The Fuzzy C-ESC retains the responsiveness of the vehicle without the driver losing control of the vehicle.

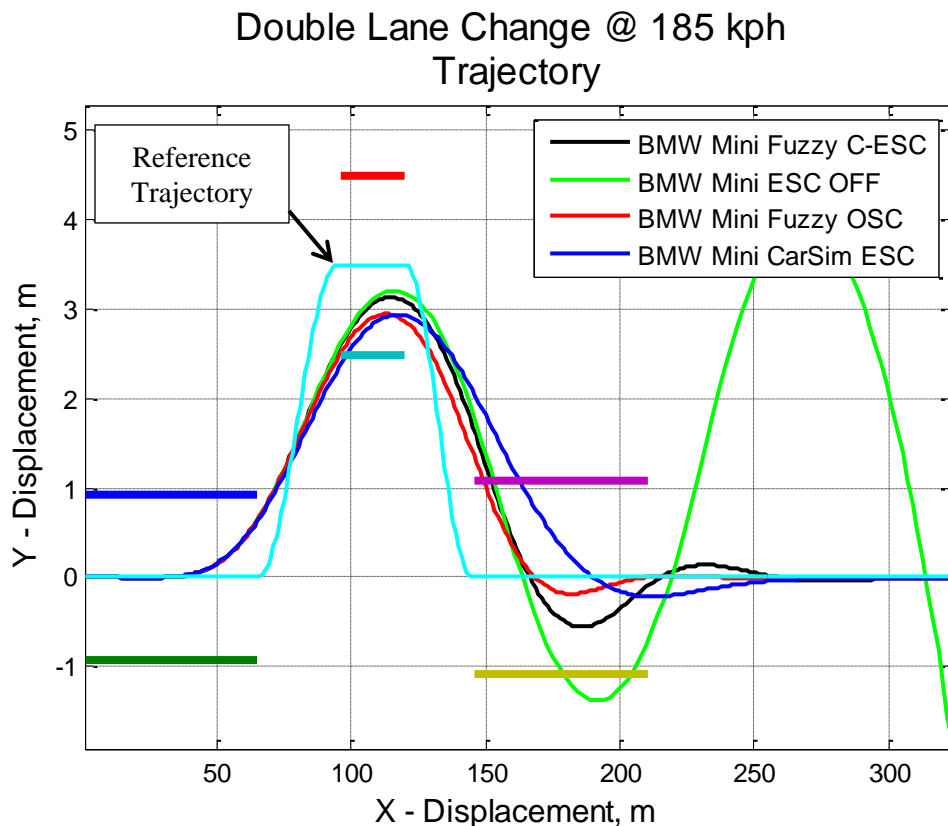


Figure 4.8 Trajectory: Case 2



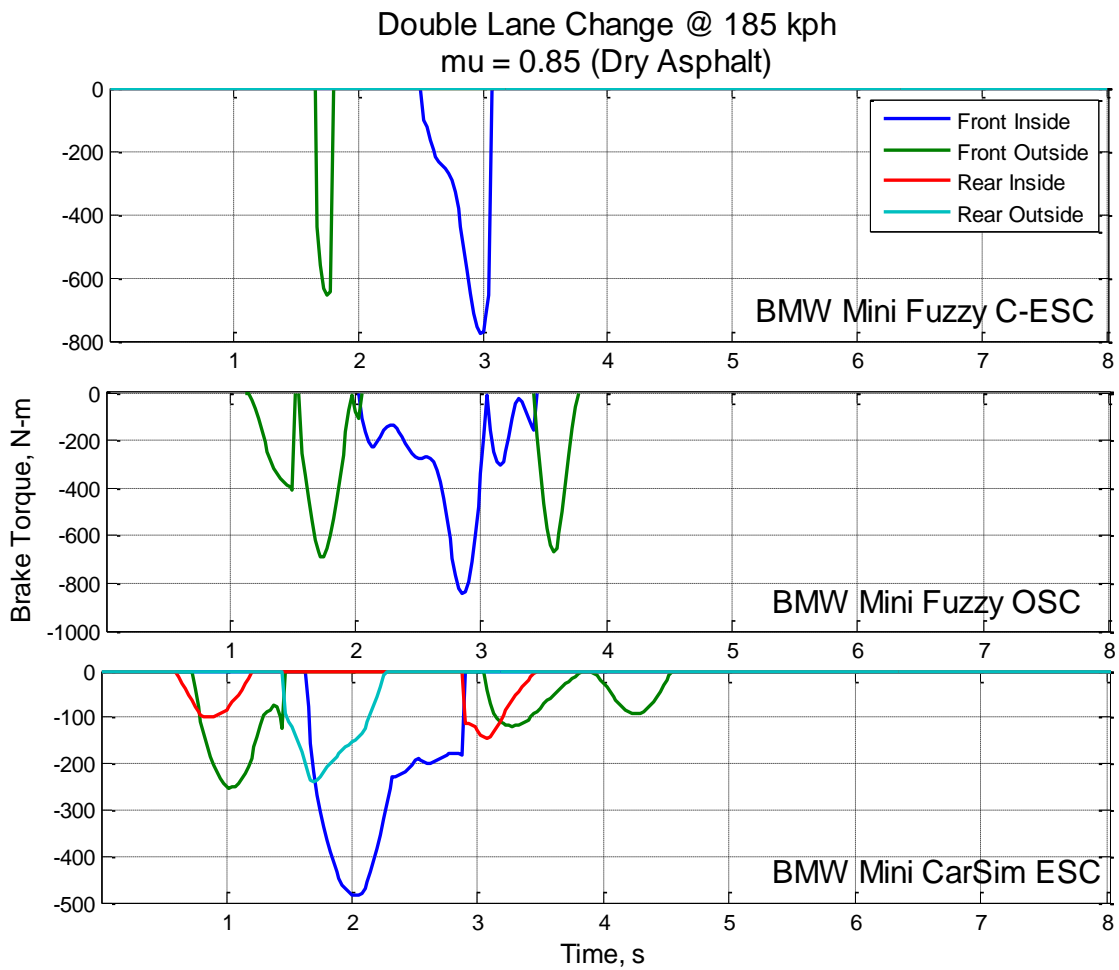


Figure 4.9 Brake Torque: Case 2

Double Lane Change @ 185 kph  
 $\mu = 0.85$  (Dry Asphalt)

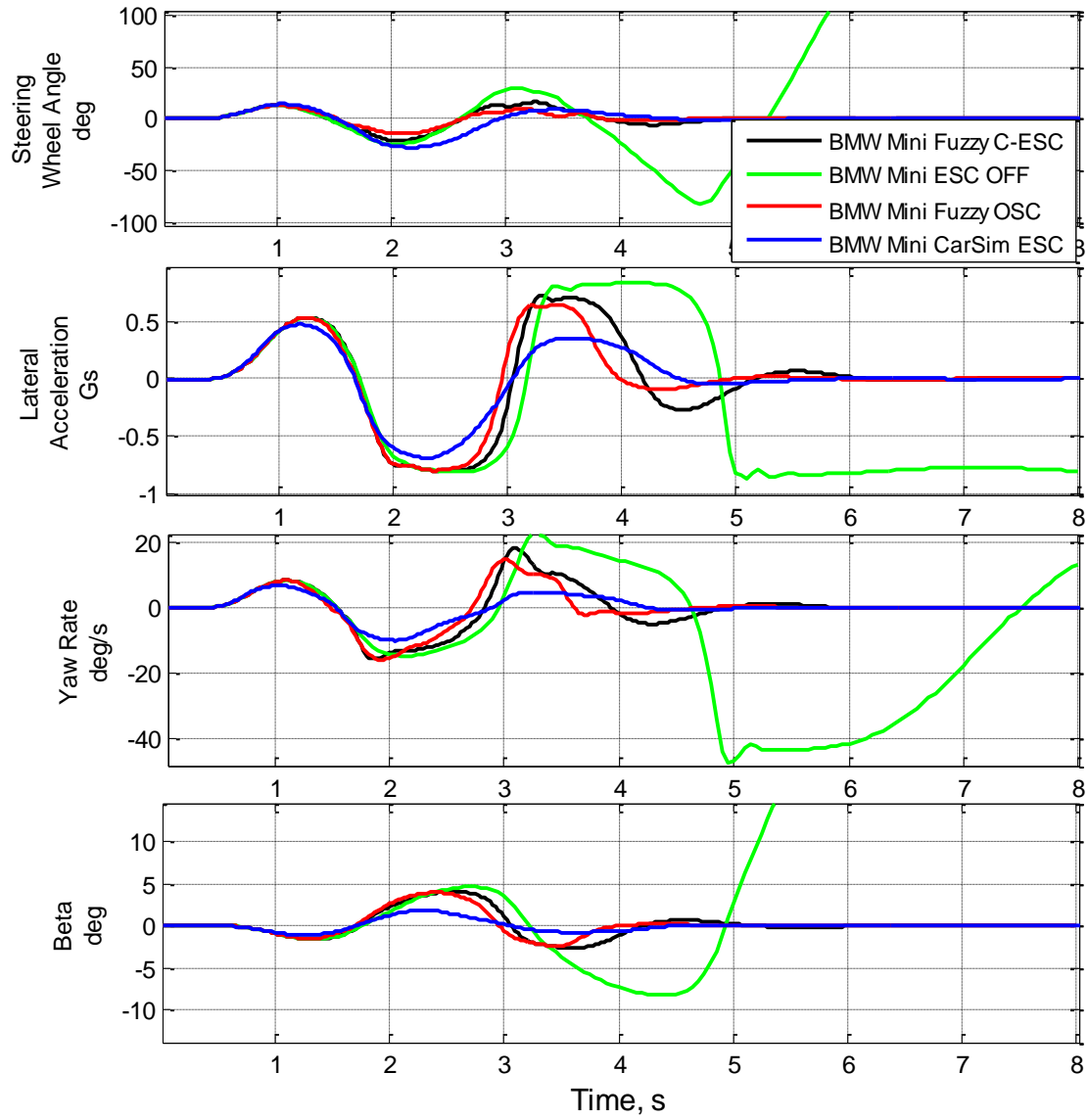
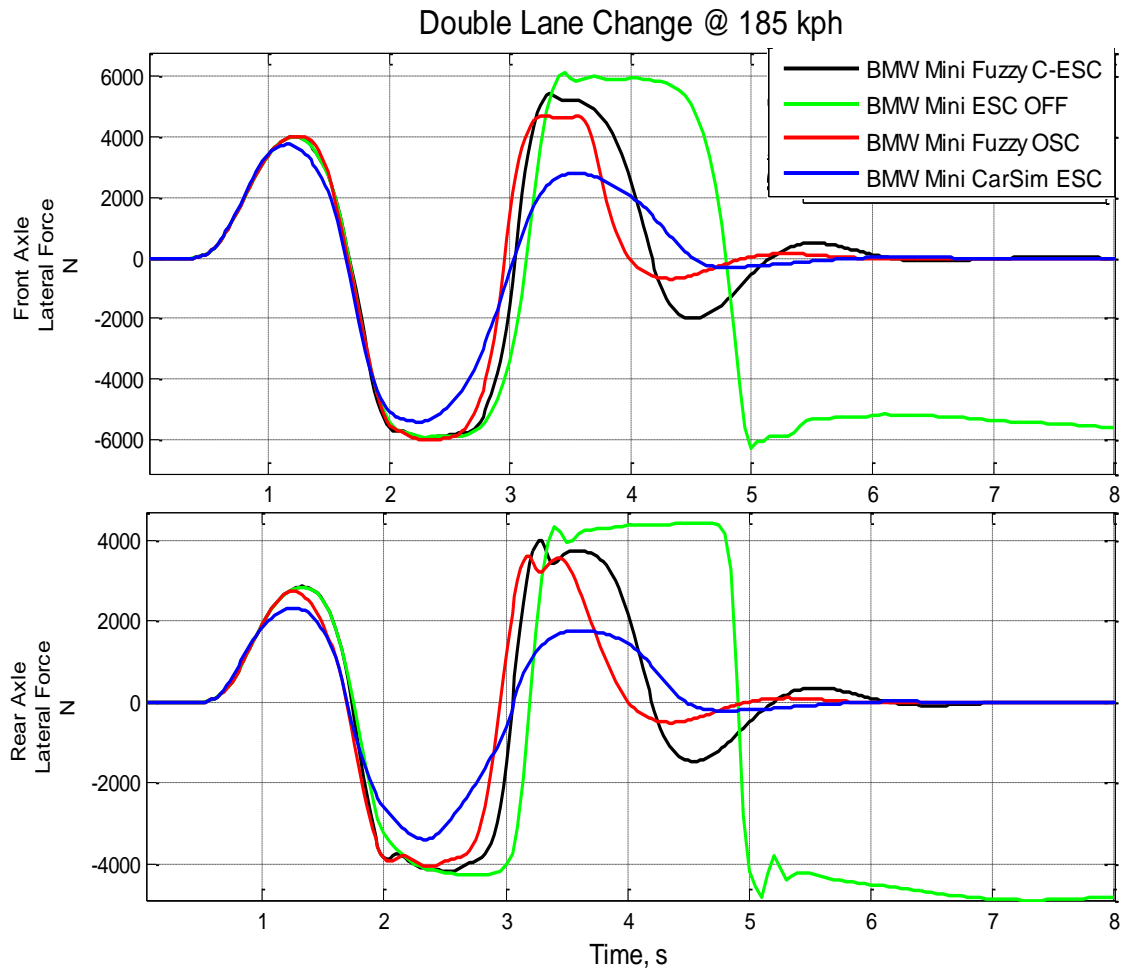


Figure 4.10 Vehicle Response: Case 2



**Figure 4.11 Lateral Force per Axle: Case 2**

### Case 3: Nominal BMW Mini, Braking-in-Turn, $\mu = 0.2$ (Ice/Snow)

This case demonstrates the performance of the controller on an ultra-low friction surface like ice or packed snow. The tires used are nominal OE tires and the simulation is carried out at **65 kph**. For this run the brake pressure resulting from driver actuated braking is lowered to **0.3 MPa**. This is reflective of the more tentative braking likely to occur on a low friction surface.

Figure 4.12 shows that even a very small braking force results in the vehicle without ESC running off the road. In contrast, the Fuzzy C-ESC equipped vehicle differentially brakes the individual wheels (Figure 4.13) and the vehicle quickly returns to the lane center. The controller applies short pulses of braking force to get the vehicle to turn in. In effect, the controller uses the brakes to ‘tug’ the vehicle into the turn. This is accomplished without excessive increase in either yaw rate or side slip angle (Figure 4.14). Both signals show distinct peaks that are reflective of what race drivers do with their steering inputs during limit under-steer to regain control of the vehicle <sup>[18]</sup>. The drop in velocity is also much smaller than for the vehicle without ESC and the lateral forces are maximized (Figures 4.15 and 4.16).

**Table 4.3 Maximum Safe Speed: Case 3**

	<b>Maximum Safe Speed (kph)</b>
<b>ESC OFF</b>	62.6
<b>Fuzzy C-ESC</b>	66.4

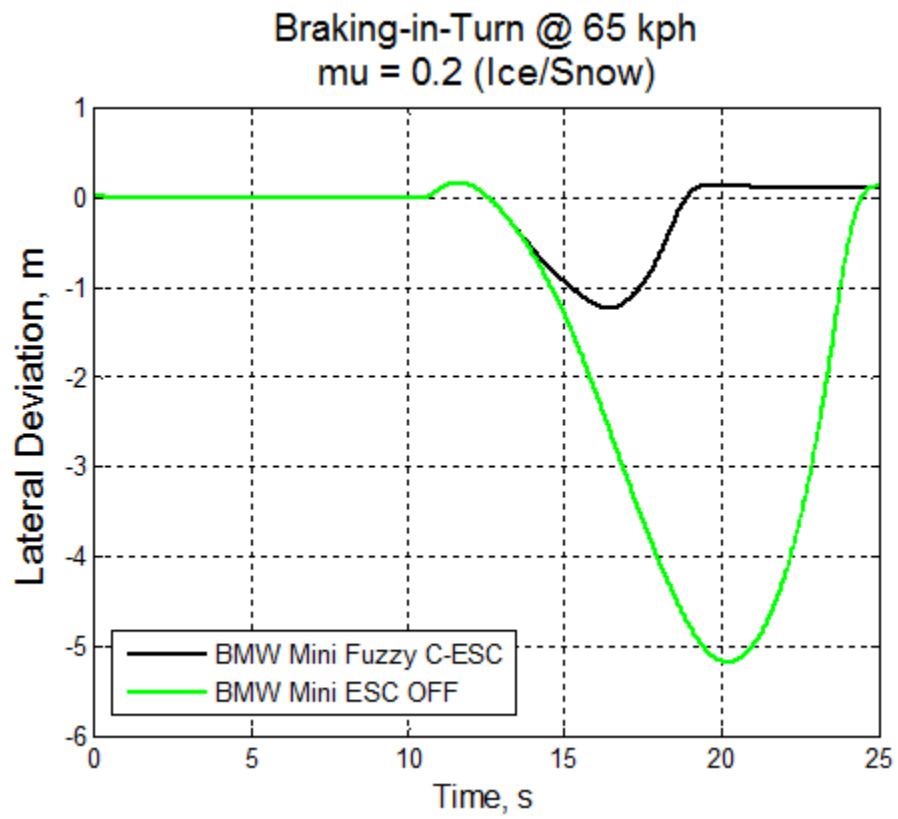


Figure 4.12 Lateral Deviation: Case 3

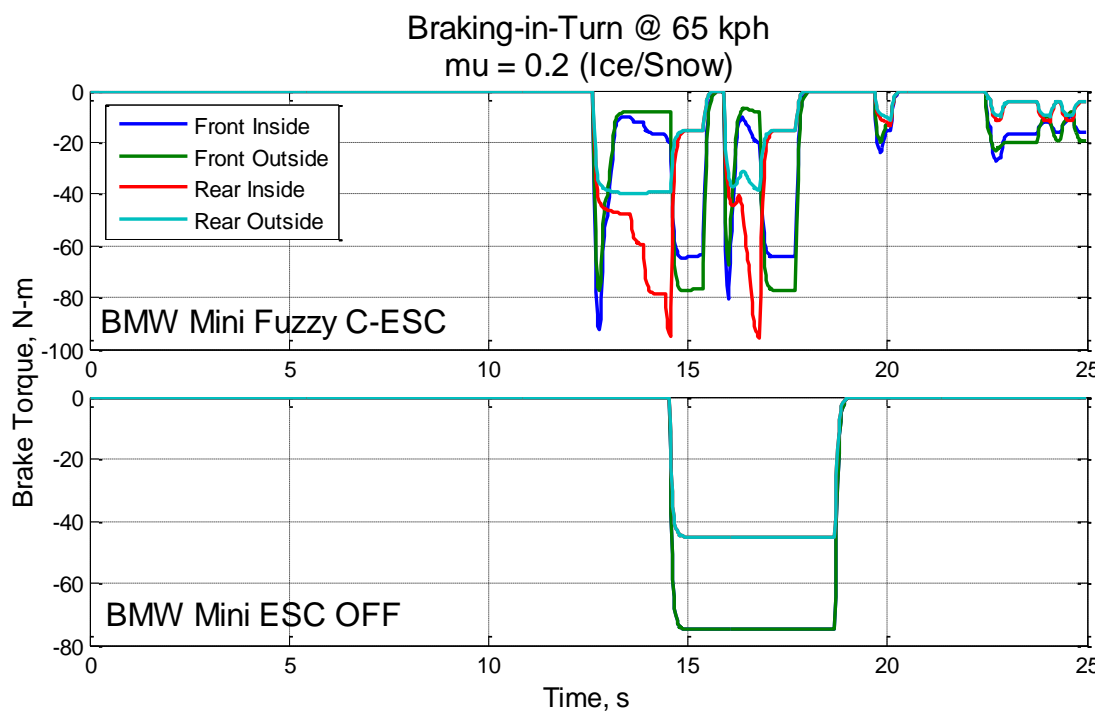


Figure 4.13 Brake Torque: Case 3

Braking-in-Turn @ 65 kph  
 $\mu = 0.2$  (Ice/Snow)

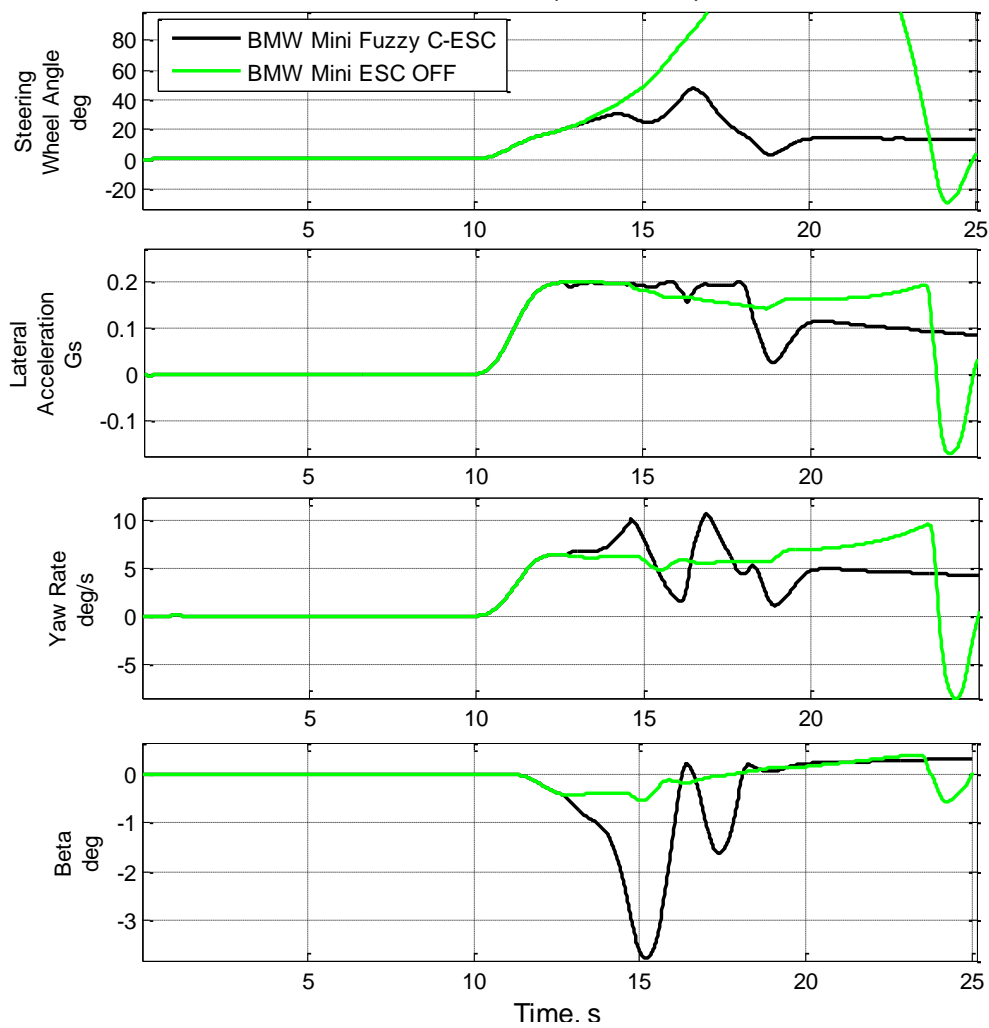


Figure 4.14 Vehicle Response: Case 3

Braking-in-Turn @ 65 kph  
 $\mu = 0.2$  (Ice/Snow)

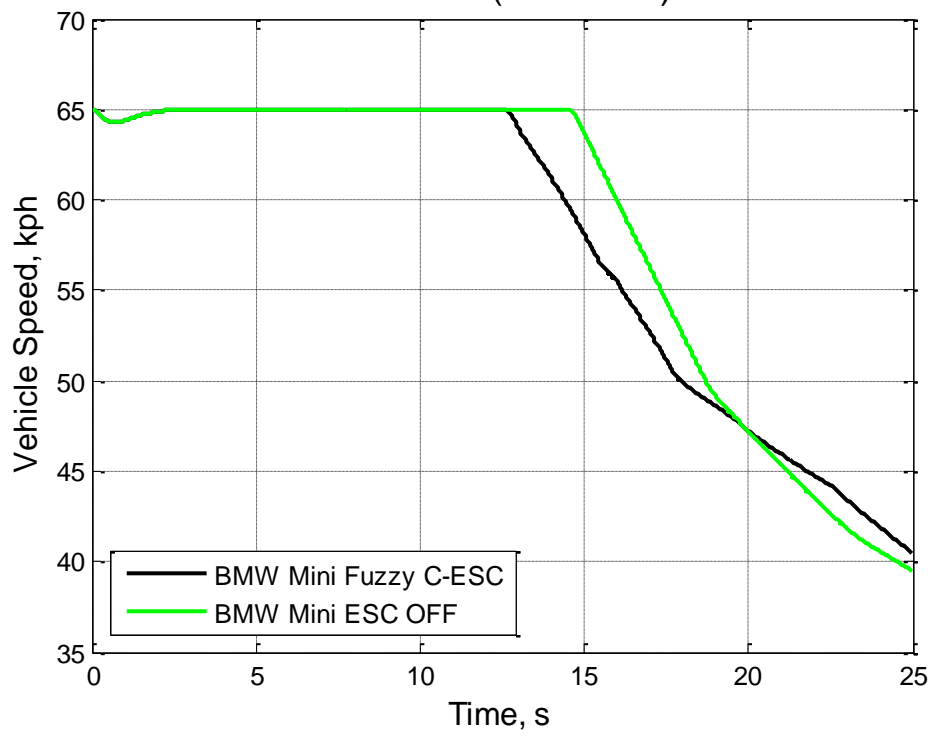


Figure 4.15 Vehicle Speed: Case 3



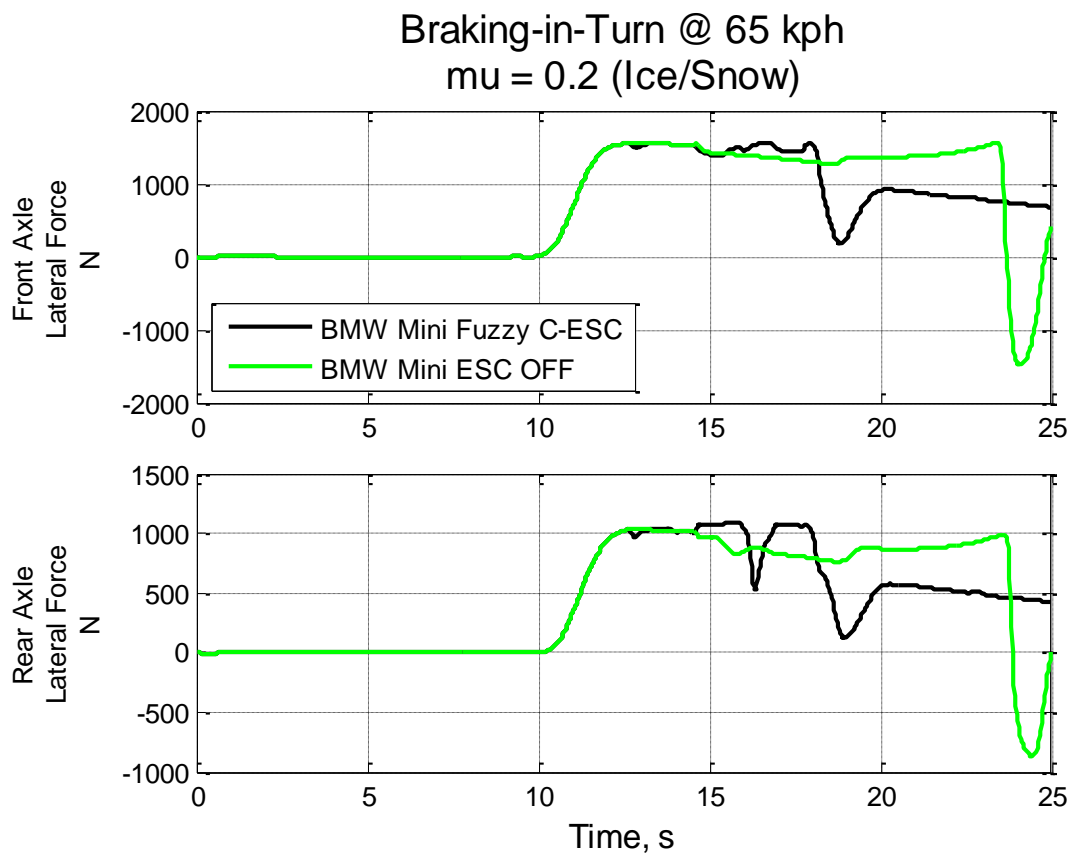


Figure 4.16 Lateral Force per Axle: Case 3

#### Case 4: Gross Vehicle Weight Mini, Braking-in-Turn, $\mu = 0.5$ (Wet Asphalt)

To study the effect of loading condition on controller performance, the BMW Mini loaded to its gross weight is simulated through the braking-in-turn maneuver on simulated wet asphalt. No changes are made to the controller algorithm. The simulation is carried out at **95 kph**.

The lateral deviation for the GVW Mini with and without ESC is shown in Figure 4.17. The ESC is again able to control the vehicle and return it to the lane center. The vehicle dynamics plots show the ‘tugging’ action of the controller (Figure 4.18). The brake pulses (Figure 4.19) are, however, shorter than the ones for Case 3. The controller detects the larger over-steer tendency of the vehicle (due to the more rear-ward weight bias) and reduces under-steer in phases so that the vehicle side-slip does not increase and result in the vehicle ‘floating’ off the road. The controller adapts to the different loading condition of the vehicle. Once again the controller is less intrusive (Figure 4.20) and maximizes the lateral forces at the axles (Figure 4.21). The vehicle without ESC loses so much speed that the side-slip angle becomes positive while the vehicle is completing the turn. This is because the velocity vector leads the vehicle at low speeds.

**Table 4.4 Maximum Safe Speed: Case 4**

	<b>Maximum Safe Speed (kph)</b>
<b>ESC OFF</b>	93
<b>Fuzzy C-ESC</b>	96.9

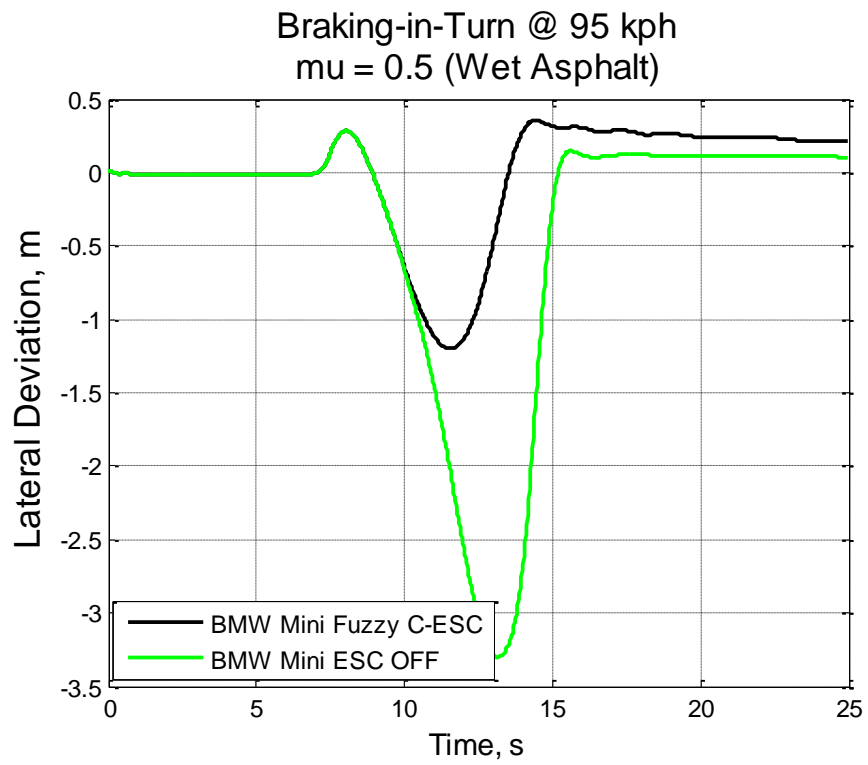


Figure 4.17 Lateral Deviation: Case 4

Braking-in-Turn @ 95 kph  
 $\mu = 0.5$  (Wet Asphalt)

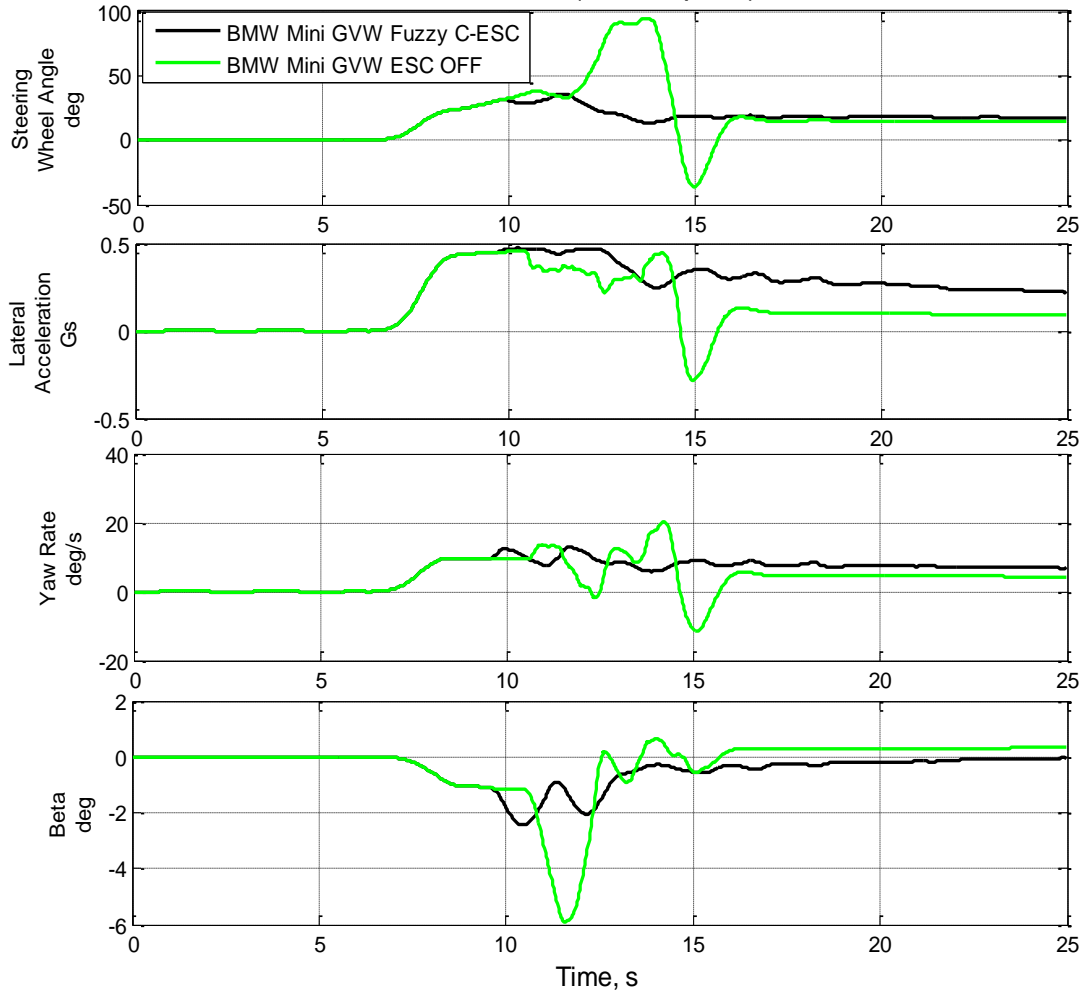


Figure 4.18 Vehicle Response: Case 4

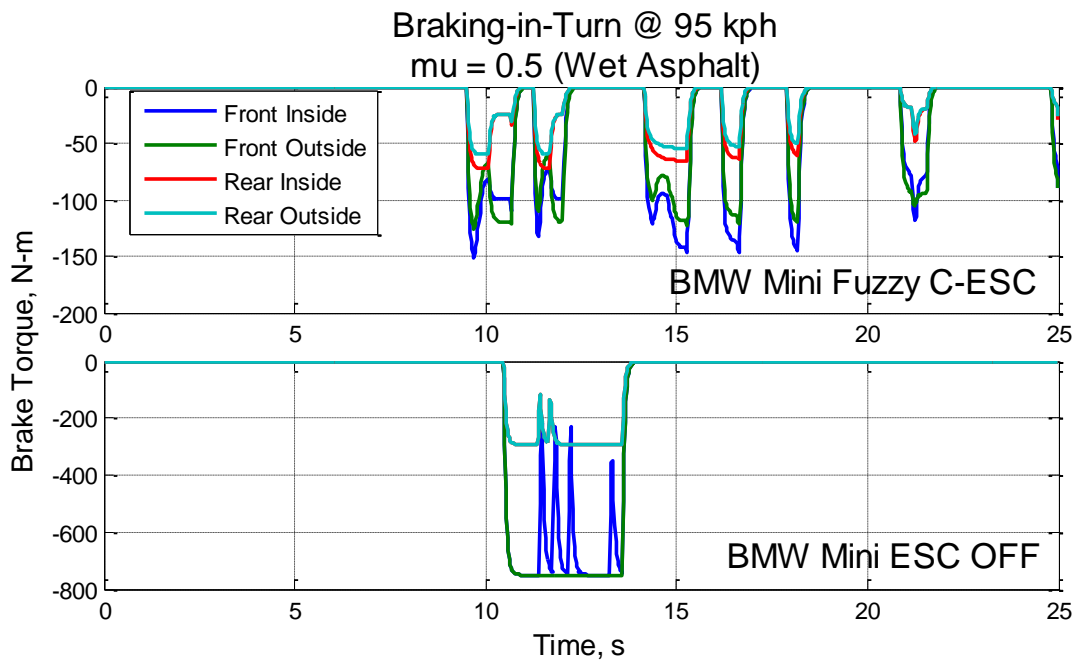


Figure 4.19 Brake Torque: Case 4

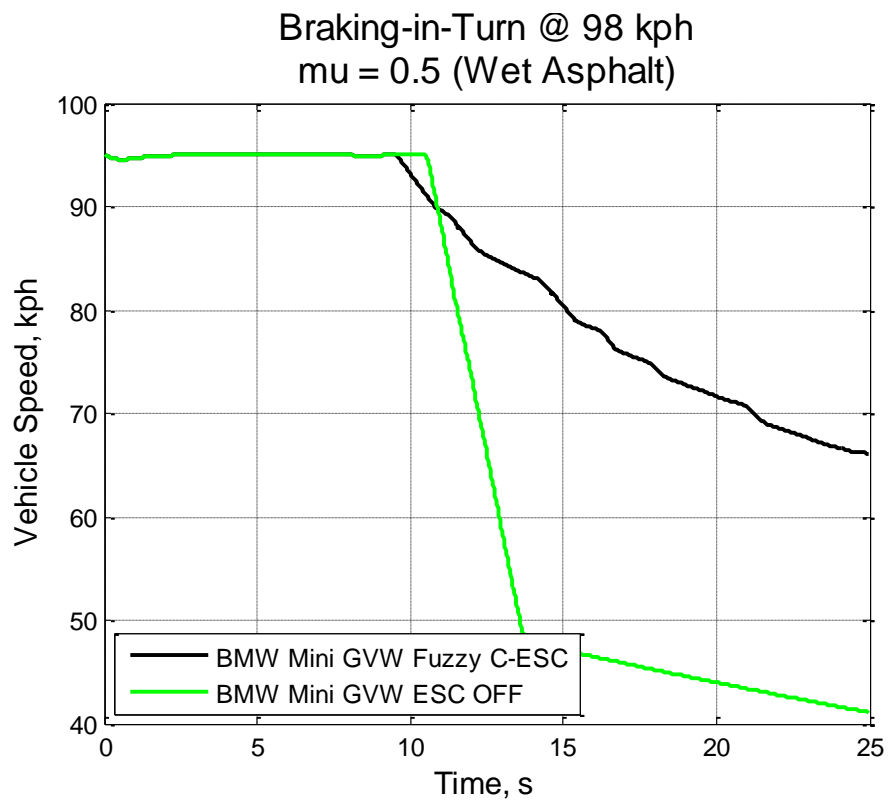


Figure 4.20 Vehicle Speed: Case 4

Braking-in-Turn @ 95 kph  
 $\mu = 0.5$  (Wet Asphalt)

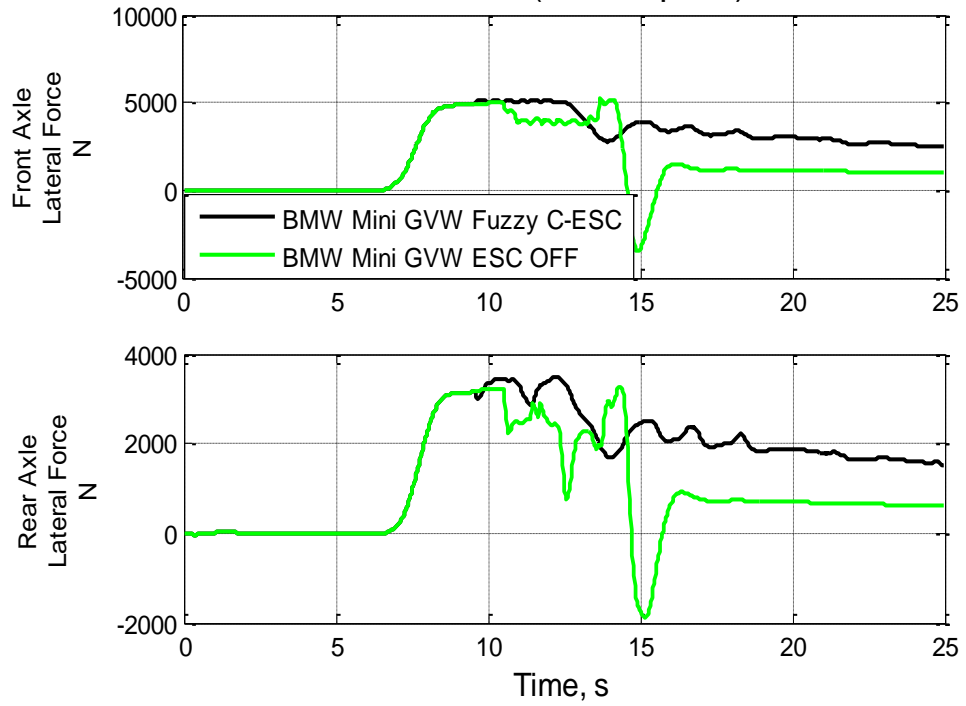


Figure 4.21 Lateral Force per Axle: Case 4

### Case 5: BMW Mini with Degraded Front tires, Braking-in-Turn, $\mu = 0.85$

Next, we will examine the effect of degraded front tires on controller performance. To do this the front tires on the BMW Mini were degraded by **25%**. This results in a reduction in front axle lateral grip. The modified tire parameters can be found in Appendix B. The road surface and loading conditions are nominal ( $\mu = 0.85$ ) and the maneuver is simulated at **115 kph**. The resulting lateral deviation is shown in Figure 4.22.

The behavior of the vehicle with the ESC is consistent, qualitatively, with that seen for the other cases. The vehicle dynamics plots and the brake torque are shown in Figures 4.23 and 4.24. The familiar ‘tugging’ action of the controller can be observed. The smaller pulses in braking also mean a smaller loss in vehicle speed (Figure 4.25). The vehicle without ESC slows down to well below 50 kph resulting in the side-slip angle becoming positive for the remainder of the left hand turn. The resulting lateral forces at the front and rear axle are shown in the Figure 4.26. The vehicle with Fuzzy C-ESC is reoriented by manipulating the rear axle lateral forces to ensure that the maximum possible lateral force is generated at the front axle.

**Table 4.5 Maximum Safe Speed: Case 5**

	<b>Maximum Safe Speed (kph)</b>
<b>ESC OFF</b>	108.4
<b>Fuzzy C-ESC</b>	118.5



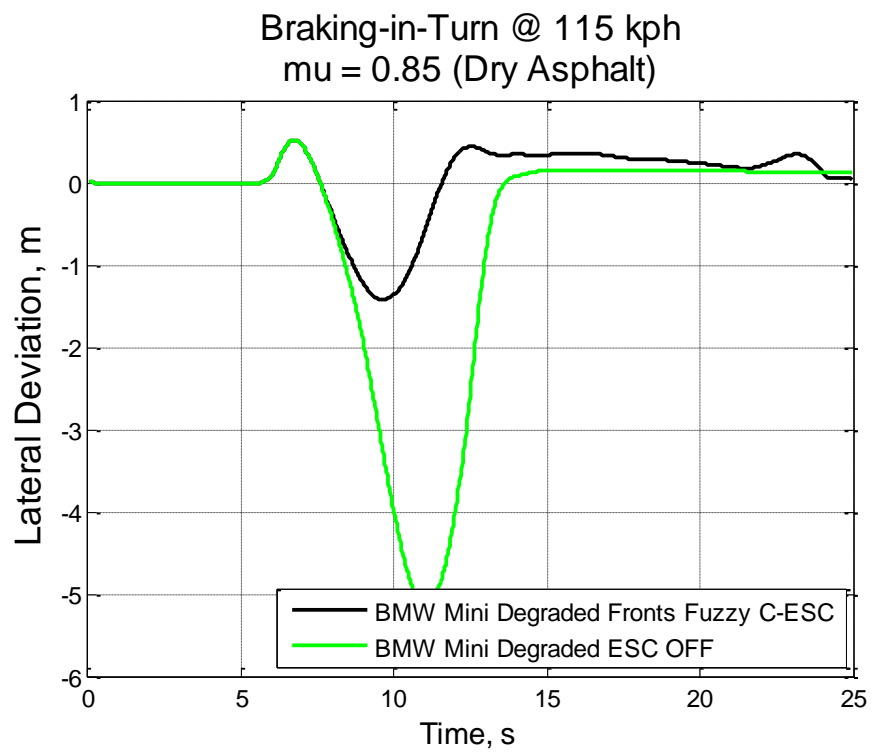


Figure 4.22 Lateral Deviation: Case 5

Braking-in-Turn @ 115 kph  
 $\mu = 0.85$  (Dry Asphalt)

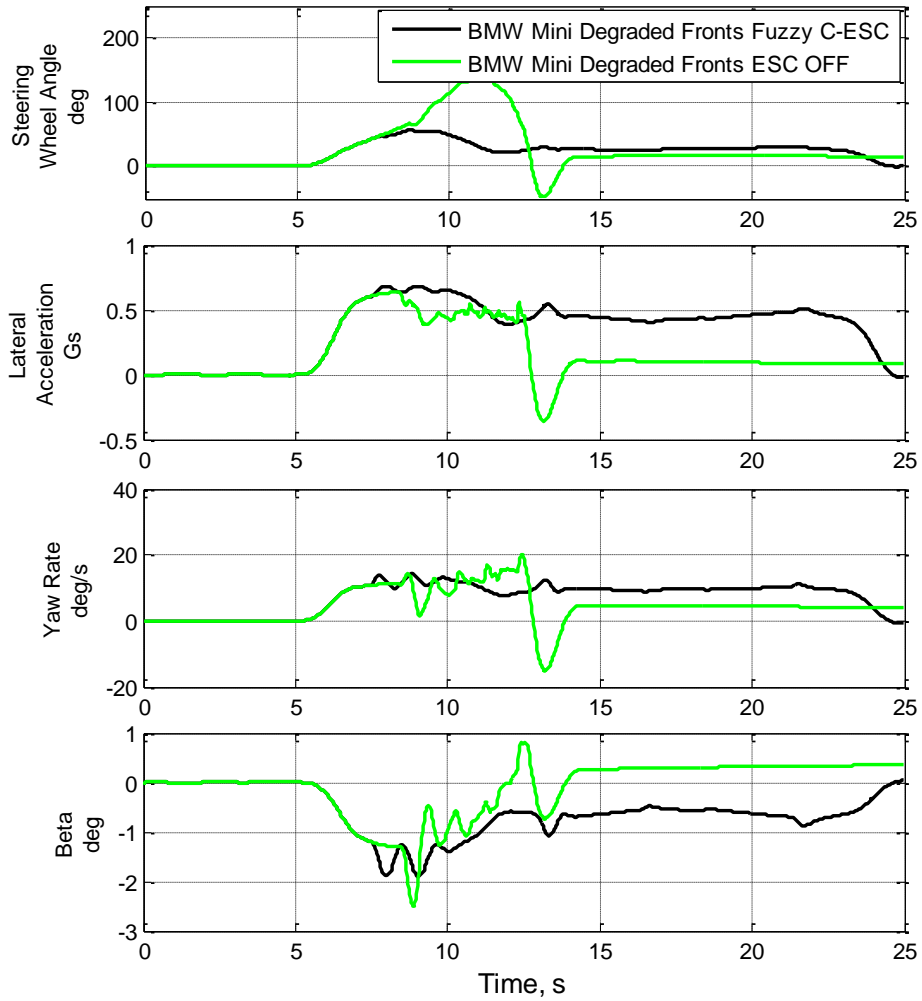


Figure 4.23 Vehicle Response: Case 5

Braking-in-Turn @ 115 kph  
 $\mu = 0.85$  (Dry Asphalt)

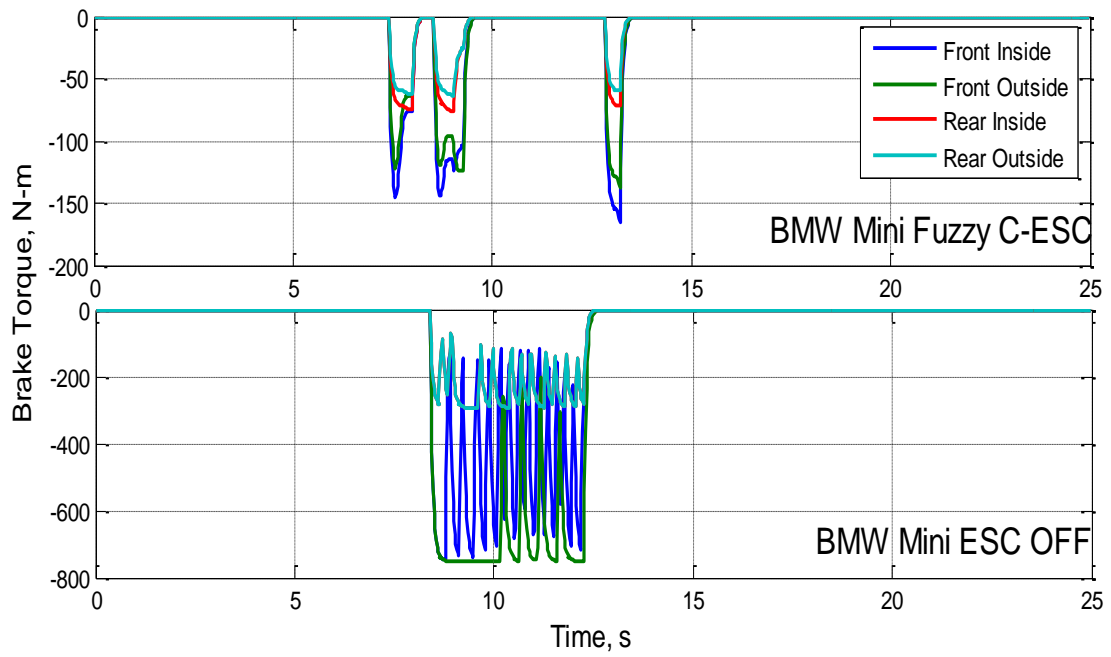


Figure 4.24 Brake Torque: Case 5

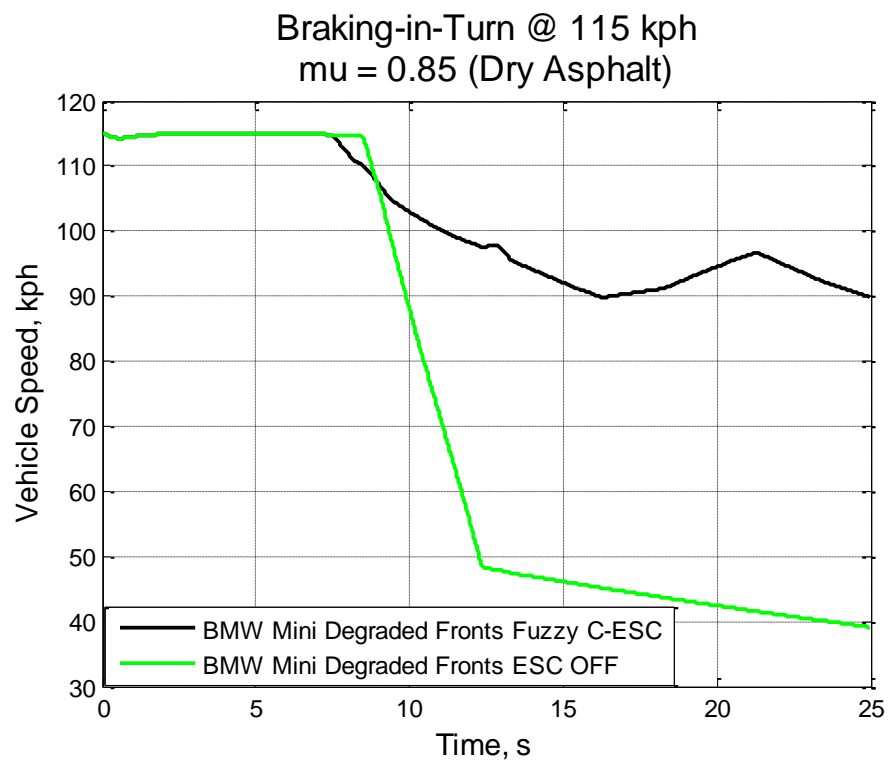


Figure 4.25 Vehicle Speed: Case 5

Braking-in-Turn @ 115 kph  
 $\mu = 0.85$  (Dry Asphalt)

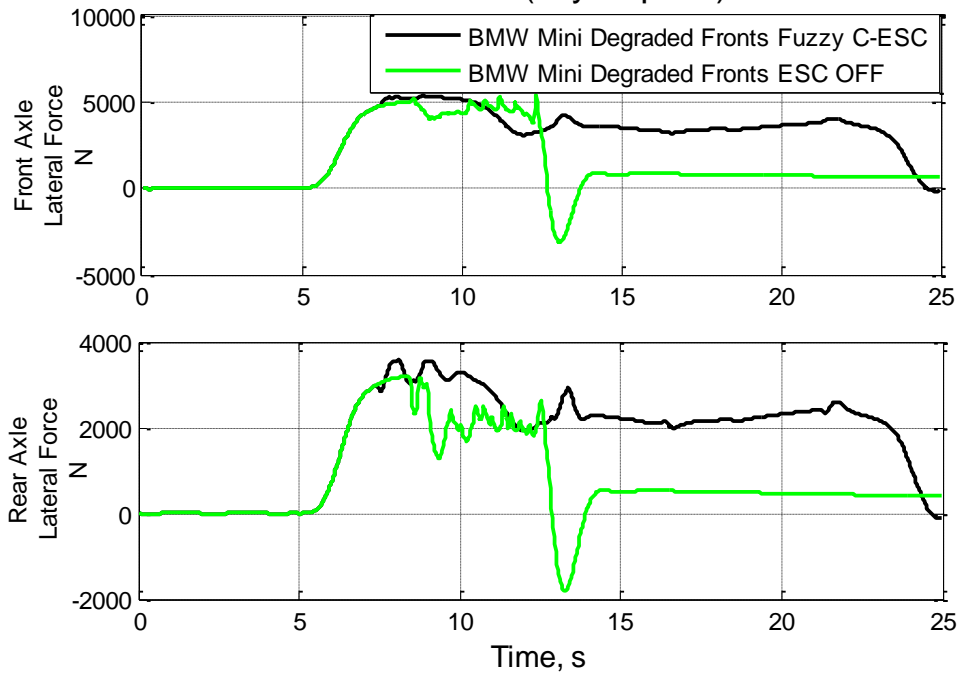


Figure 4.26 Lateral Force per Axle: Case 5

### **Case 6: Nominal D-Class Sedan, Braking-in-Turn, $\mu = 0.5$ (Wet Asphalt)**

In this case, a nominal sedan is simulated executing the braking-in-turn maneuver at **92 kph** on a low friction surface representing wet asphalt. Static values of the vehicle parameters, yaw inertia, front track and the rolling radius of the front wheels are updated in the MATLAB workspace to the values for the sedan. The remaining algorithm is unchanged. The three quantities above are used to compute the braking force during an over-steer event as described in [4,5]. The vehicle specifications and tire data can be found in the Appendices A and B. The resulting lateral deviations for the vehicle with and without the Fuzzy C-ESC are shown in Figure 4.27. The corresponding vehicle dynamics are shown in Figure 4.28.

The controller works very smoothly for this case. Once again the controller applies short pulses of braking force to get the vehicle to turn in (Figure 4.29). The first pulse has an extended rear wheel braking. This is due to a larger under-steer number ( $US > 5$ ) detected by the controller. The controller, in this case, detects that the vehicle has a much lower over-steer tendency and allows the extended rear wheel braking. As a result a large peak in side-slip angle is observed (Figure 4.28). The remaining pulses ensure the vehicle continues to traverse the circular trajectory. The quick variations in braking are very effective in this case. The driver's steering input barely changes as the vehicle is quickly controlled.

The vehicle without ESC again slows down to well below 50 kph (Figure 4.30) resulting in the side-slip angle becoming positive for the remainder of the left hand turn. A small amount lateral force and lateral acceleration is then required to complete the turn.

Table 4.6 Maximum Safe Speed: Case 6

	Maximum Safe Speed (kph)
ESC OFF	86.8
Fuzzy C-ESC	92.4

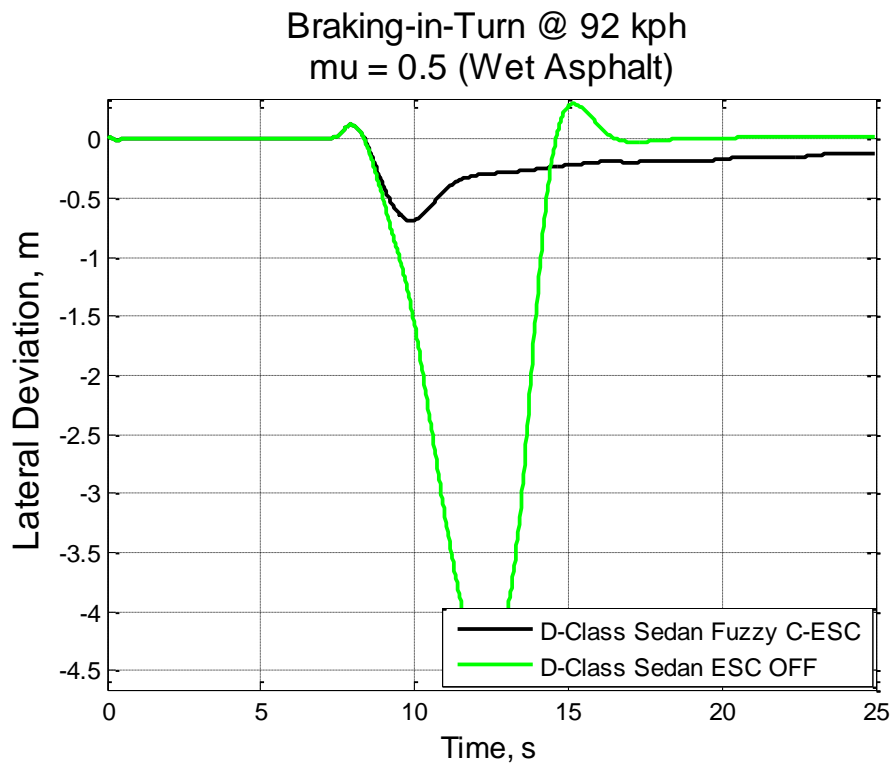


Figure 4.27 Lateral Deviation: Case 6

Braking-in-Turn @ 92 kph  
 $\mu = 0.5$  (Wet Asphalt)

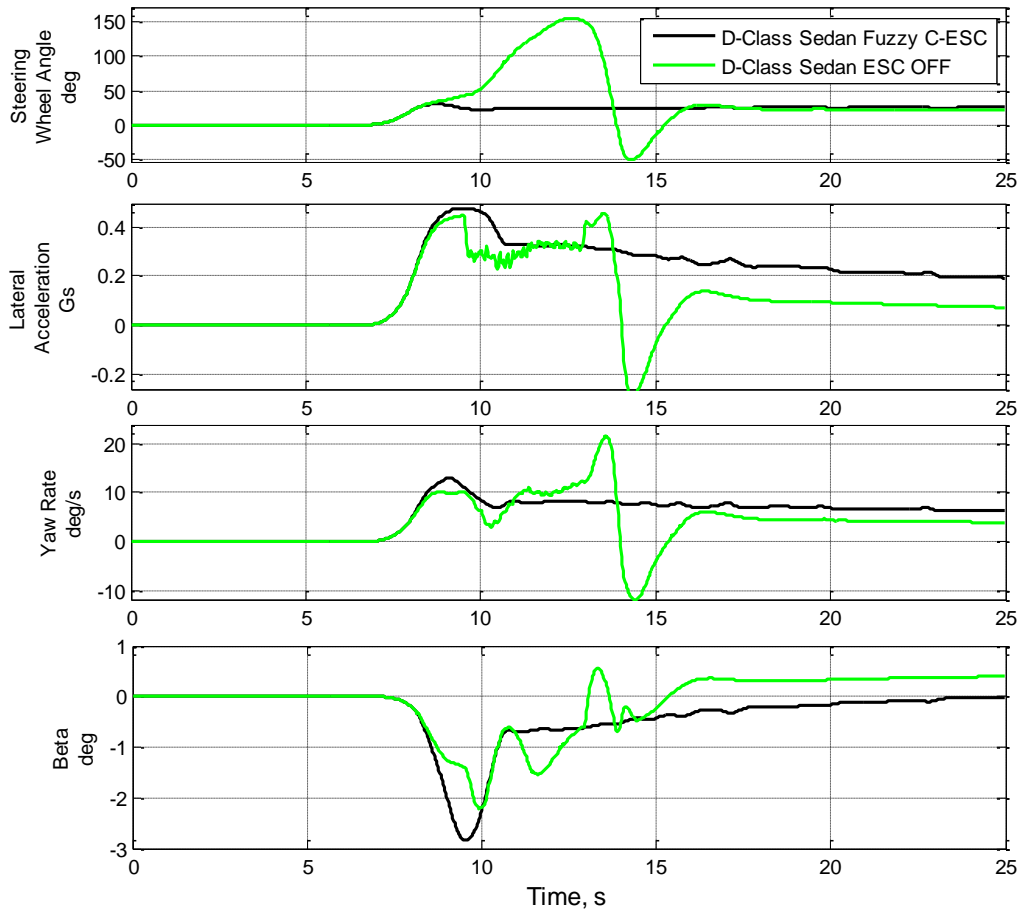


Figure 4.28 Vehicle Response: Case 6



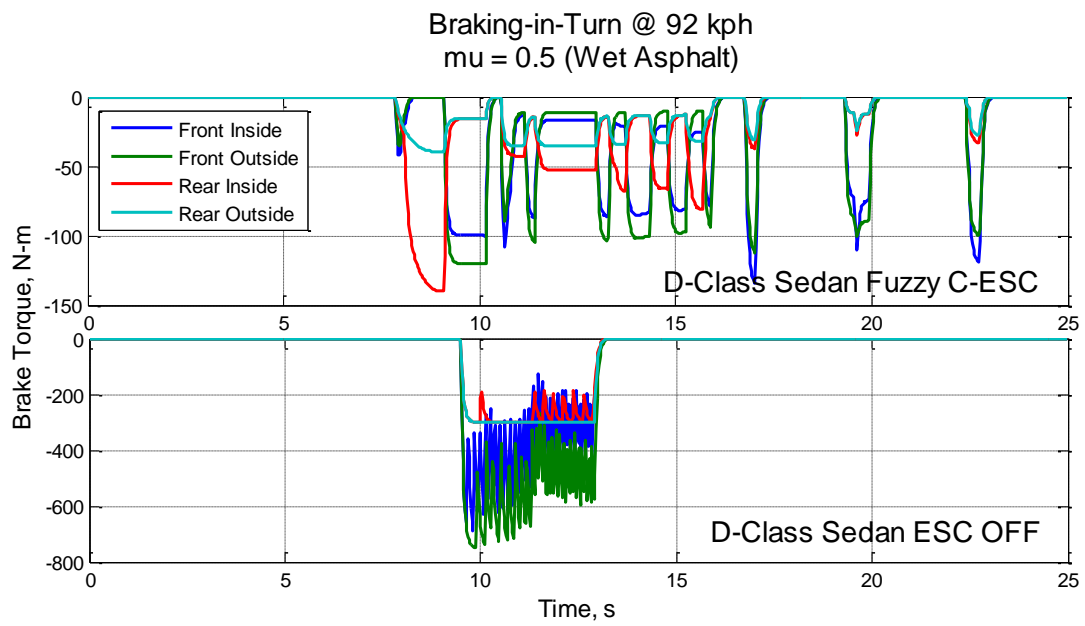


Figure 4.29 Brake Torque: Case 6

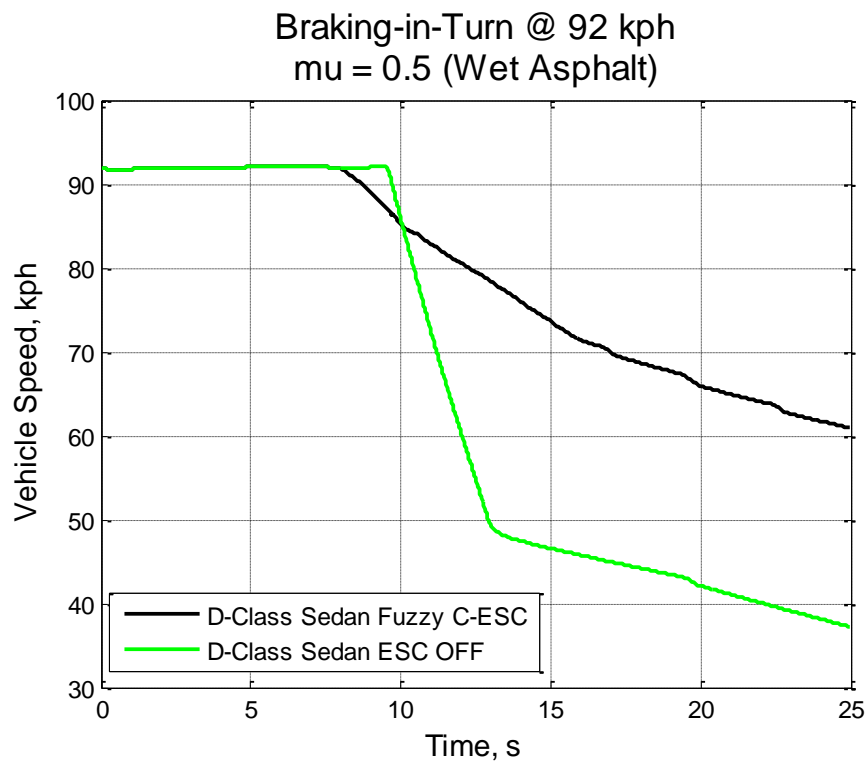


Figure 4.30 Vehicle Speed: Case 6

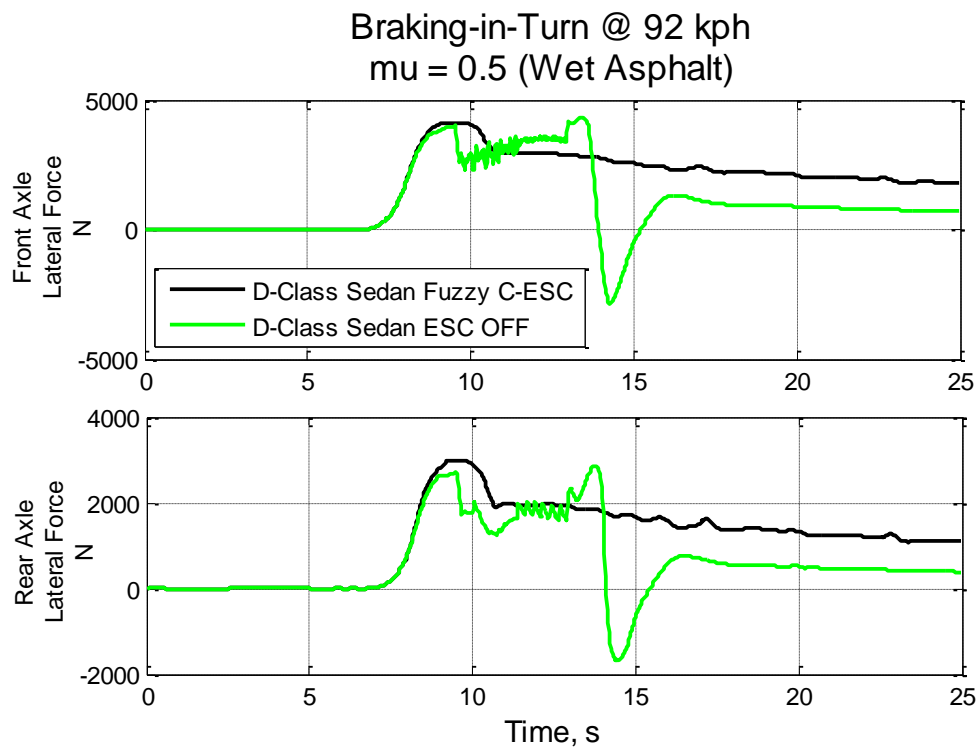


Figure 4.31 Lateral Force per Axle: Case 6

### **Case 7: Nominal D-Class Sedan, Braking-in-Turn, $\mu = 0.85$**

This case demonstrates how a vehicle changes its behavior from under- to over-steer during a maneuver and the adaptability of the controller to this change. The simulation is run at **110 kph** for a nominal D-Class Sedan with a tire-to-ground friction of **0.85**, which is similar to that of dry pavement. The lateral deviation for the vehicle with and without ESC is shown in Figure 4.32.

As is evident the vehicle without ESC has a large overshoot while returning to the lane center. The driver has to counter steer heavily to avoid spinning out as the vehicle side-slip and yaw rate increase rapidly (Figure 4.33). The vehicle without ESC initially under-steers and the driver applies the brakes (Figure 4.34) to reduce vehicle speed. The resulting load transfer to the front causes the rear wheels to reach their limit lateral force and the vehicle threatens to spin-out.

The Fuzzy C-ESC applies pulsing brake pressure that causes the vehicle to turn in while preventing a spin-out. The peak brake torque for the ESC equipped vehicle is only 20% of that applied by the driver (Figure 4.34). The controller intervention is barely perceptible to the driver as seen in the steering wheel angle plot. The first braking pulse again has extended rear wheel braking. This indicates that the under-steer number must be above '5' and the vehicle was under-steering heavily justifying the hard braking by the driver. The C-ESC reduces the lateral deviation to the outside and then prevents a spin-out. For this case, maximizing lateral force is not the ideal way to complete the maneuver. The per axle lateral forces for the two configuration are shown in Figure 4.35. The Fuzzy C-ESC equipped vehicle has lower, but smoother, peaks in the lateral forces.

**Table 4.7 Maximum Safe Speed: Case 7**

	<b>Maximum Safe Speed (kph)</b>
<b>ESC OFF</b>	110
<b>Fuzzy C-ESC</b>	119

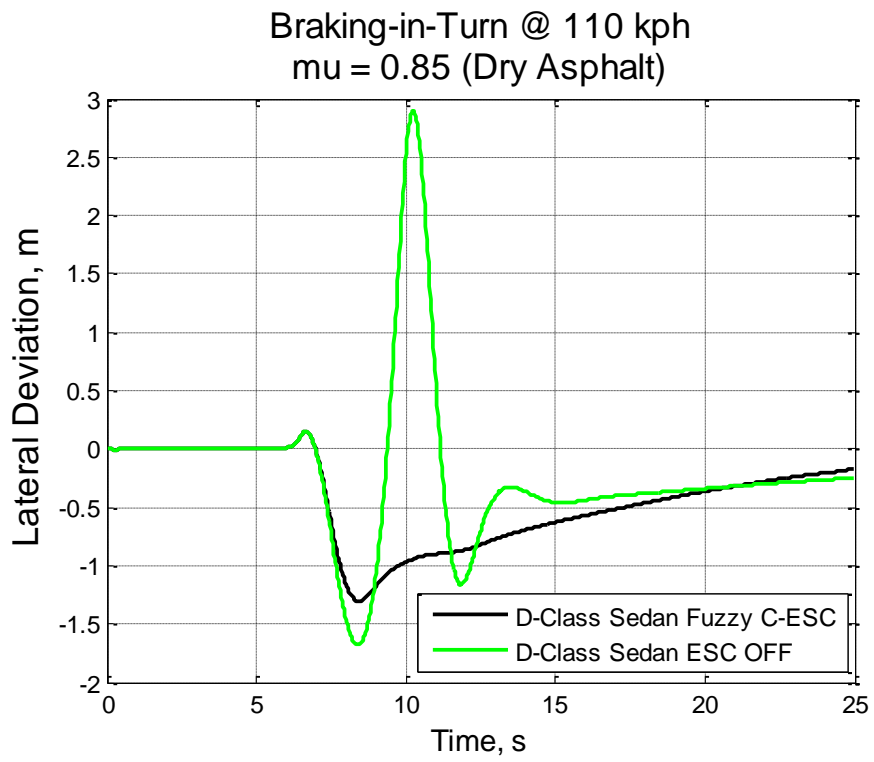


**Figure 4.32 Lateral Deviation: Case 7**

Braking-in-Turn @ 110 kph  
 $\mu = 0.85$  (Dry Asphalt)

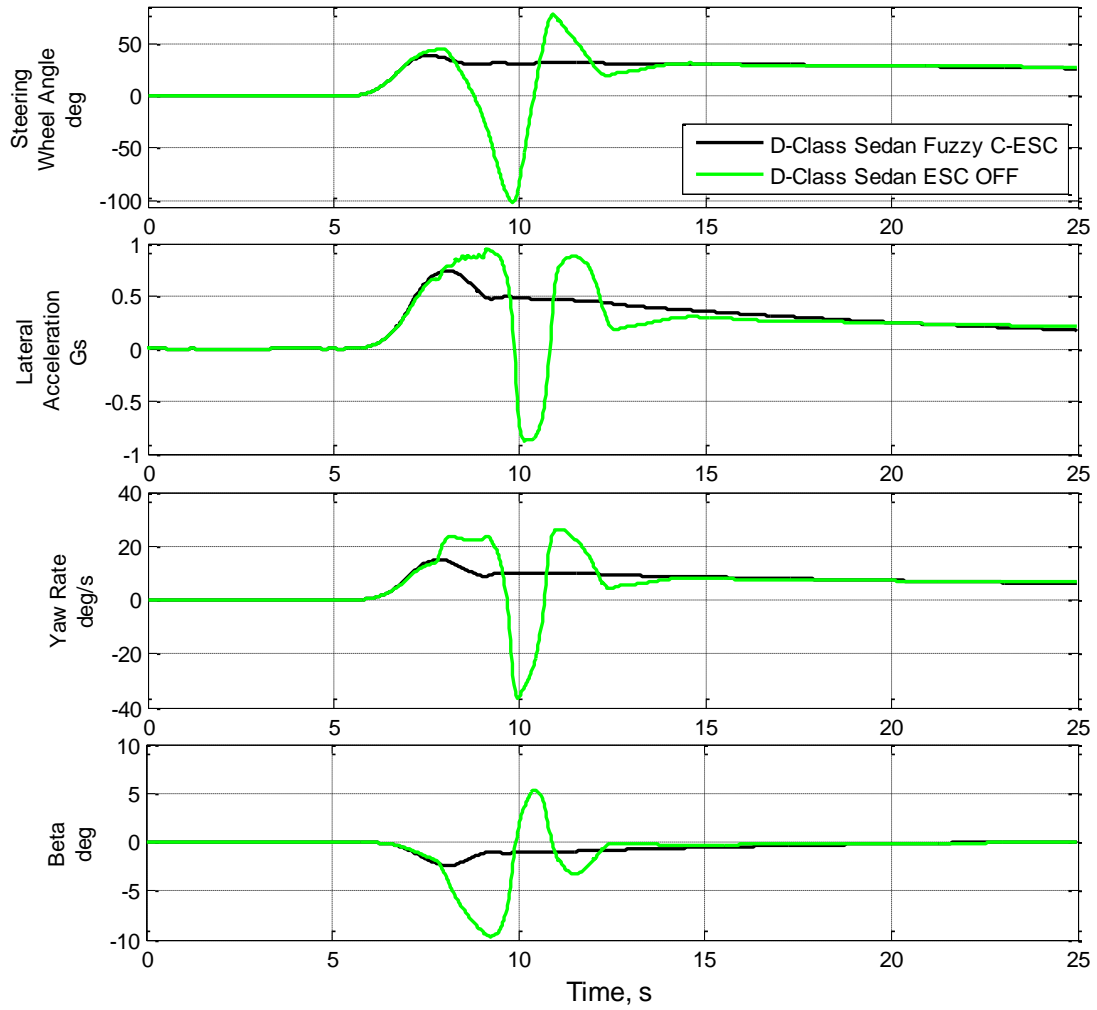


Figure 4.33 Vehicle Response: Case 7

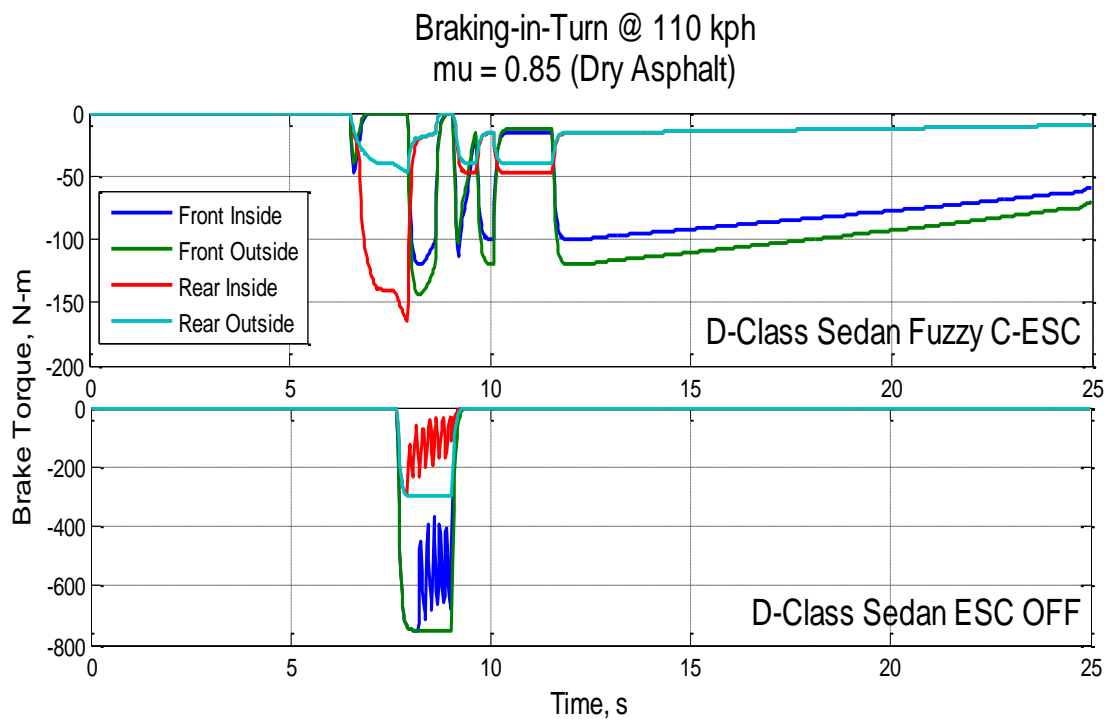


Figure 4.34 Brake Torque: Case 7

Braking-in-Turn @ 110 kph  
 $\mu = 0.85$  (Dry Asphalt)

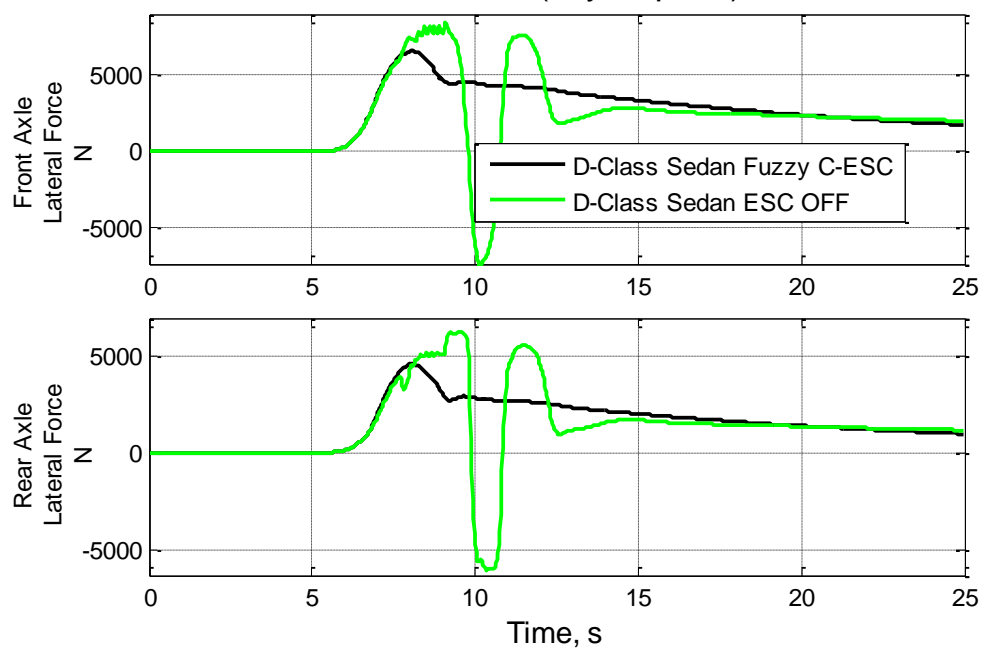


Figure 4.35 Lateral Force per Axle: Case 7



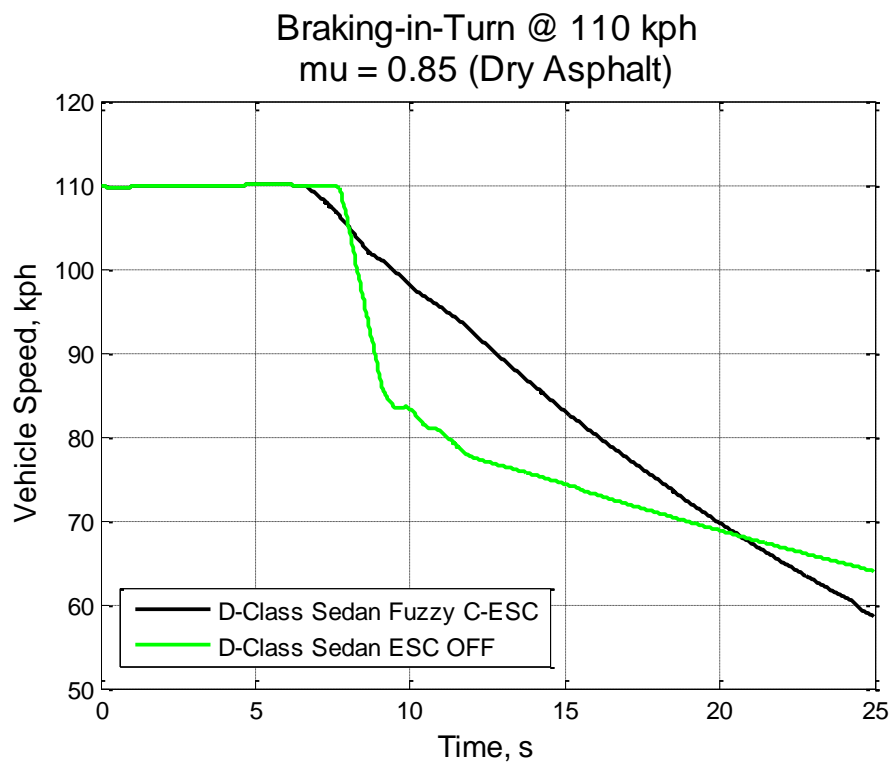


Figure 4.36 Vehicle Speed: Case 7

### **Case 8: Nominal E-Class SUV, Braking-in-Turn, $\mu = 0.5$**

This case simulates a large sport utility vehicle (SUV) executing the braking-in-turn maneuver at **85 kph** on a wet surface. The vehicle parameters are again updated in the MATLAB workspace to match those of the SUV. The nominal SUV has a larger mass and, more importantly, a higher C.G. location. This affects the load transfer dynamics and hence the brake distribution. However, the algorithm is unchanged for this vehicle as well. As we will see, the controller adapts to the change in behavior of the vehicle.

The lateral deviation and the vehicle dynamics plots are shown in Figures 4.37 and 4.38. The fuzzy controller detects that a quick initial braking along with the throttle cut are sufficient to result in a load transfer that improves the lateral force capability of the vehicle. The driver actuated braking is over-ridden when the controller detects that the vehicle is about to under-steer (Figure 4.39). However, no additional braking is actuated because of the vehicle's propensity to over-steer. The vehicle then 'cruises' till there is no over- or under-steer detected. Short pulses in braking then ensure that the vehicle continues to move along the circular trajectory.

In contrast, the vehicle without ESC has large values of both steering input and side-slip angle. The driver is trying hard to turn the vehicle but it only 'floats' off the road. This situation is particularly hazardous for an SUV because of its tendency to rollover. The vehicle, without ESC, may hit a curb sideways and 'trip' over the railing. The controller is again less intrusive (Figure 4.40) and maximizes the lateral forces at the front and rear axle (Figure 4.41).

Table 4.8 Maximum Safe Speed: Case 8

	Maximum Safe Speed (kph)
ESC OFF	82.8
Fuzzy ESC	87.7

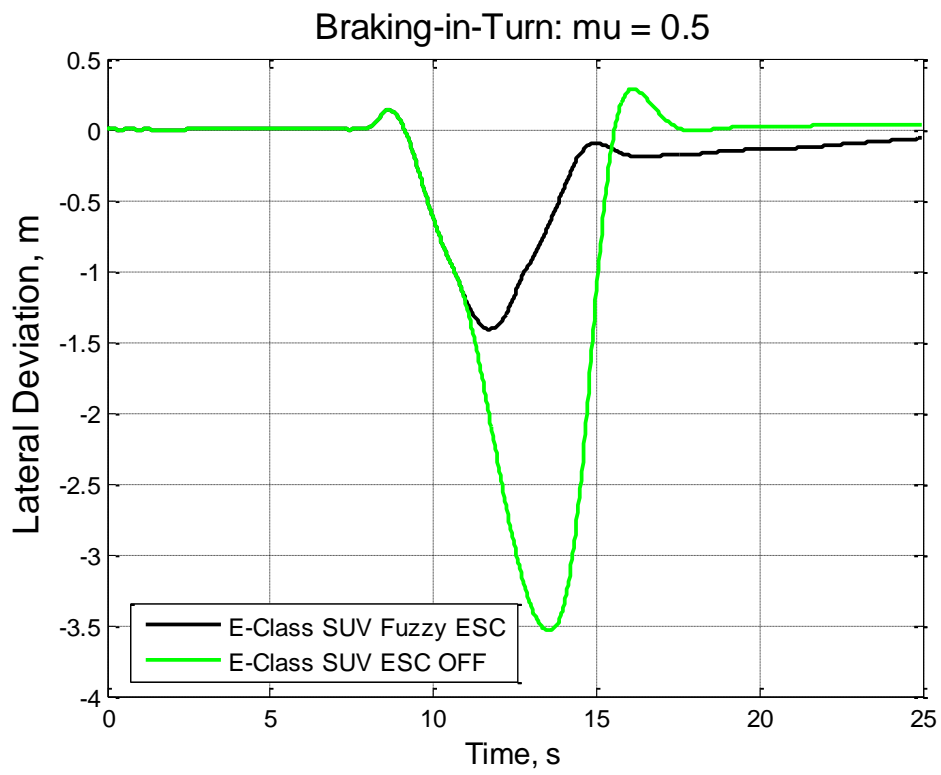


Figure 4.37 Lateral Deviation: Case 8

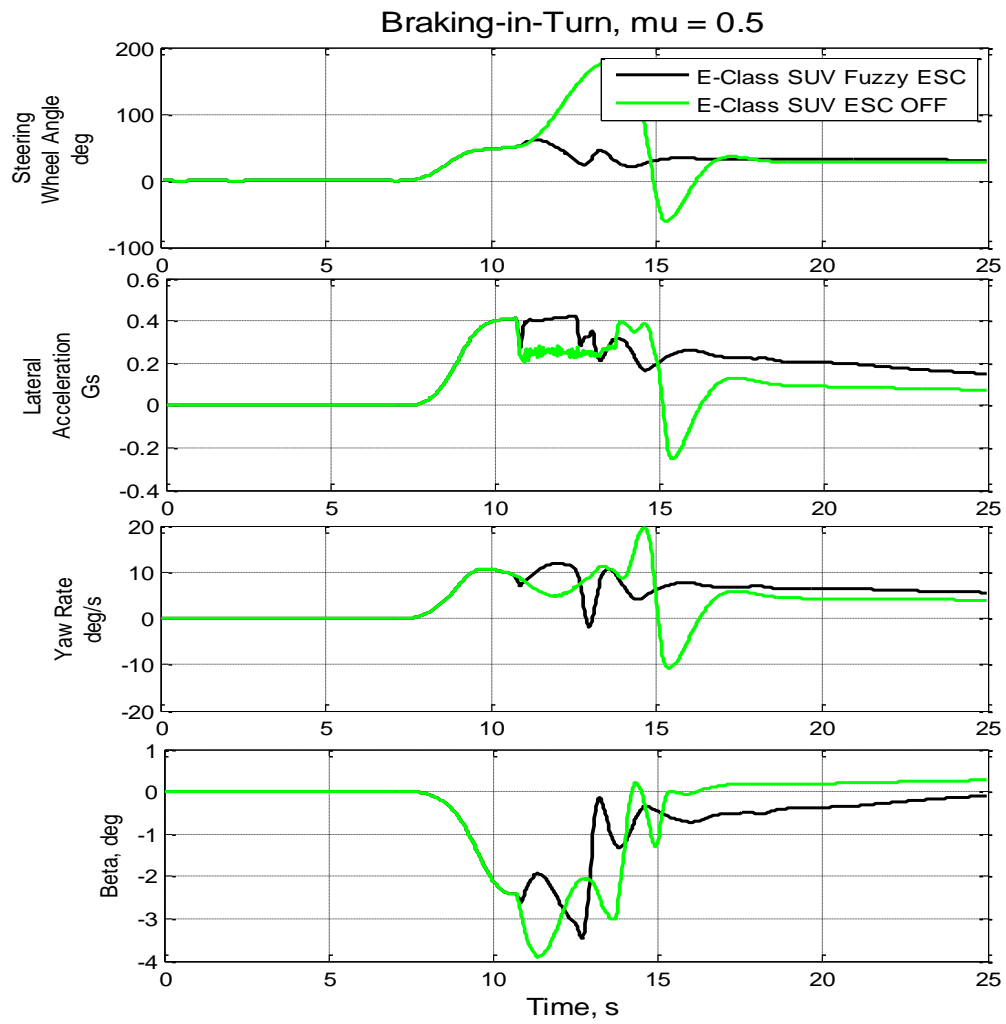


Figure 4.38 Vehicle Response: Case 8

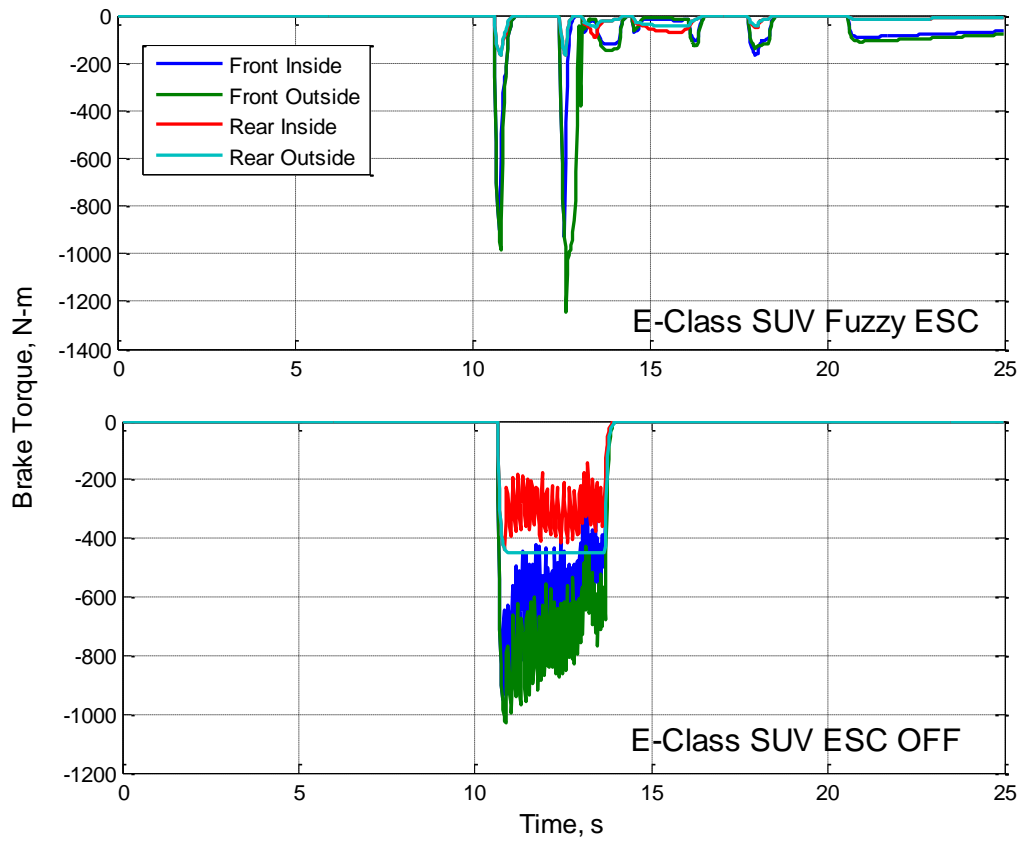


Figure 4.39 Brake Torque: Case 8

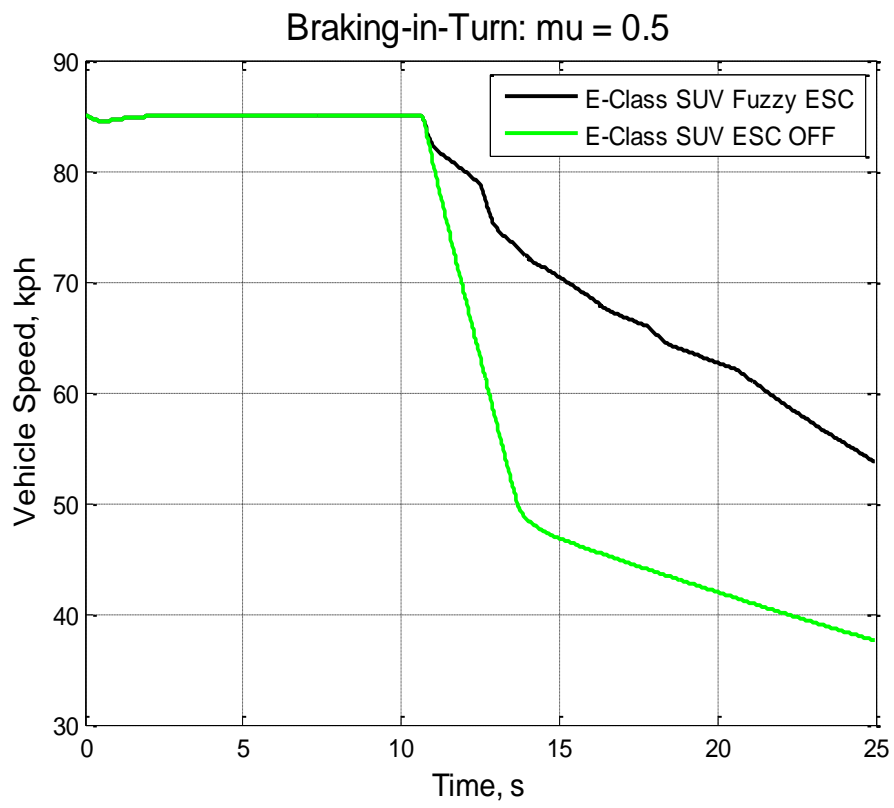


Figure 4.40 Vehicle Speed: Case 8

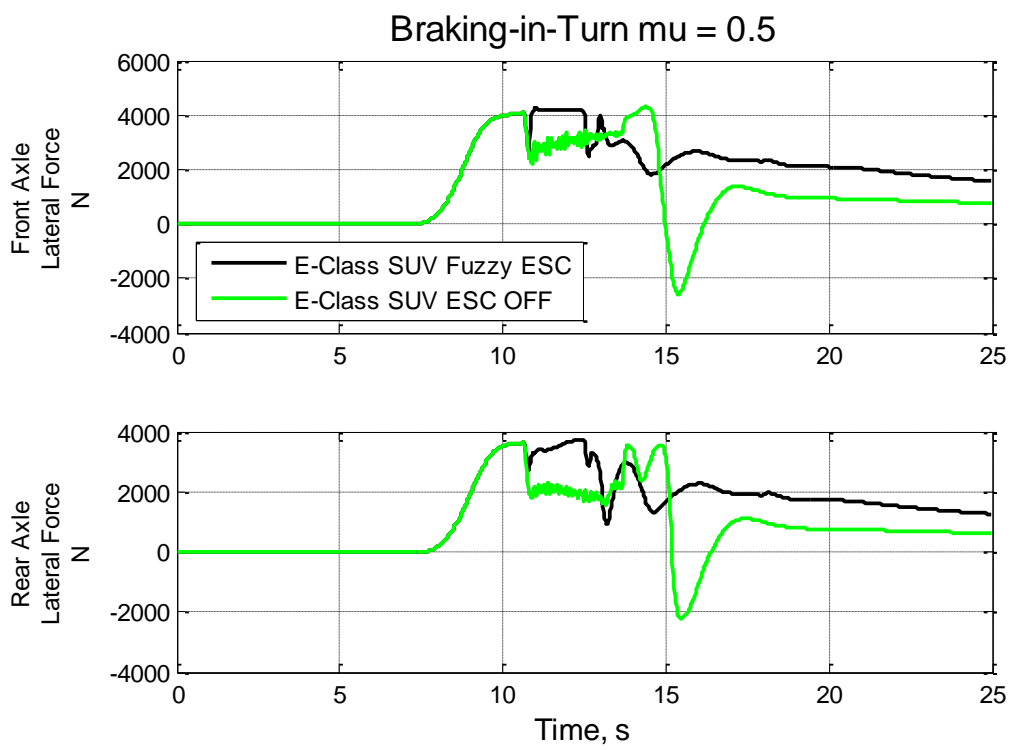


Figure 4.41 Lateral Force per Axle: Case 8

## Summary

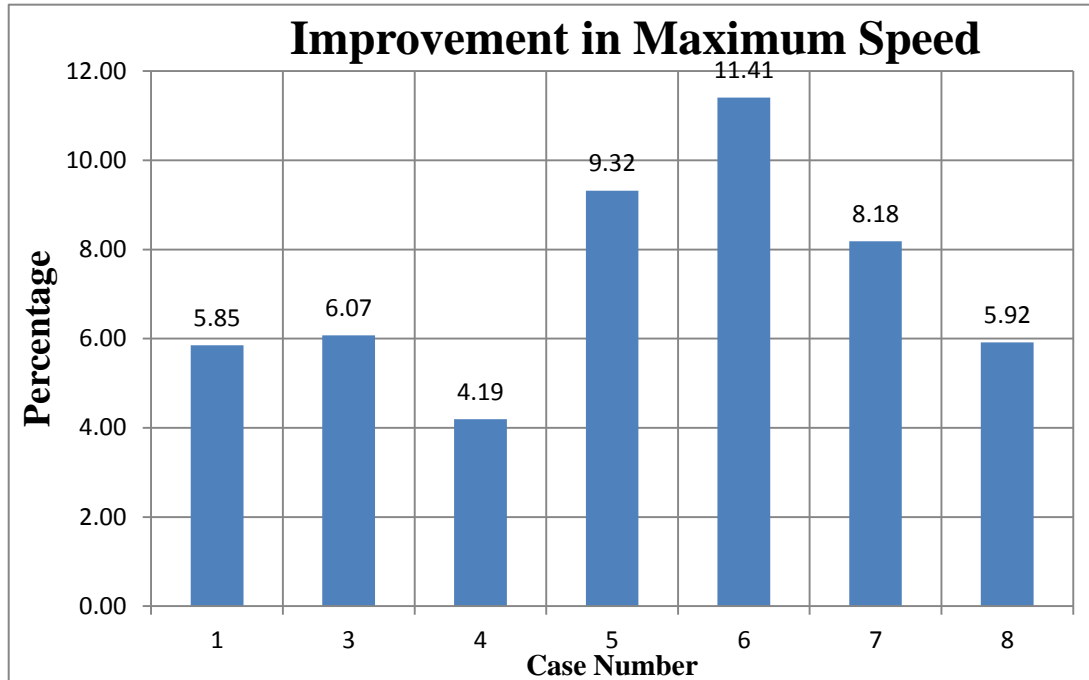
A fuzzy logic based electronic stability controller is developed and its performance tested using simulations. It combined an existing over-steer controller <sup>[4,5]</sup> with a new under-steer controller developed as part of this project. The majority of the work in this project focused on reducing the under-steer tendency of a vehicle. In order to validate this behavior a test maneuver, braking-in-turn, was developed that simulates a situation most likely to cause limit under-steer.

Table 4.9 lists the maximum safe speeds with and without Fuzzy ESC for the seven cases in which the braking-in-turn maneuver is simulated. The maximum safe speed is that speed at which the vehicle completes the maneuver without its lateral deviation exceeding 2 m. For each case the improvement in maximum speed as a percentage of the ESC OFF configuration is also shown. There is an average improvement of **7.28%** in maximum speed due to the presence of the controller. The same data is presented graphically in Figure 4.22.



**Table 4.9 Percent Improvement in Maximum Speed: Braking-in-Turn**

Case	Vehicle	Configuration	Friction Coefficient	Maximum Safe Speed (kph)		% Gain	Average
				ESC OFF	Fuzzy C-ESC		
1	BMW Mini	Nominal	$\mu = 0.5$	94	99.5	5.85	<b>7.28</b>
3	BMW Mini	Nominal	$\mu = 0.2$	62.6	66.4	6.07	
4	BMW Mini	Gross Vehicle Weight	$\mu = 0.5$	93	96.9	4.19	
5	BMW Mini	Degraded Front Tires	$\mu = 0.85$	108.4	118.5	9.32	
6	D-Class Sedan	Nominal	$\mu = 0.5$	86.8	96.7	11.4	
7	D-Class Sedan	Nominal	$\mu = 0.85$	110	119	8.18	
8	E-Class SUV	Nominal	$\mu = 0.5$	82.8	87.7	5.92	



**Figure 4.42 Percent Improvement in Maximum Speed**

## CHAPTER 5

### CONCLUSIONS AND RECOMMENDATIONS

#### Conclusion

The model-based ESC systems described in the open literature are generally dependent on the accuracy of the vehicle model. Extensive tests need to be carried out to characterize the model and to account for effects of load, tire wear, banking, etc. The process needs to be repeated for each vehicle that uses the ESC. A model-free approach would save a lot of time and expense.

A simple measure to quantify under-steer in a vehicle, fractional drop, is developed in this thesis. This measure is then used to attenuate under-steer in the vehicle. It was found that fractional drop is very robust to changes in vehicle, tire and road parameters and does not require a vehicle model to predict vehicle behavior. Fuzzy logic is then used to filter and control signal flow as well as obtain efficient brake actuation for a stability controller.

The controller is shown to significantly improve the road holding capability of a vehicle. It uses only real-time, easily measurable signals (lateral acceleration, yaw rate and steering wheel angle), to make control decisions and does not use a vehicle or tire model to estimate vehicle states. An experimentally validated vehicle model, a BMW Mini, and several other vehicle models from CarSim were used to test the robustness of the controller. The same algorithm was used for all cases. It was shown that the controller

consistently improves the vehicle performance in situations of limit under-steer. It improves the maximum possible speed for negotiating a given curve by 4 to 11%.

Finally, the under-steer controller was combined with an existing fuzzy logic based over-steer controller, with modifications, to obtain a model-free ESC system. It was shown that the combined ESC has comparable performance to the pure over-steer controller in case of an over-steer situation while adding the ability to control under-steer. The model-free controller is also shown to have significant advantage over a model-based CarSim ESC system.

#### Future Work

The next stage of development should focus on developing the simulation based controller into a fully operational prototype ESC system. Validation of the control algorithm should be done using actual vehicle tests. The algorithm may need to be tuned for signal noise as well as response lag in the vehicle. An additional safety measure for when the driver over-reacts should be developed.

A unified and optimized braking strategy should be developed that maximizes grip at individual tires. Patterns in wheel speed may be investigated to this end. Integration of this strategy into the existing control algorithm should improve vehicle performance. Addition of other actuation methods such as traction control and active anti-roll should be investigated.

## APPENDICES

## Appendix A

### Vehicle Parameters

Vehicle parameters for the different vehicle models used in this work are listed in Table A.1. Tire data is presented in Appendix B.

**Table A.1 Vehicle Parameters**

Parameter	Units	Nominal BMW Mini	Degraded Front Tires BMW Mini	GVW BMW Mini	CarSim Sedan	CarSim SUV
<b>Inertial Properties:</b>						
Total Vehicle Mass	kg	1323.45	1323.45	1852.93	1530	1920
Sprung Mass	kg	1071.45	1071.45	1600.83	1370	1650
Front Weight per Wheel	N	3893.59	3893.59	5451.03	4424	4959
Rear Weight per Wheel	N	2595.73	2595.73	3634.02	3078	4458.7
CG Height	m	0.517	0.517	0.517	0.54	0.781
Yaw Moment of Inertia	kg-m <sup>2</sup>	1750	1750	2450	4605	3763.2
<b>Tire Properties:</b>						
Front Effective Rolling Radius	mm	290	290	290	335	393
Rear Effective Rolling Radius	mm	290	290	290	335	393
<b>Vehicle Dimensions:</b>						
Wheelbase	m	2.468	2.468	2.468	2.78	3.05
Front Track Width	m	1.453	1.453	1.453	1.55	1.575
Rear Track Width	m	1.475	1.475	1.475	1.55	1.575

## Appendix B

### Tire Data

The tire data for the various tire sets used in the vehicle models is presented in this appendix. The BMW Minis use OE 205/45 R17 Run-flat Goodyear tires. The degraded tires case is achieved by reducing this data set by a factor of 0.25. The Mini tire data is shown in Figures B.1 to B.4. This data was obtained in flat track testing of the tires. The tire data for the CarSim Sedan and SUV are shown in Figures B.5 to B.8.

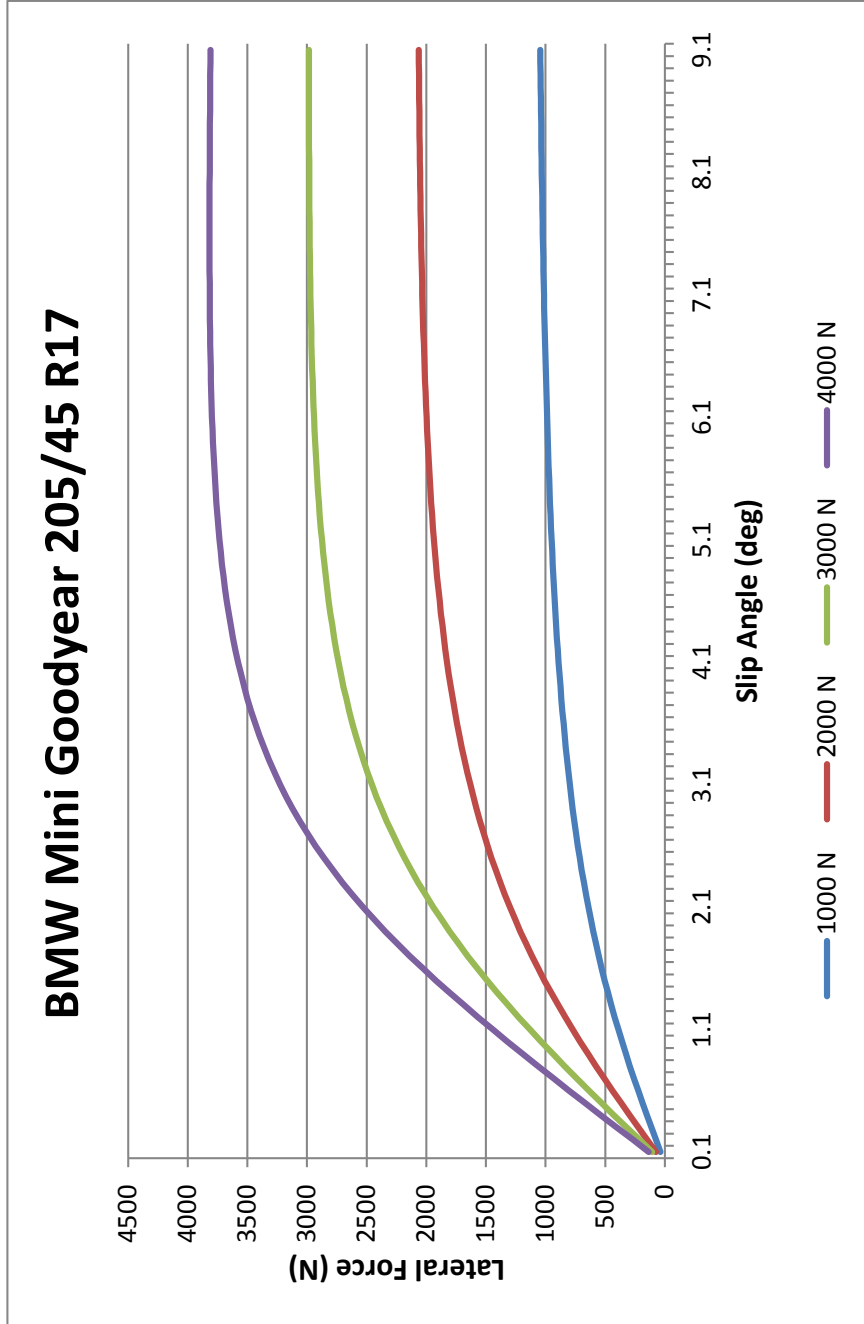


Figure B.1 BMW Mini: Nominal:  $F_y$  vs.  $\alpha$

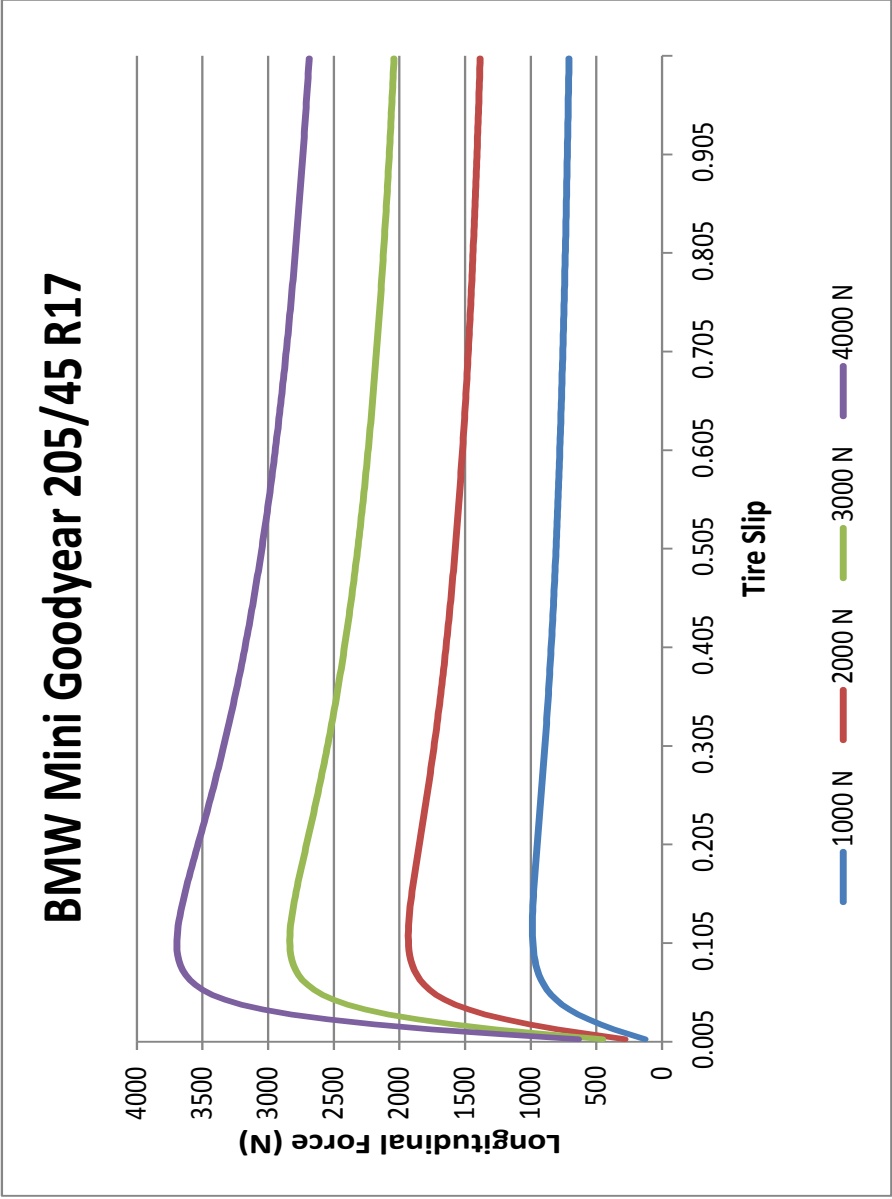


Figure B.2 BMW Mini: Nominal: Fx vs.  $\kappa$



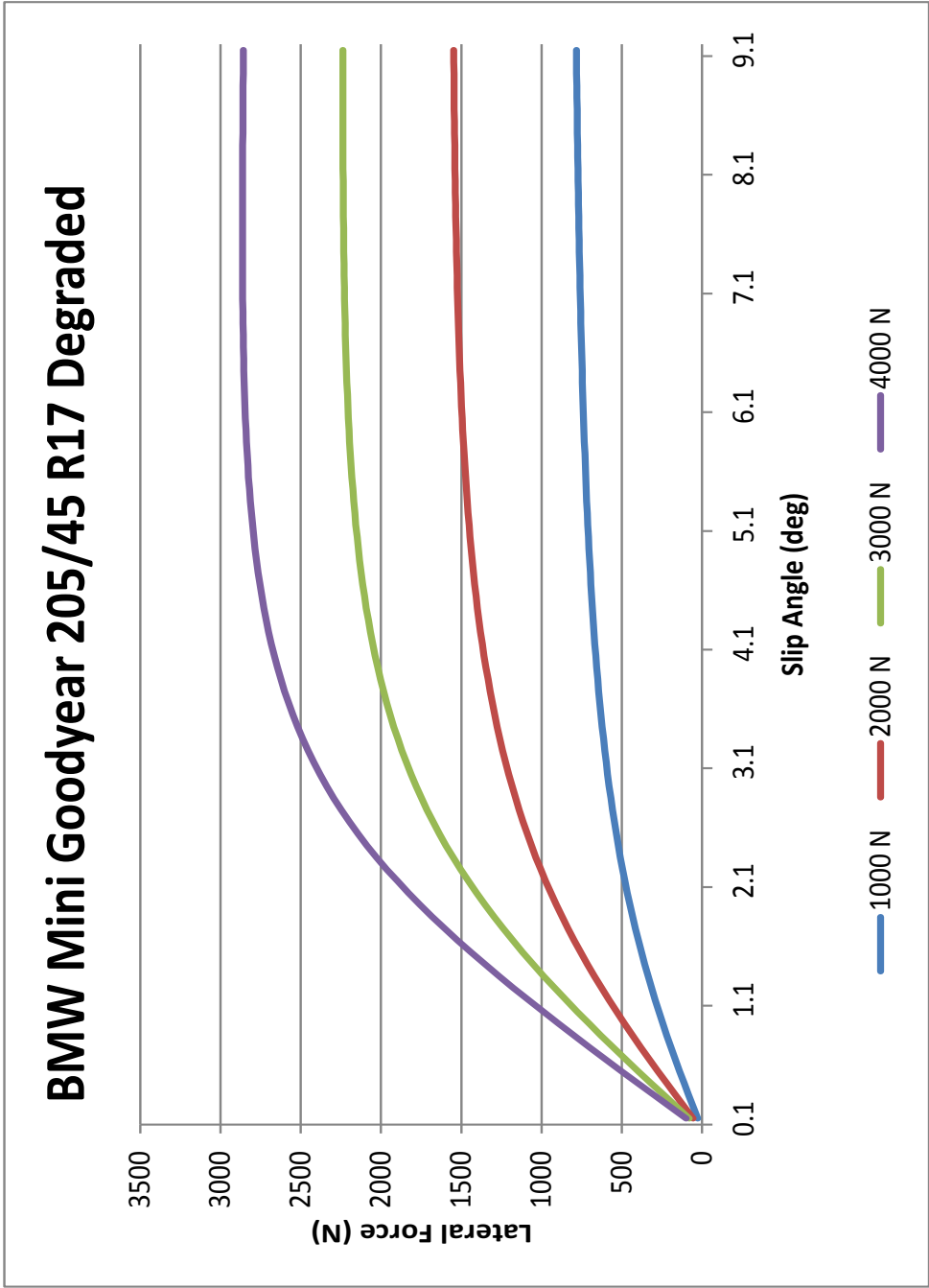


Figure B.3 BMW Mini: Degraded Tires:  $F_y$  vs.  $\alpha$

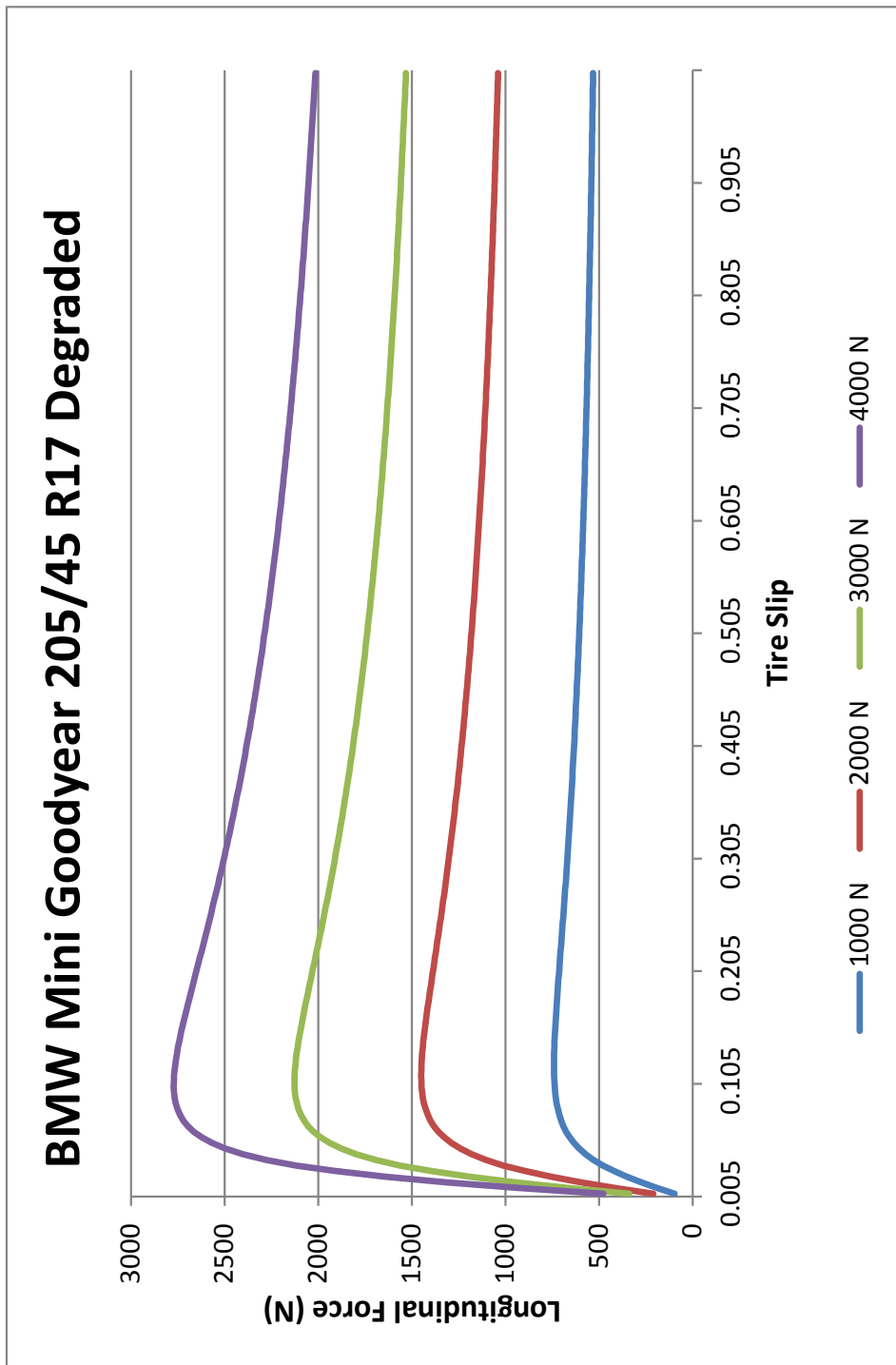


Figure B.4 BMW Mini: Degraded Tires:  $F_x$  vs.  $\kappa$

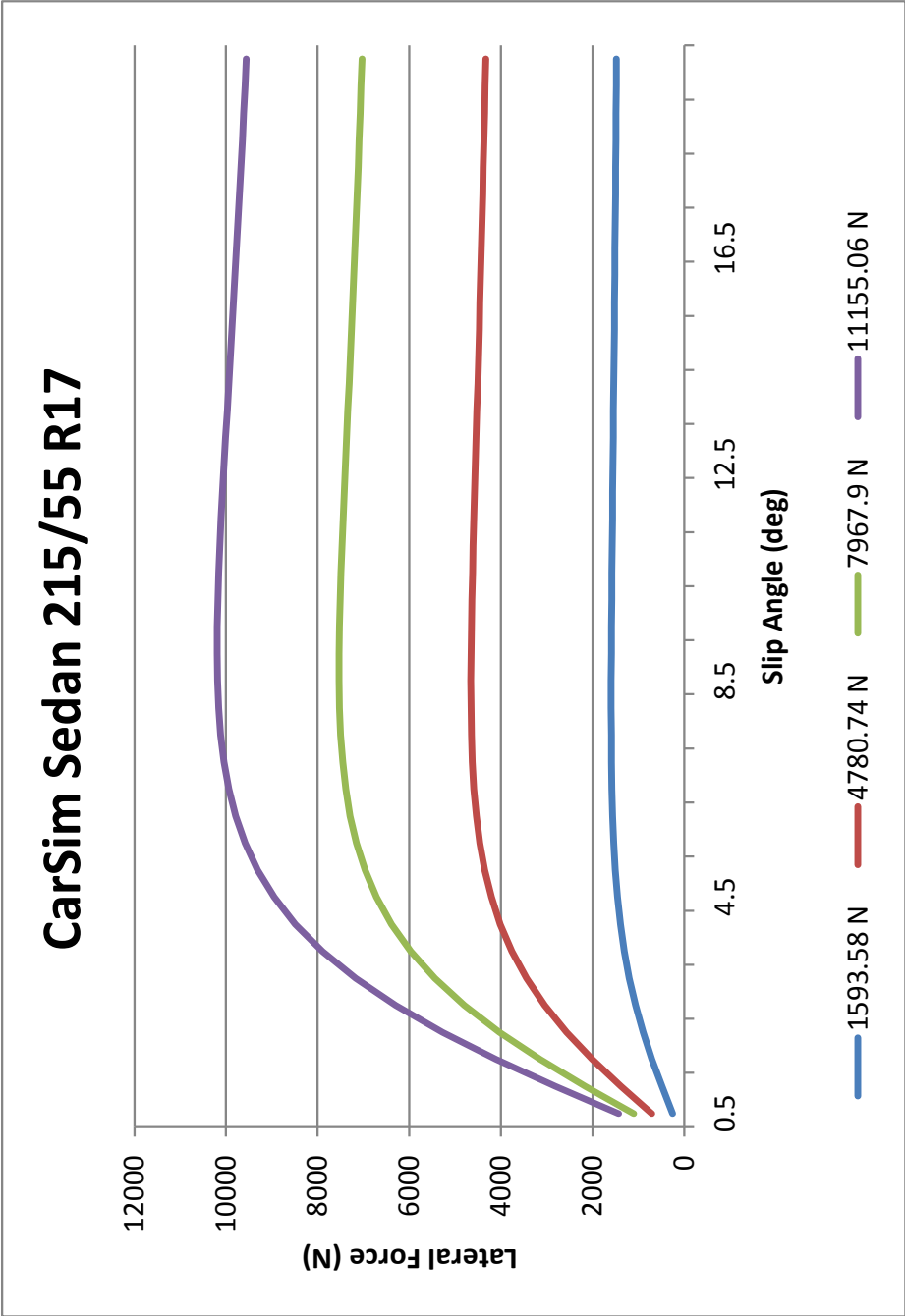


Figure B.5 CarSim Sedan: Nominal:  $F_y$  vs.  $\alpha$

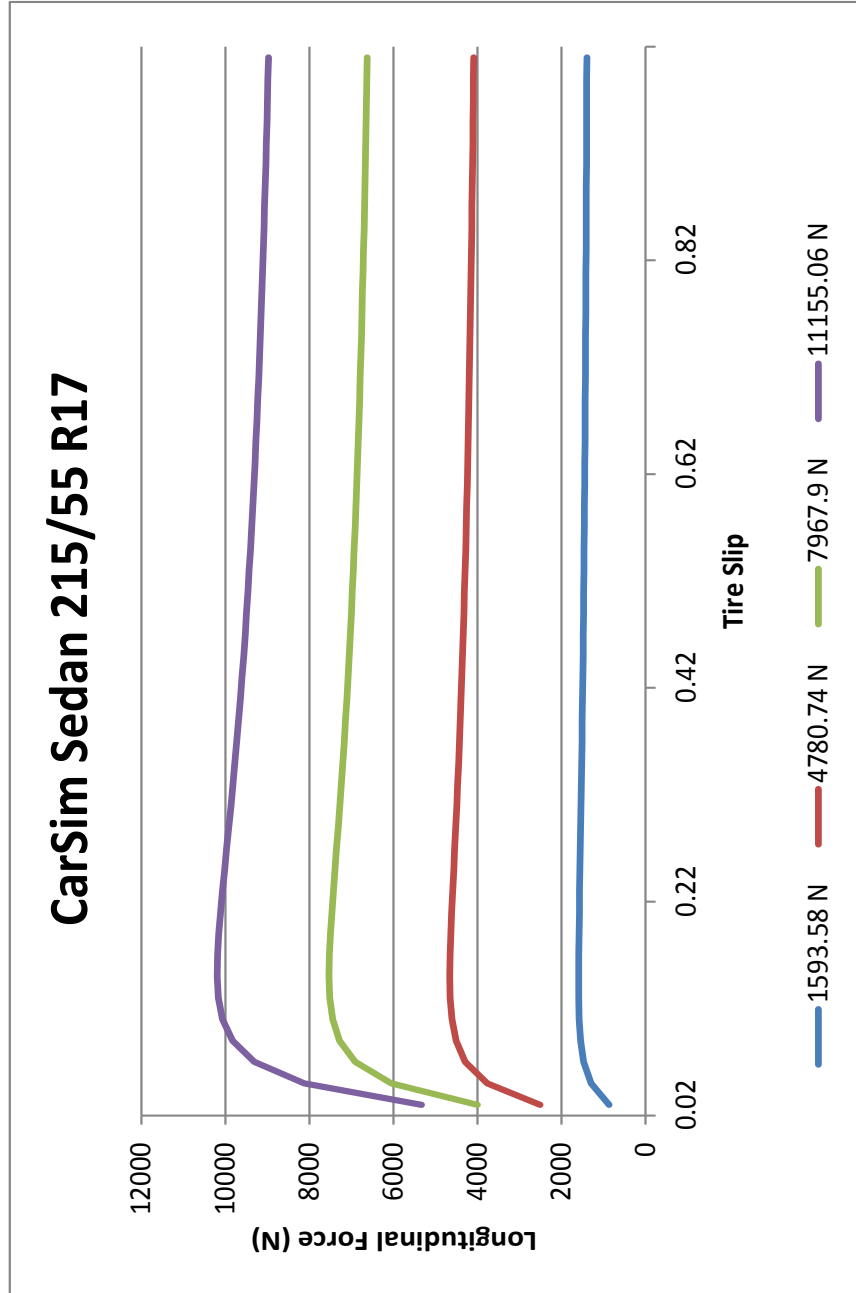


Figure B.6 CarSim Sedan: Nominal: Fx vs.  $\kappa$

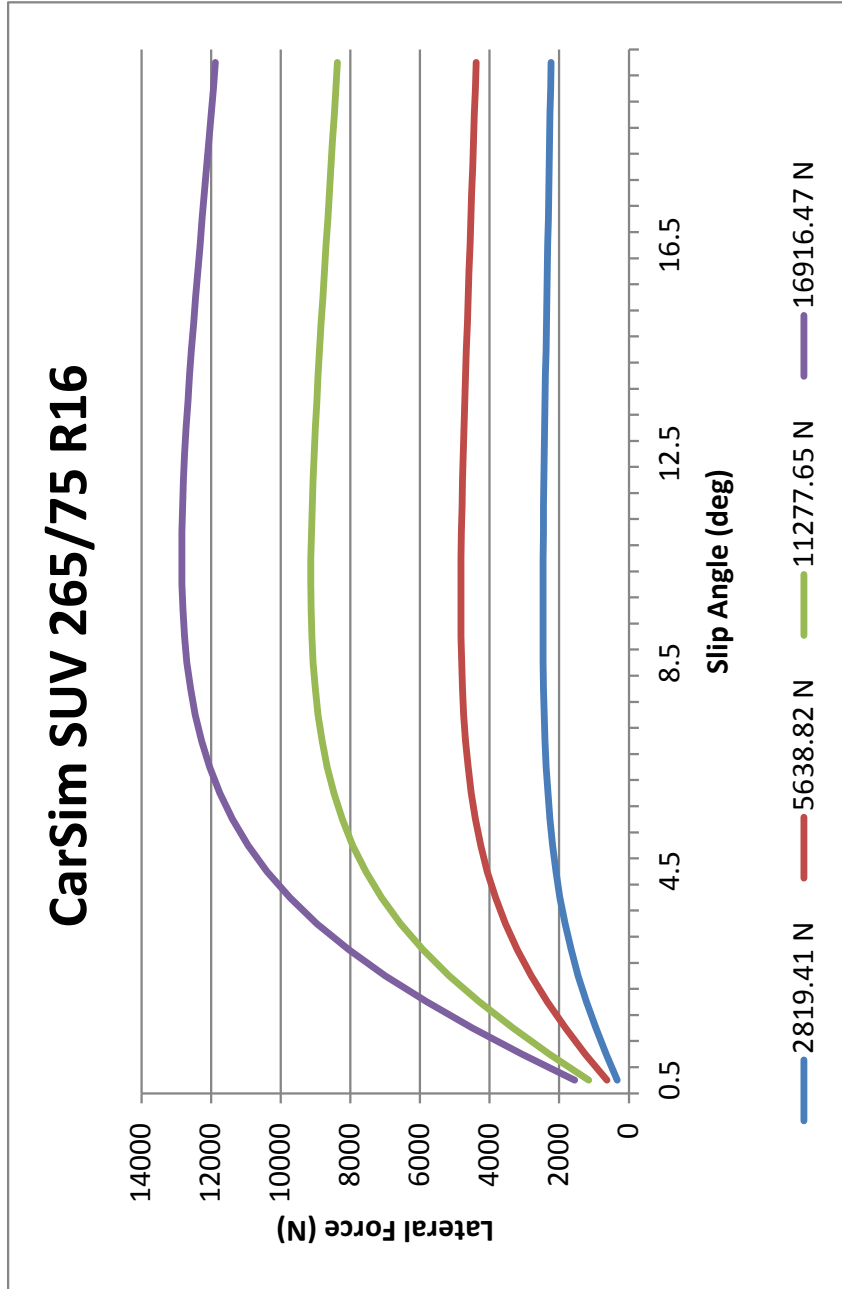


Figure B.7 CarSim SUV: Nominal:  $F_y$  vs.  $\alpha$

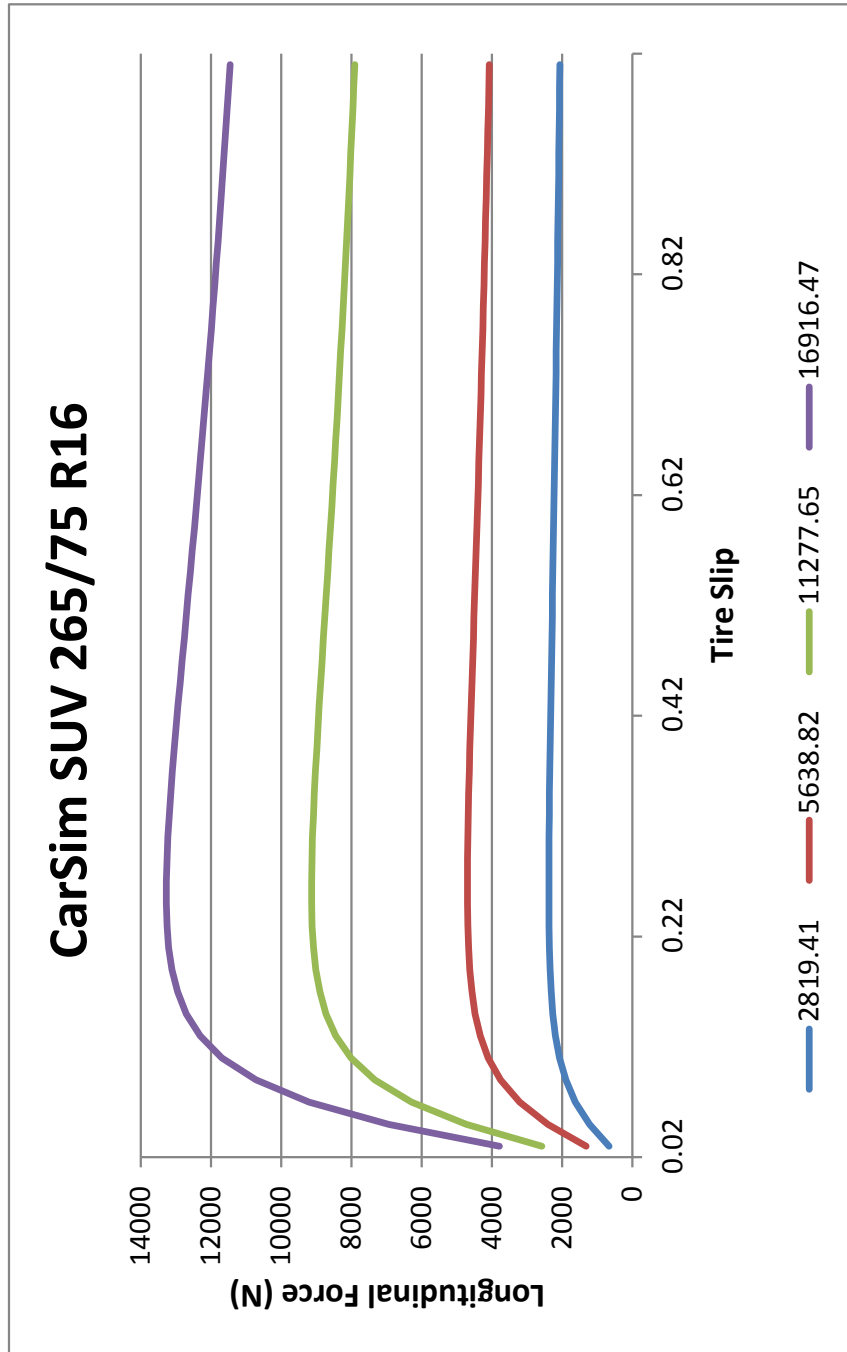


Figure B.8 CarSim SUV: Nominal: Fx vs.  $\kappa$

## Appendix C

### MATLAB and Simulink Documentation

This section details the Simulink model of the controller along with the subsystems and the associated MATLAB codes. An overview of the controller is provided in Figure

C.1. The controller has four main sections:

- Input-Output Interface with CarSim
- Controller
- Actuator
- CarSim ABS

The input and output interface is used to import the measured signals from vehicle model and to export the control signals, brake pressure and engine throttle.

The CarSim ABS (Figure C.2) system is included in the Simulink model so that the under-steer override, which is the line pressure in the brakes, can be applied at the appropriate section in the braking system. The Controller and Actuator modules have been discussed in detail in Chapter 3.

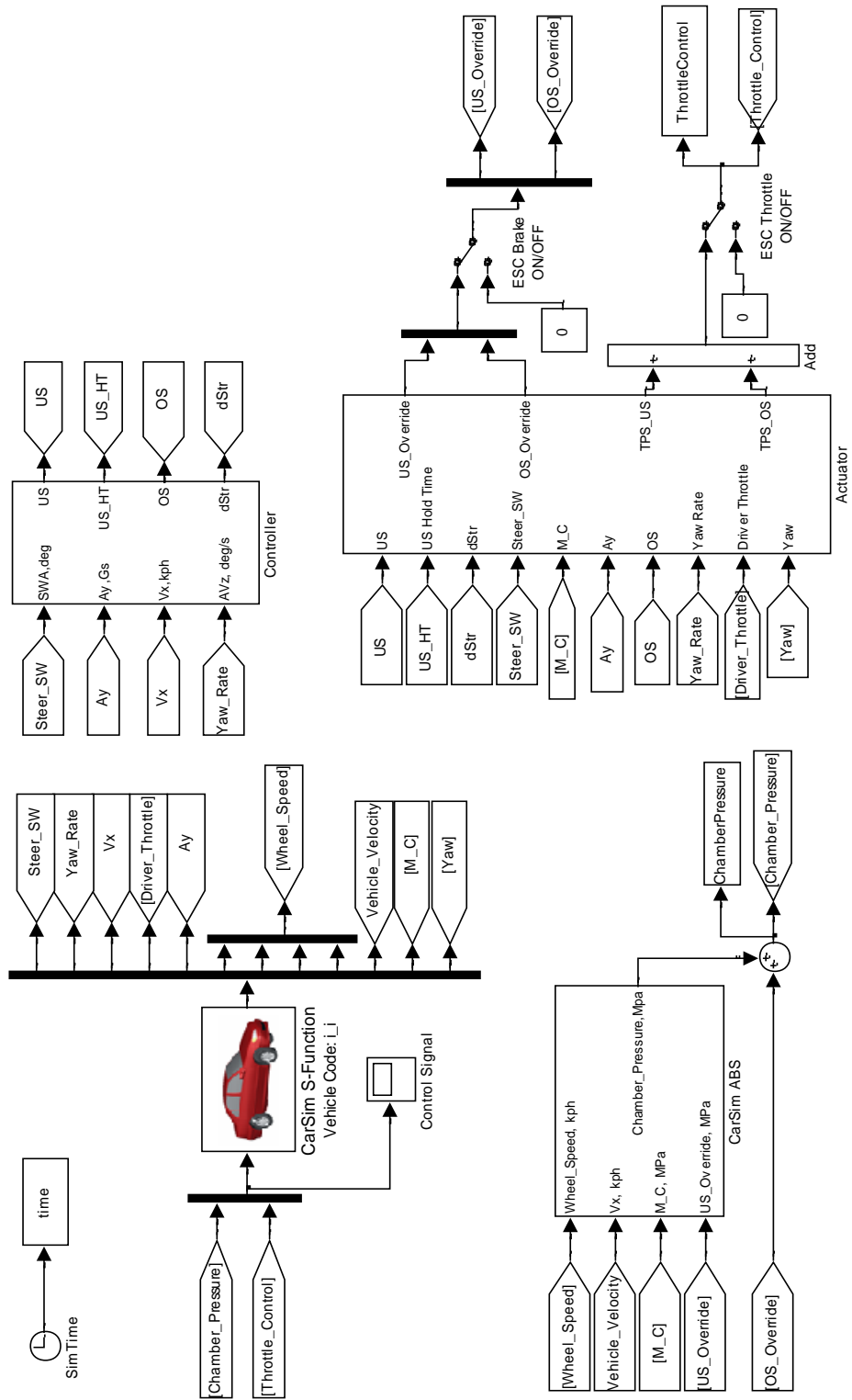


Figure C.1 Complete ESC: Overview



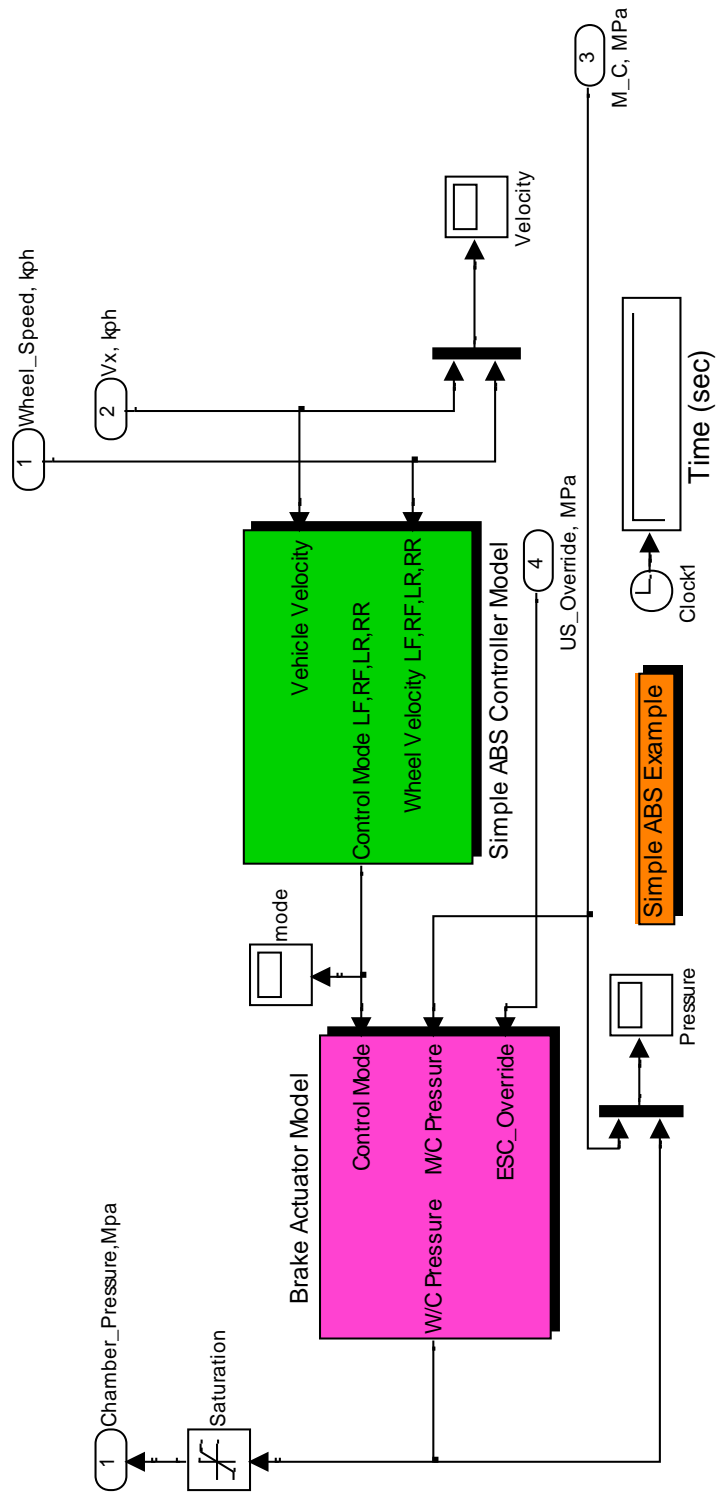


Figure C.2 CarSim ABS

## Control Module

The control module for the Fuzzy C-ESC has subsystems for both under-steer and over-steer. The working of the various under-steer subsystems in the control module has been explained in detail in Chapter 3. An overview of the control module is included in Figure C.3. A hold block (Figure C.4) is placed within both US and OS control modules and is used to keep track of the start and end of every under-and over-steer event respectively. The two signals are sent to the decision module to generate the final under-and over-steer numbers used for brake actuation. The associated MATLAB code is attached below.

### **Decision Module: Embedded MATLAB script**

```
function [US,OS] = fcn(US_HT,USN,OSN,OS_HT)
% This block supports an embeddable subset of the MATLAB language.
% See the help menu for details.

% US = 0;
% OS = 0;

if USN > 0 && OSN > 2 % Both US & OS numbers will initiate
actuation
    if US_HT > OS_HT % Under-steer event starts before over-
steer

        US = USN;
        OS = 0;

    else

        US = 0;
        OS = OSN;

    end
else
    US = USN;
    OS = OSN;

end
```

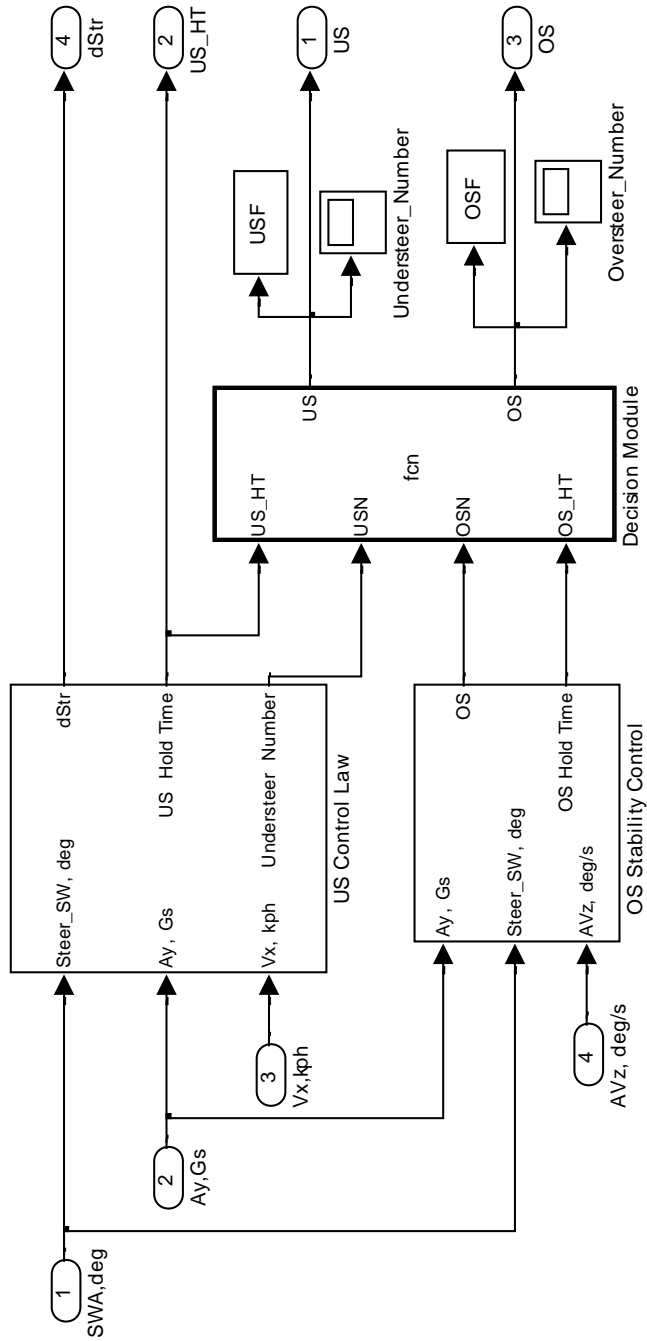


Figure C.3 ESC Control Module

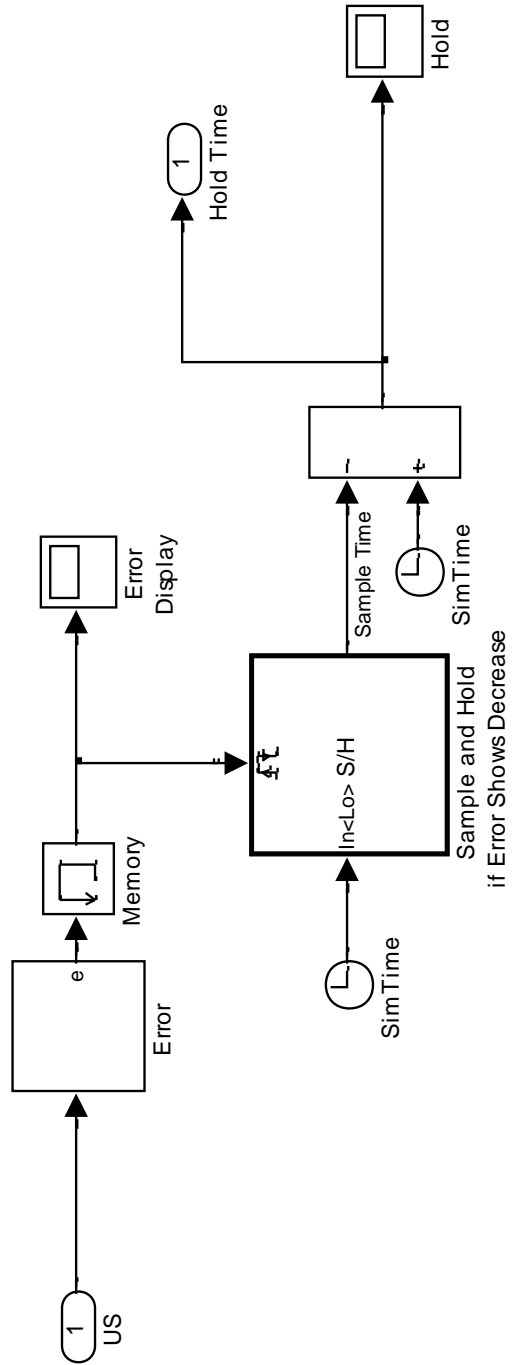


Figure C.4 US Hold Time

## Actuator Module

The actuator module for the Fuzzy C-ESC shown in Figure C.5 includes sections for under-steer and over-steer attenuation. The throttle control block (Figure C.6) has two embedded MATLAB scripts. The first is used to store the last ‘safe’ value of throttle input and the second is used to over-ride and re-introduce throttle as required.

The brake force distributor has an embedded MATLAB script that assigns brake pressure at individual wheels based on the value of understeer and lateral acceleration of the vehicle. The MATLAB code associated with the brake pressure assignment is attached below. The overview of the brake force distributor is shown in Figure C.7.

### **Safe Throttle: Embedded MATLAB Script**

```
function k2 = fcn(driver_throt,US,Hold,Time,k1)
% This block supports an embeddable subset of the MATLAB language.
% See the help menu for details.

if US <= 0 && Time <= Hold % before the first instance of under-
steer
    k2 = driver_throt;      % driver throttle is passed

else
    k2 = k1;                % after under-steer is detected the last
end                        % 'safe' value of throttle is held
```

### **Throttle Over-ride: Embedded MATLAB Script**

```
function eng_throt = fcn(k,driver_throt,US,Hold,Time)
% This block supports an embeddable subset of the MATLAB language.
% See the help menu for details.
```

```

    if US > 0 && Time <= Hold
        eng_throt = -driver_throt;    % throttle is cut when US is
detected

    elseif US <= 0 && Time > Hold    % throttle is re-introduced in
steps
        if Hold <= 2
            eng_throt = -driver_throt;
        elseif Hold > 2 && Hold <= 3
            eng_throt = -driver_throt + 0.2 * k;
        elseif Hold > 3 && Hold <= 5
            eng_throt = -driver_throt + 0.8 * k;
        elseif Hold > 5 && Hold <= 8
            eng_throt = -driver_throt + 1.2 * k;
        else
            eng_throt = 0;
        end

    elseif US <= 0 && Time <= Hold    % all intervention is removed
        eng_throt = 0;

    else
        eng_throt = -driver_throt;

    end
end

```

### **Brake Force Distributor: Embedded MATLAB Script**

```

function [fl,fr,rl,rr] = fcn(US,str_rate,swa,ht,brk,po,pf,OS)
% This block supports an embeddable subset of the MATLAB language.
% See the help menu for details.

k = 0.4;    % braking reduction factor at the rear axle in the
ABS
b = 1.2;    % ratio of brake pressure at the inside wheel to the
           % outside wheel per axle
c = 1;    % front brake status

% Inside to outside brake distribution based on US number
if US < 3.5
    b = 1.2;
elseif US >= 3.5 && US < 4
    b = 1.5;
elseif US >= 4 && US < 4.5
    b = 2.0;
elseif US >= 4.5 && US < 5
    b = 2.5;
elseif US >=5
    b = 3.5;

```

```

end

% Decide front brake status based on US number
if US <= 5
    c = 1;
else
    c = 0;
end

% Assign brake pressure to individual wheels and override driver
applied brake (brk), if any

if US > 0
    if swa > 0 && str_rate >= 0
        rl = -brk + po*b/k;
        rr = -brk + po/k;
        fl = -brk + po*b*pf*c;
        fr = -brk + po*pf*c;
    elseif swa < 0 && str_rate <= 0
        rl = -brk + po/k;
        rr = -brk + po*b/k;
        fl = -brk + po*pf*c;
        fr = -brk + po*b*pf*c;
    elseif swa >= 0 && str_rate < 0
        rl = -brk + po;
        rr = -brk + po;
        fl = -brk + po;
        fr = -brk + 1.2*po;
    elseif swa <= 0 && str_rate > 0
        rl = -brk + po;
        rr = -brk + po;
        fl = -brk + 1.2*po;
        fr = -brk + po;
    else
        rl = -brk + po;
        rr = -brk + po;
        fl = -brk + po;
        fr = -brk + po;
    end

elseif US <= 0 && ht < 1.5 && OS <= 2
    fl = -brk;
    rl = -brk;
    rr = -brk;
    fr = -brk;

elseif OS > 2
    fl = -brk;
    rl = -brk;
    rr = -brk;
    fr = -brk;

else
    fl = 0;

```

```
rl = 0;  
rr = 0;  
fr = 0;  
end
```



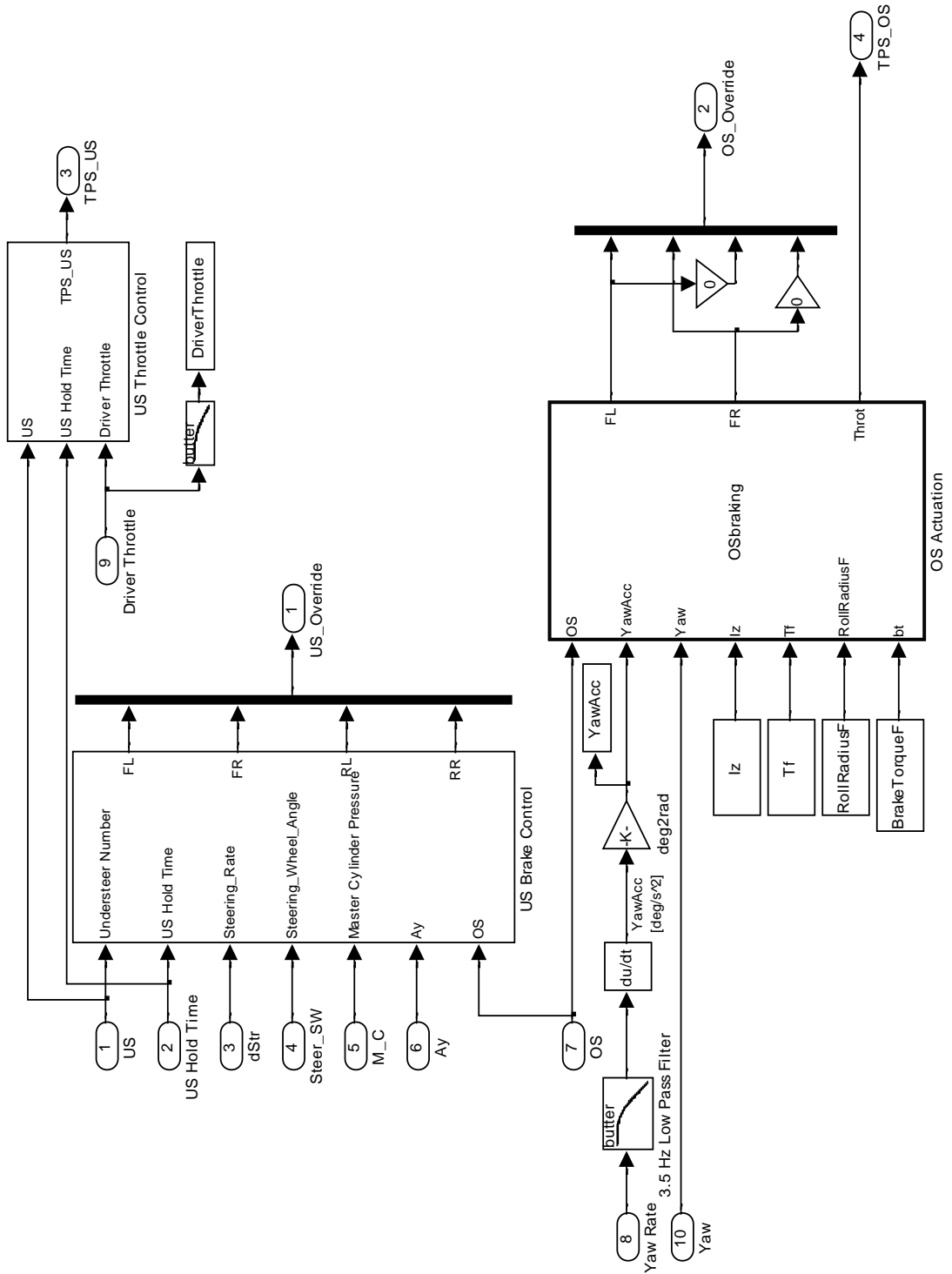


Figure C.5 Actuator Module

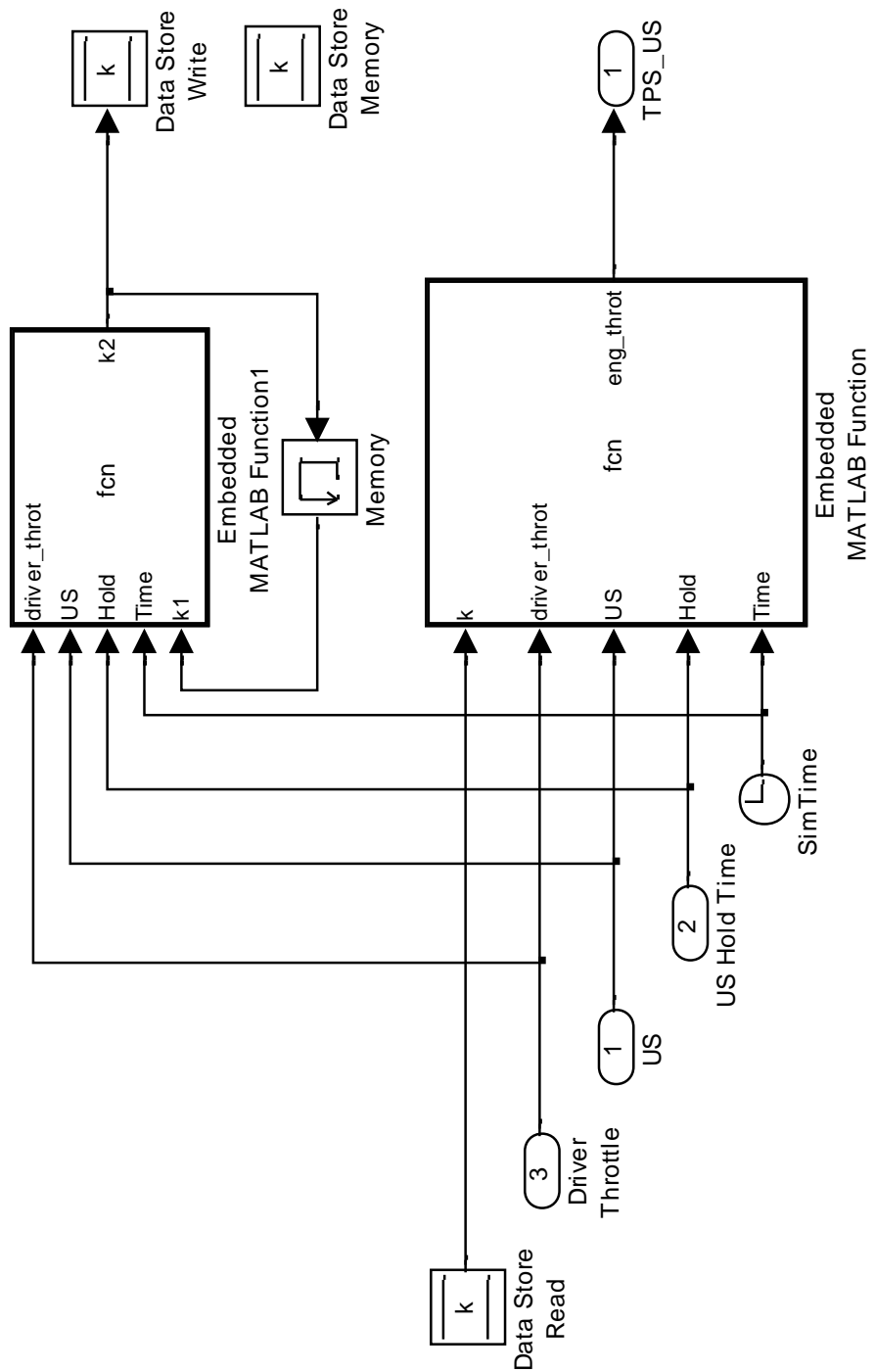


Figure C.6 US Throttle Control

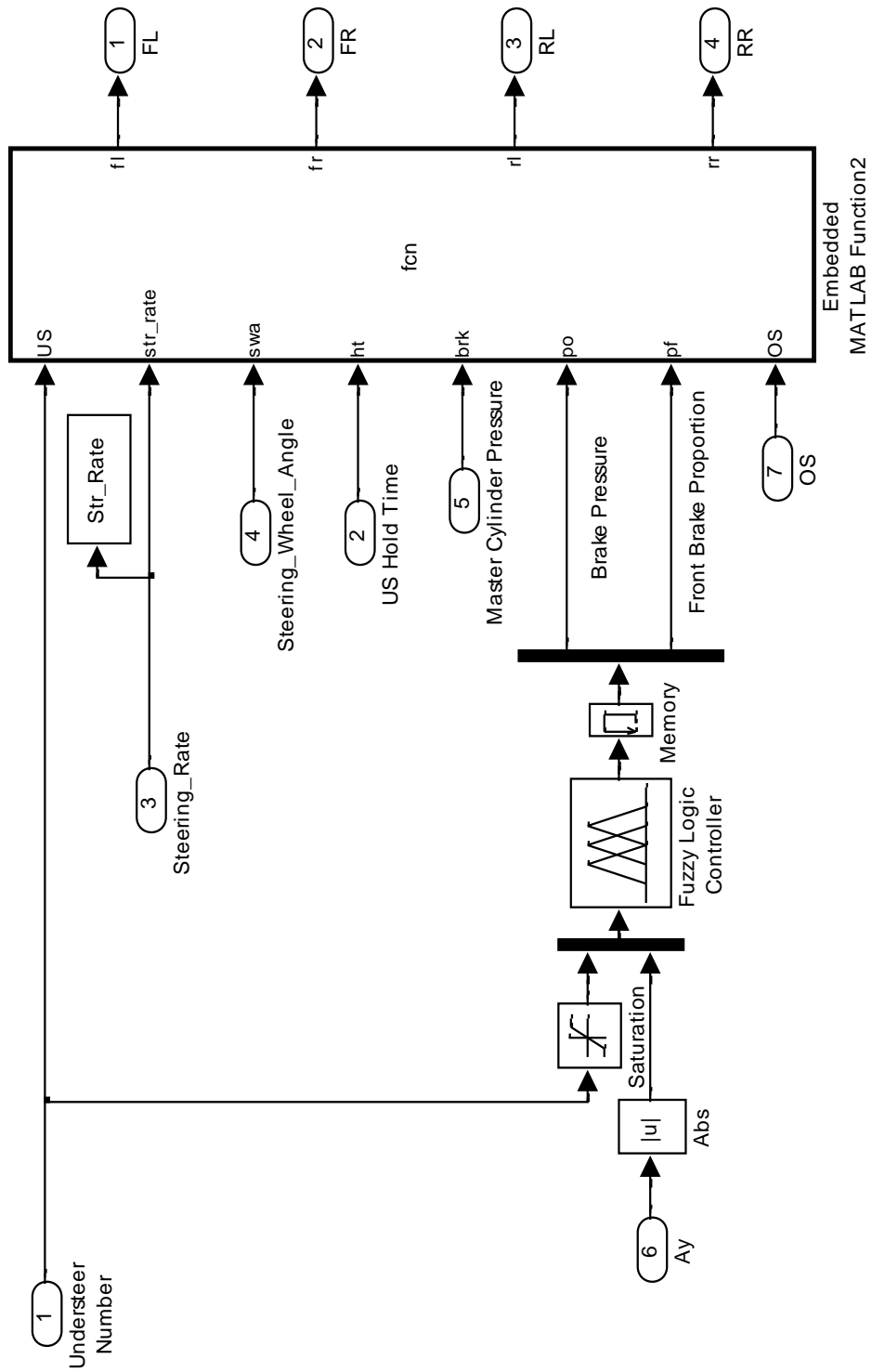


Figure C.7 Brake Force Distributor

## Appendix D

### Fuzzy Inference Systems

The fuzzy inference systems developed in this work are detailed in this section. The four FISs that will be discussed are:

1. Indicated Under-steer
2. Under-steer
3. Modified Possible Over-steer
4. Brake Balance

The unmodified version of FIS ‘Over-steer Indicating Fuzzy Logic’ imported from Anderson’s work <sup>[4, 5]</sup> has not been discussed here. The reader is referred to [4,5] for details.

#### **Indicated Under-steer**

This FIS is placed in the Under-steer Computation block (Figure D.1) and transforms the fractional drop computed into an under-steer number between 0 and 10. The FIS has one input, ‘NormE’ (Fractional Drop), and one output, ‘IUS’. The input and output membership functions are shown in Figure D.2.

The FIS has one rule and the evaluation can be understood with an example. Let the input value be ‘0.33’. The fuzzy rule is:

If ‘NormE’ is *high* Then ‘IUS’ is *high*

Figure D.3a shows the input variable with an input ‘0.33’ and the resulting membership value of ‘0.333’. There is only one input and hence no fuzzy operators.

Therefore, the degree of membership for the output variable is ‘0.333’. The output membership function is truncated such that the highest degree of membership is ‘0.333’ (Figure D.3b).

The aggregate output membership function is the same as that for the fuzzy rule. The defuzzification method used for this FIS is ‘smallest of maximum’. Hence, the smallest absolute output value associated with the maximum degree of membership in the aggregate output MF is the defuzzified output (Figure D.3c). For an input value of 0.33, the defuzzified output is ‘3’.

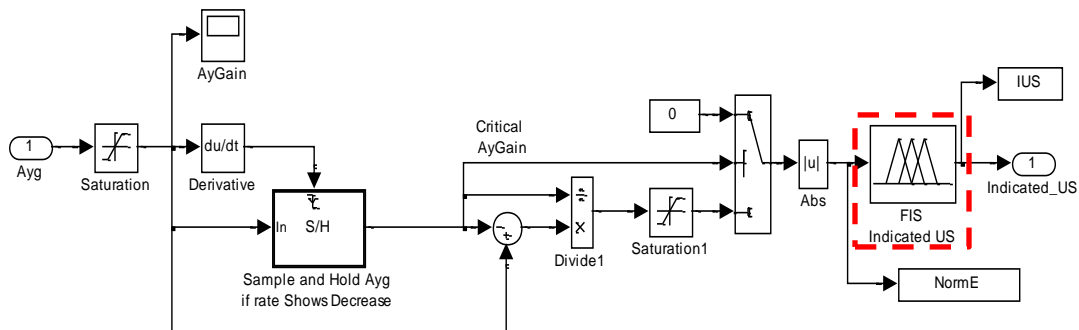


**Figure D.1 Under-Steer Computation Block**

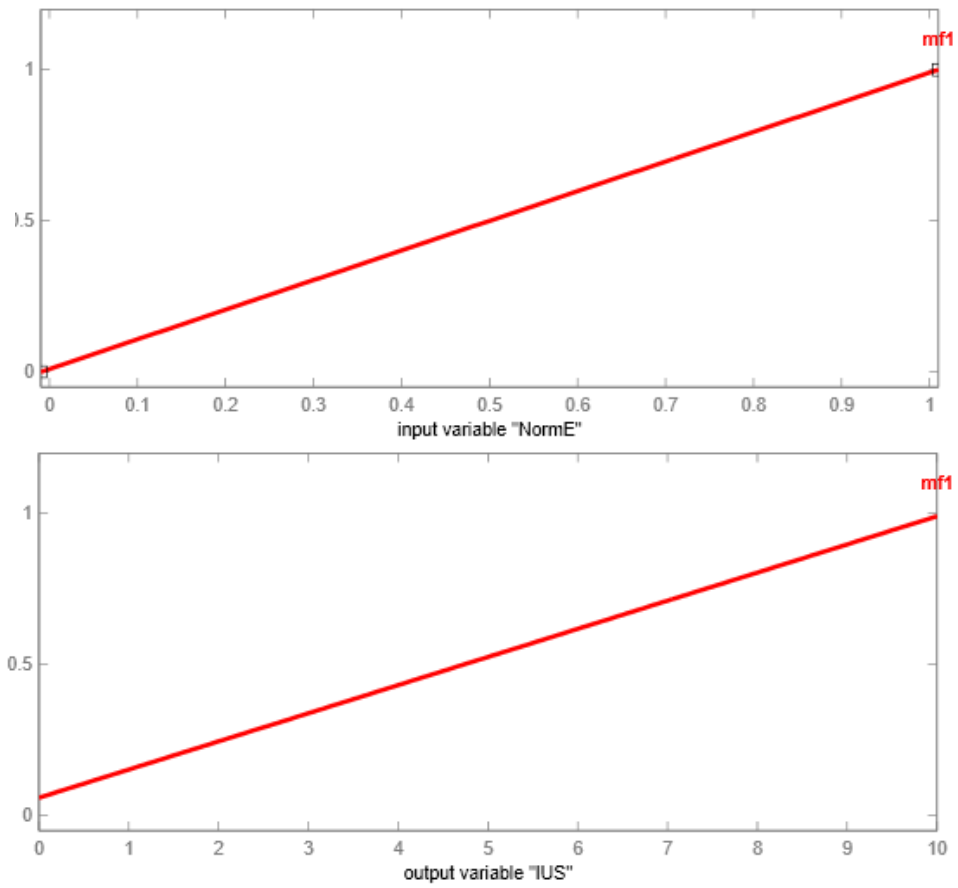
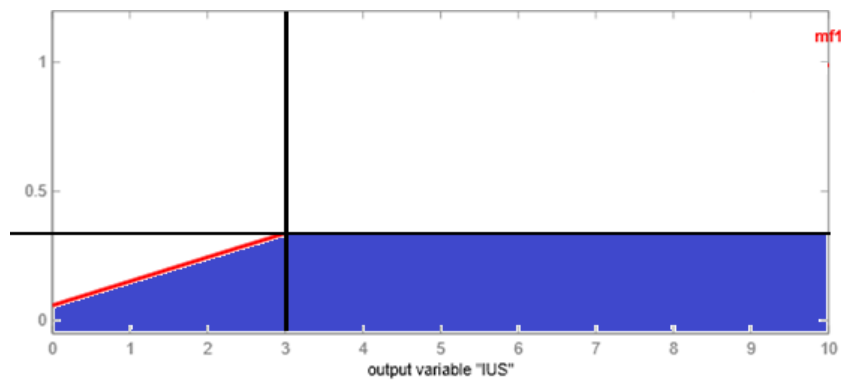
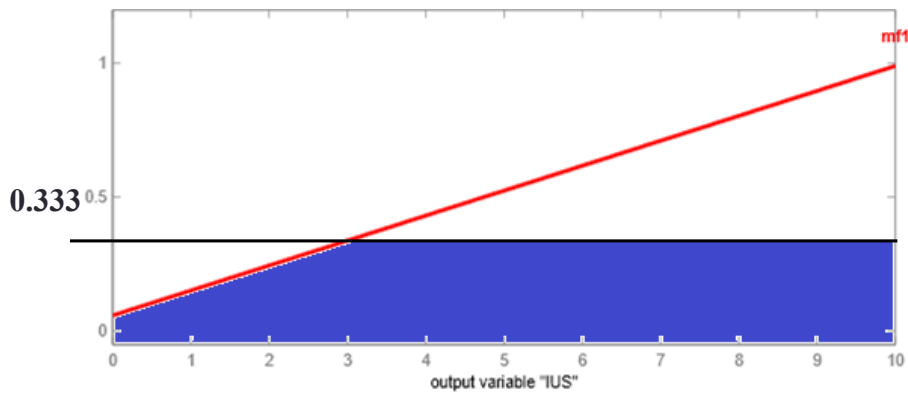
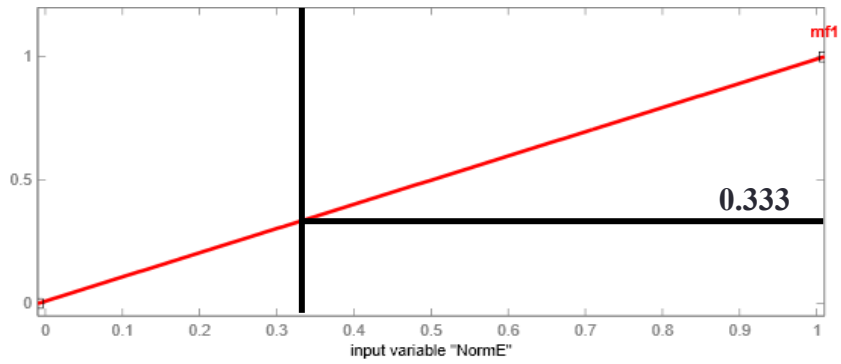


**Figure D.2 FIS Indicated Under-steer: Input and Output Membership Functions**

NormE = 0.33



Indicated Under-steer = 3

Figure D.3 Indicated Under-steer: Rule 1 Evaluation and Defuzzified Output

## Under-steer

This FIS is placed in the Under-Steer control module (Figure D.4). It is used to prevent unnecessary brake actuation during straight line and parking lot driving. The FIS has three inputs:

- Vehicle speed,  $V_x$  (kph)
- Steering Wheel Angle, SWA (deg)
- Indicated Under-steer, IUS

It has one output, 'Under-steer'. The input and output membership functions are shown in Figure D.5. The FIS has only one rule. Consider input values:

$$V_x = 80 \text{ kph}$$

$$\text{SWA} = 30 \text{ deg}$$

$$\text{IUS} = 3$$

The fuzzy rule for the FIS is:

If ' $V_x$ ' is *high* AND 'SWA' is *high* AND 'IUS' is *high* then 'Under-steer' is *high*

Figure D.5 shows the input and output membership values for the given set of input values. The membership values for  $V_x$  and SWA are '1' where as the membership value for IUS is '0.306'. The fuzzy operator used is 'AND' and hence the smallest membership value from among the inputs (0.306) is assigned to the output. The truncated output membership function will have the highest degree of membership of 0.306.

The aggregate output membership function is the same as that seen in figure D.6d because there is only one rule. The defuzzification method used is 'smallest of maximum' and the defuzzified output value is '3.6'.



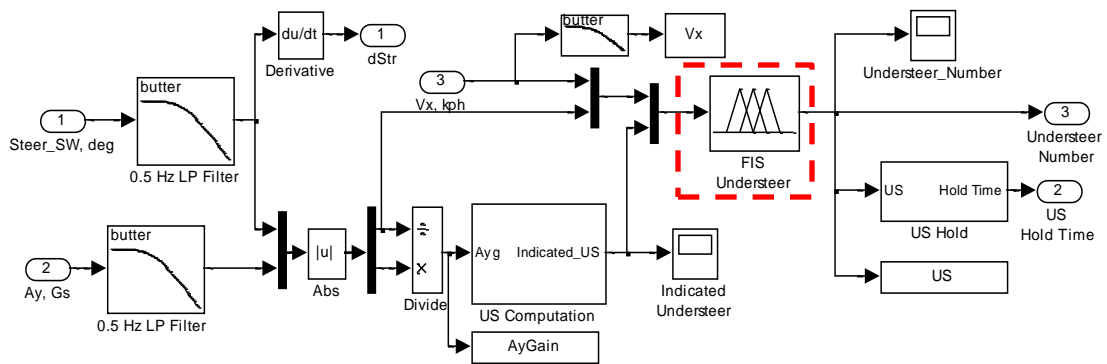
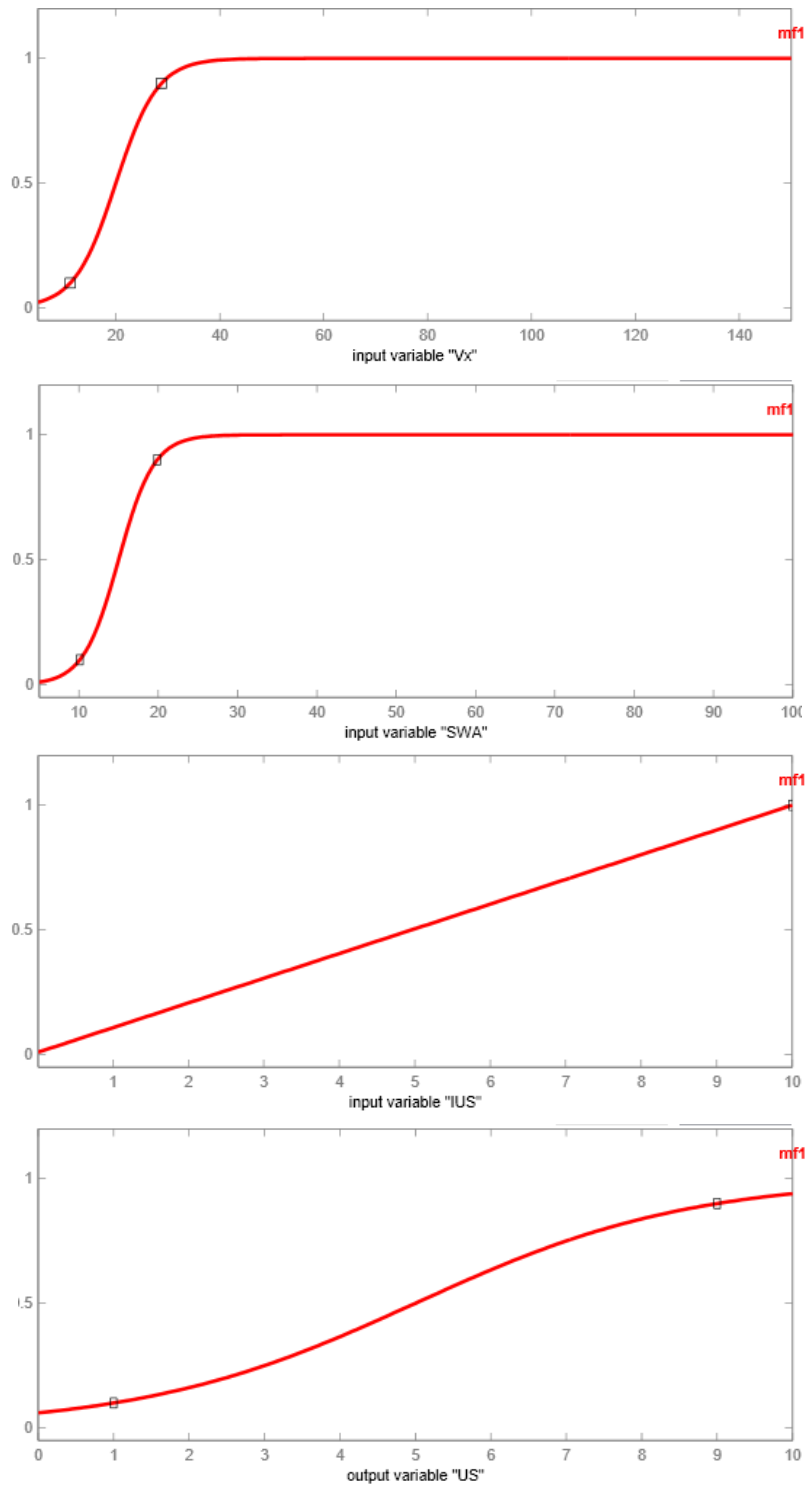
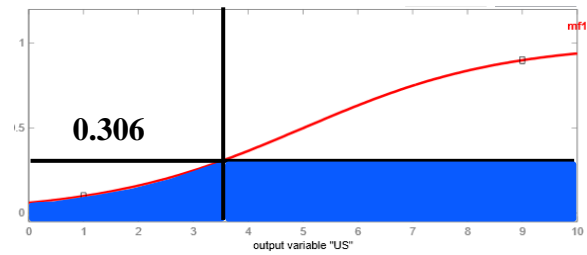
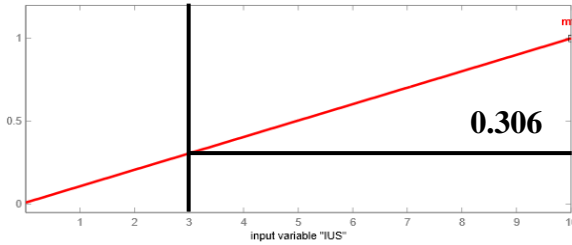
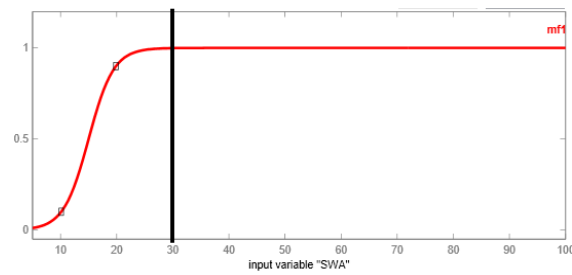
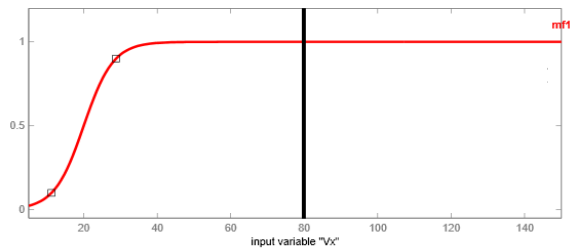


Figure D.4 Under-Steer Control Module



**Figure D.5 FIS Under-steer: Input and Output Membership Functions**



**Under-steer = 3.6**

**Figure D.6 Under-steer: Rule 1 Evaluation and Defuzzified Output**

## Possible Unstable Event

This FIS is placed in the ‘Over-steer Indicator’ block (Figure D.7) and computes the possibility of over-steer in the vehicle at any time. The FIS has two inputs and one output.

Inputs:

- Lateral Acceleration,  $A_y$  (Gs)
- Yaw Acceleration, YawAcc ( $\text{deg/s}^2$ )

Output:

- Event

The membership functions for the inputs and the output are shown in Figure D.8. The FIS has nine fuzzy rules:

1. If  $A_y$  is ‘Small’ *and* YawAcc is ‘Slow’ Then Event is ‘Stable’
2. If  $A_y$  is ‘Med’ *and* YawAcc is ‘Slow’ Then Event is ‘Stable’
3. If  $A_y$  is ‘Large’ *and* YawAcc is ‘Slow’ Then Event is ‘Mod\_Stable’
4. If  $A_y$  is ‘Small’ *and* YawAcc is ‘Med’ Then Event is ‘Stable’
5. If  $A_y$  is ‘Med’ *and* YawAcc is ‘Med’ Then Event is ‘Mod\_Stable’
6. If  $A_y$  is ‘Large’ *and* YawAcc is ‘Med’ Then Event is ‘Mod\_Unstable’
7. If  $A_y$  is ‘Small’ *and* YawAcc is ‘Fast’ Then Event is ‘Stable’
8. If  $A_y$  is ‘Med’ *and* YawAcc is ‘Fast’ Then Event is ‘Mod\_Unstable’
9. If  $A_y$  is ‘Large’ *and* YawAcc is ‘Fast’ Then Event is ‘Unstable’

Figure D.9 shows the input variable membership functions for input values [0.4 0.8] i.e.  $A_y = 0.4 \text{ Gs}$  and YawAcc =  $0.8 \text{ deg/s}^2$ . The lateral acceleration has non-zero

membership values for the ‘Small’ and ‘Med’ membership functions and the yaw acceleration has non-zero membership values for the ‘Med’ and ‘Fast’ membership functions. The FIS uses the ‘AND’ operator for all the rules and the smaller membership value from among the inputs will dictate the output membership value for each rule. Hence, rules 1, 2, 3, 6 and 9 will have zero membership value for the associated output membership functions. The evaluation of the fuzzy rules for the input values defined above is shown in Figure D.10.

The aggregate output membership function is obtained by overlapping the output membership areas for the rules 4, 5, 7 and 8. The defuzzification method used is the ‘centroidal’ method. The value associated with the centroid of the area of the aggregate output membership function is the final output value. For the given input the defuzzified output is ‘5.26’.

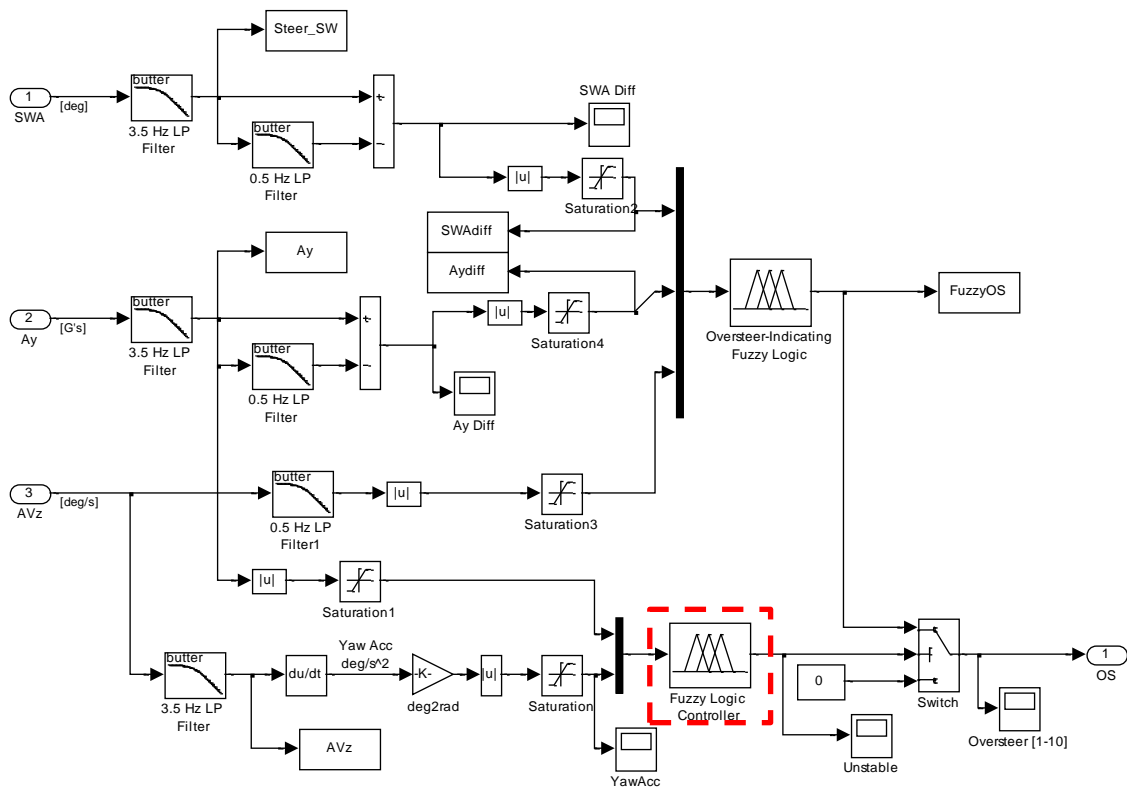
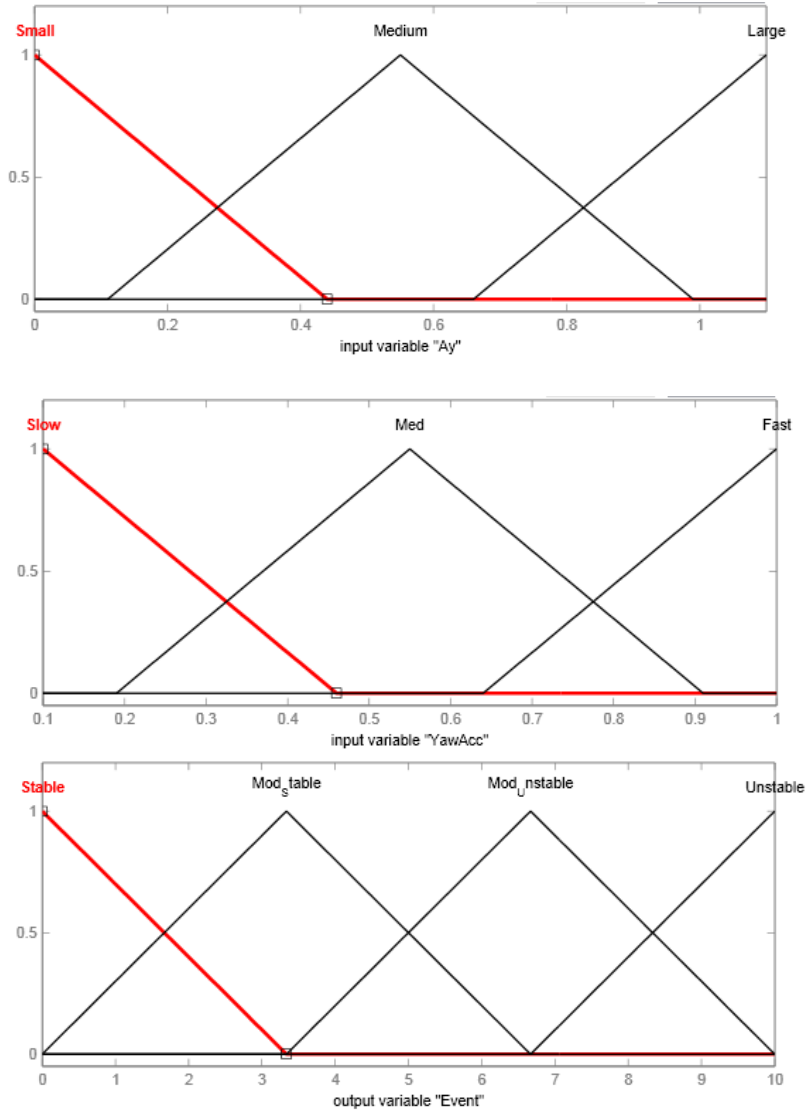


Figure D.7 Over-Steer Indicator block



**Figure D.8 FIS Possible Unstable Event: Input and Output Membership Functions**

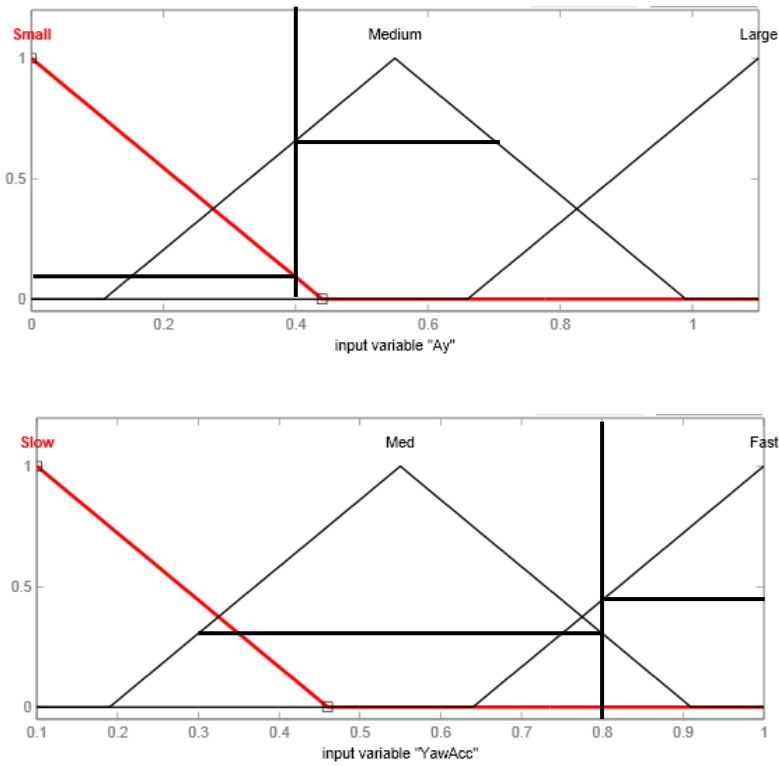


Figure D.9 Possible Unstable Event: Input Membership Functions for Input [0.4 0.8]

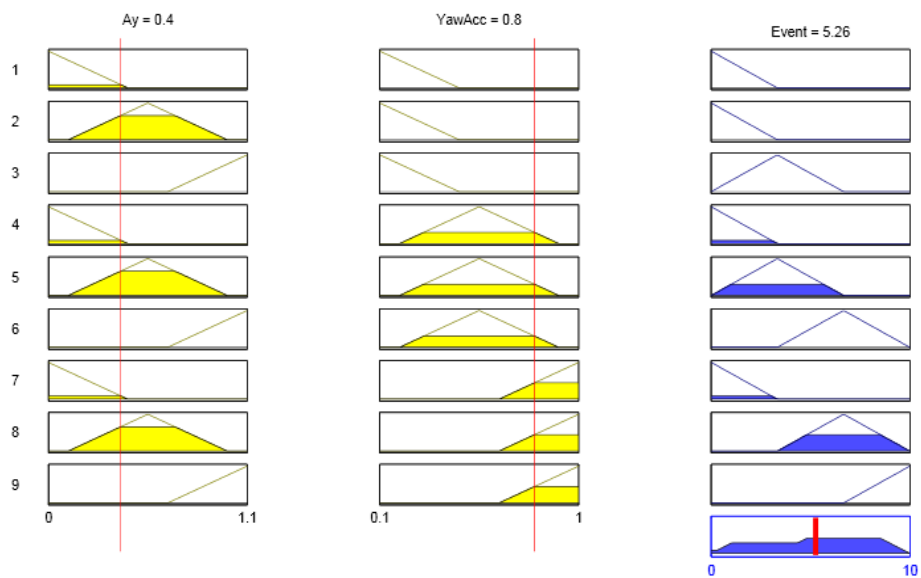


Figure D.10 Possible Unstable Event: Evaluation of Rules for Input [0.4 0.8]



## **Brake Balance**

This FIS is placed in the Under-Steer Brake Force Distributor block (Figure D.11) and is used to compute the brake distribution to the front axle during the first stage of braking as well as the nominal brake pressure during an under-steer event. The FIS has two inputs and two outputs.

Inputs:

- Under-steer, US
- Lateral Acceleration,  $A_y$  (Gs)

Outputs:

- Nominal Brake Pressure, Pressure (MPa)
- Front Brake Proportion, FrontBrake

The membership functions for the four variables are shown in Figure D.12. There are seven fuzzy rules for this FIS.

- If US is 'No' Then FrontBrake is 'High'
- If US is 'Low' Then FrontBrake is 'Med'
- If US is 'Med' Then FrontBrake is 'Low'
- If US is 'High' Then FrontBrake is 'No'
- If  $A_y$  is 'Low' Then Pressure is 'Low'
- If  $A_y$  is 'Med' Then Pressure is 'Med'
- If  $A_y$  is 'High' Then Pressure is 'High'

Figure D.13 shows the input variable membership functions for input values [1.5 0.8] i.e.  $US = 1.5$  and  $A_y = 0.8$  Gs. The under-steer number has non-zero membership values for 'Low' and 'med' membership functions and the lateral acceleration has non-zero membership values for the 'Med' and 'Large' membership functions.

In this FIS the two inputs do not interact and there is no operator used for any rule. For each rule, the membership value of the output membership function is the same as the membership value of the input membership function associated with that rule. Hence, rules 1, 4 and 5 will have zero membership value for the associated output membership functions. The evaluation of the fuzzy rules for the input values defined above is shown in Figure D.14.

The aggregate output membership function is obtained by overlapping the output membership areas for the rules 2, 3, 6 and 7 for Pressure and Front Brake separately. The outputs are aggregated separately and the defuzzification method used is the 'centroidal' method for both outputs. The value associated with the centroid of the area of the aggregate output membership function for each of the outputs is the final output value. For the given inputs the defuzzified outputs are Pressure = 0.55 and FrontBrake = 0.794.

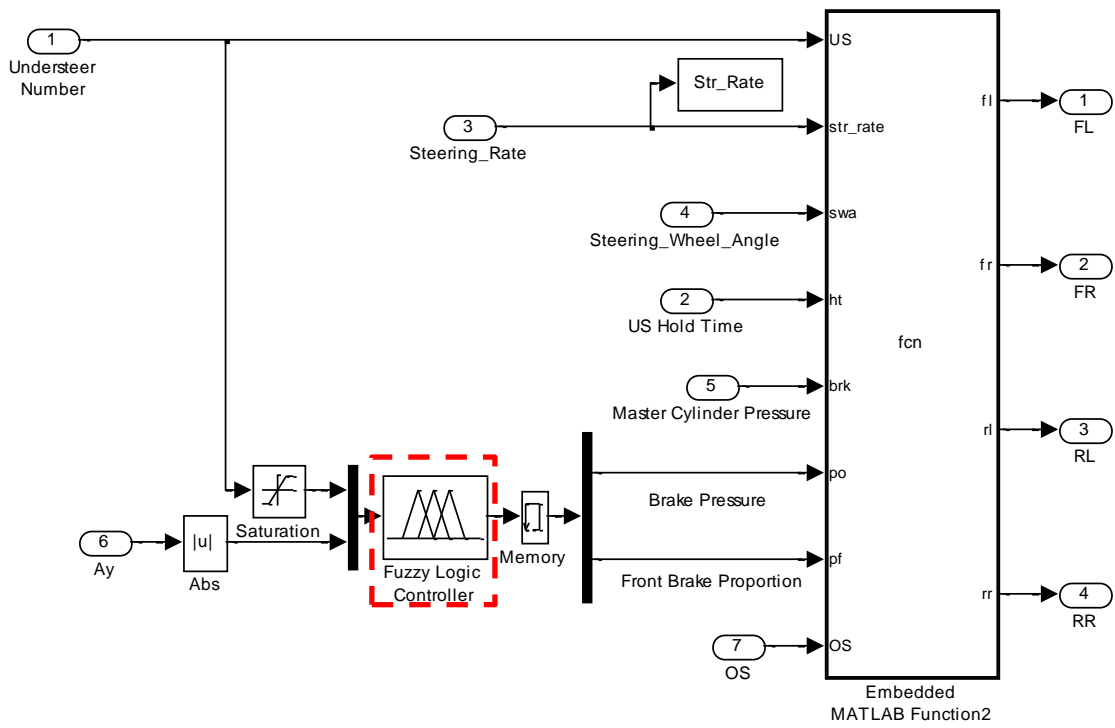


**Figure D.11 Under-Steer Brake Force Distributor block**

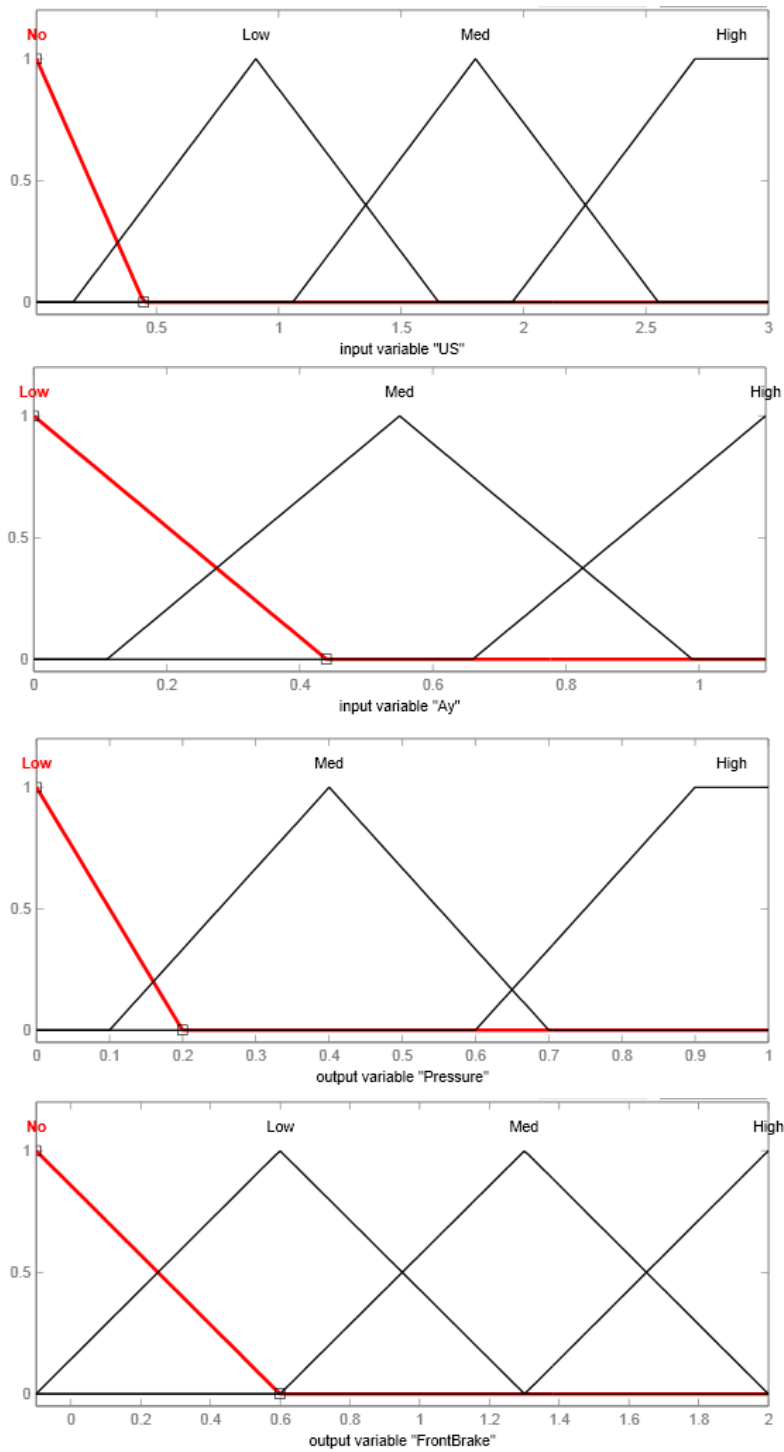


**Figure D.12 Brake Balance: Input and Output Membership Functions**

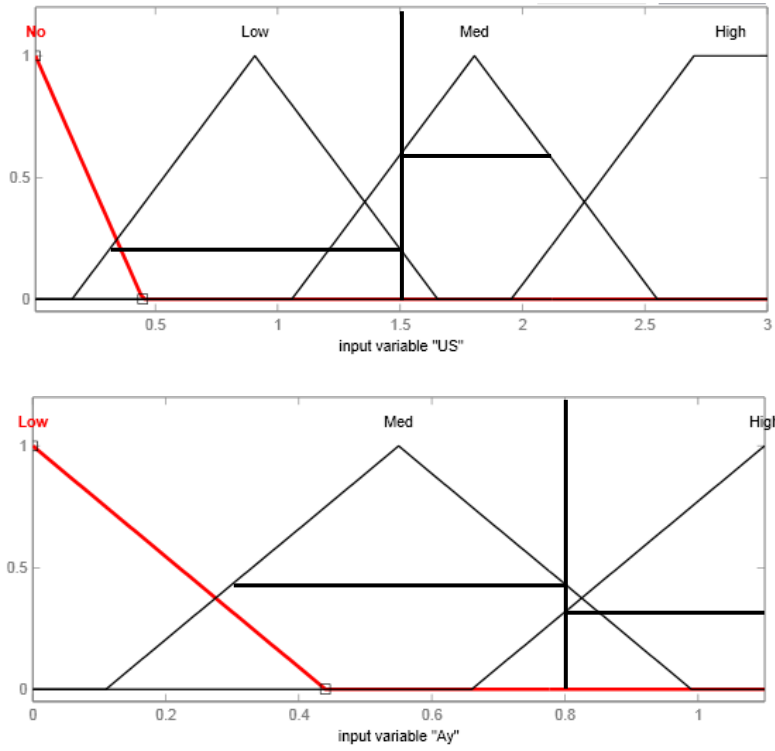


Figure D.13 Brake Balance: Input Membership Functions for Input [1.5 0.8]

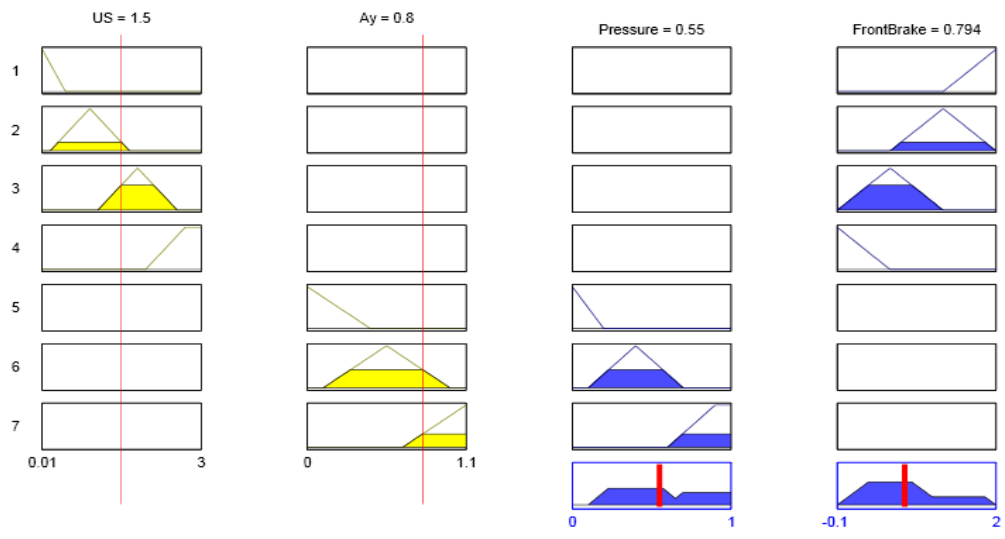


Figure D.14 Brake Balance: Evaluation of Rules and Defuzzified Outputs

## REFERENCES

- [1] Dang J.N., "Statistical Analysis of the Effectiveness of Electronic Stability Control (ESC) Systems-Final Report," **NHTSA Technical Report DOT HS 810 794**, 2007.
- [2] Milliken W.F. and Milliken D.L., "Race Car Vehicle Dynamics," SAE International, Warrendale, PA, ISBN 1-56091-526-9, 1995.
- [3] Zadeh L.A., "Fuzzy Sets," *Inform. Control* **8**(3):338-353, 1965, doi: 10.1016/S0019-9958(65)90241-X.
- [4] Anderson J.R., "Fuzzy Logic Approach to Vehicle Stability Control," M.S. Thesis, Clemson University, Clemson, SC, 2010.
- [5] Anderson J.R. and Law E.H., "Fuzzy Logic Approach to Vehicle Stability Control of Oversteer," *SAE Int.J.Passeng.Cars - Mech.Syst.* **4**(1):241-250, 2011, doi: 10.4271/2011-01-0268.
- [6] van Zanten , Anton T., Erhardt R., and Pfaff G., "VDC, The Vehicle Dynamics Control System of Bosch," *SAE Technical Paper 950759*, 1995, doi:10.4271/950759.
- [7] "Automotive Handbook," Robert Bosch GmbH, Plochingen, Germany, ISBN 978-0-7680-1953-7, 2007.
- [8] Guo J., Chu L., Zhou F., Cao L., "Integrated Control of Variable Torque Distribution and Electronic Stability Program Based on Slip Angle Phase," 2011 International Conference on Electronic and Mechanical Engineering and Information Technology (EMEIT), 2011, doi:10.1109/EMEIT.2011.6023881.
- [9] Yuan Chao-chun, Chen Long, Wang Shao-hua, Jiang Hao-binm, "Research of Electronic Stability Program Based on the Mu Control Theory," 2010 International Conference on Computer and Communication Technologies in Agriculture Engineering (CCTAE), 2010.
- [10] Jangyeol Yoon, Wanki Cho, Bongyeong Koo, and Kyongsu Yi, "Unified Chassis Control for Rollover Prevention and Lateral Stability," *IEEE Transactions on Vehicular Technology* **58**(2):596-609, 2009.

- [11] McLellan D.R., Ryan J.P., Browalski E.S., and Heinrich J.W., "Increasing the Safe Driving Envelope - Abs, Traction Control and Beyond," *SAE 92C014*, 1992.
- [12] Sutton R., "Modelling Human Operators in Control System Design," Research Studies Press; Taunton, England ISBN 0-471-92909-3, 1990.
- [13] Tong R.M., "Control Engineering Review of Fuzzy Systems," *Automatica* **13**(6):559-569, 1977, doi: 10.1016/0005-1098(77)90077-2.
- [14] Johannsen G. and Rouse W.B., "Mathematical Concepts for Modeling Human Behavior in Complex Man-Machine Systems," *Human Factors: The Journal of the Human Factors and Ergonomics Society* **21**(6):733-747, 1979.
- [15] Daley S. and Gill K., "A Justification for the Wider Use of Fuzzy Logic Control Algorithms," *Proc.Inst.Mech.Eng.Part C* **199**(1):43-49, 1985.
- [16] Murakami S., "Automobile Speed Control System Using a Fuzzy Logic Controller," *Industrial Applications of Fuzzy Control*: 43-48, 1985.
- [17] "An Autopilot for Ships Designed with Fuzzy Sets," Proc IFAC Conference on Digital Computer Applications to Process Control, 1977.
- [18] Vaduri S.S.V., "Development of Computer Tools for Analysis of Track Test Data and for Prediction of Dynamic Handling Response for Winston Cup Cars," PhD Dissertation, Clemson University, Clemson, SC, 1999.
- [19] Fey B., "Data Power: Using Racecar Data Acquisition," Towery Pub, Memphis, ISBN 1-88109-601-7, 1993.
- [20] Ghoneim Y., Lin W., Sidlosky D., Chen H., et al., "Integrated Chassis Control System to Enhance Vehicle Stability," *Int.J.Veh.Des.* **23**(1-2):124-144, 2000, doi:10.1504/IJVD.2000.001887.
- [21] Tseng H.E., Ashrafi B., Madau D., Allen Brown T., et al., "The Development of Vehicle Stability Control at Ford," *IEEE/ASME Transactions on Mechatronics*, **4**(3):223-234, 1999.
- [22] van Zanten, A. T., "Bosch ESP Systems: 5 Years of Experience," *SAE Technical Paper 2000-01-1633*, 2000, doi:10.4271/2000-01-1633.
- [23] Gulley N. and Jang J.R., "Fuzzy Logic Toolbox User's Guide," *The MathWorks, Inc.*, **24**, 1995.

- [24] Law E.H., "Transient Handling Analysis of a 2007 BMW Mini Equipped with TWEELs: Comparison of Tests and Simulation and Parameter Studies," *Clemson University, Department of Mechanical Engineering Report TR-08-119-ME-MMS*, 2009.
- [25] U.S. Department Of Transportation, National Highway Traffic Safety Administration, "FMVSS No. 126 Electronic Stability Control Systems-Final Regulatory Impact Analysis," **49 CFR Parts 571 & 585**, 2007.
- [26] U.S. Department Of Transportation, National Highway Traffic Safety Administration, "FMVSS No. 126 Electronic Stability Systems-Final Rule," **49 CFR Parts 571 and 585 [Docket No. NHTSA-2007-27662]**, 2007.